

NATIONAL CENTER FOR EARTHQUAKE  
ENGINEERING RESEARCH

State University of New York at Buffalo

---

---

# FREQUENCY RESPONSE OF SECONDARY SYSTEMS UNDER SEISMIC EXCITATION

by

J.A. HoLung, J. Cai and Y.K. Lin

Center for Applied Stochastics Research

Florida Atlantic University

Boca Raton, Florida 33431-0991

Technical Report NCEER-87-0013

July 31, 1987

This research was conducted at Florida Atlantic University and was supported by the  
National Science Foundation under Grant No. ECE 86-07591.

## NOTICE

This report was prepared by Florida Atlantic University as a result of research sponsored by the National Center for Earthquake Engineering Research (NCEER). Neither NCEER, associates of NCEER, its sponsors, Florida Atlantic University, nor any person acting on their behalf:

- a. makes any warranty, express or implied, with respect to the use of any information, apparatus, method, or process disclosed in this report or that such use may not infringe upon privately owned rights; or
- b. assumes any liabilities of whatsoever kind with respect to the use of, or the damages resulting from the use of, any information, apparatus, method or process disclosed in this report.

Y.-P. Wang 4/16/90

---

**FREQUENCY RESPONSE OF SECONDARY SYSTEMS  
UNDER SEISMIC EXCITATION**

by

J. A. HoLung<sup>1</sup>, J. Cai<sup>1</sup> and Y. K. Lin<sup>2</sup>

July 31, 1987

Technical Report NCEER-87-0013

NCEER Contract Number 86-3023

NSF Master Contract Number ECE 86-07591

1 Research Assistants, Center for Applied Stochastics Research, College of Engineering, Florida Atlantic University

2 Schmidt Professor of Engineering and Director, Center for Applied Stochastics Research, Florida Atlantic University

**NATIONAL CENTER FOR EARTHQUAKE ENGINEERING RESEARCH**

State University of New York at Buffalo

Red Jacket Quadrangle, Buffalo, New York 14261

---



## ABSTRACT

A component-mode synthesis procedure is applied to determine the frequency response of one or several secondary systems which receive seismic excitations indirectly through the supporting primary structure. In this procedure, the interactive forces at the interfaces are added to the equations of motion for the primary and secondary systems separately. These equations are then combined by imposing the compatibility conditions at the interfaces, and in so doing the interactive forces are automatically cancelled in the final set of equations. The analysis is mathematically exact if all the independent degrees of freedom are included in the formulation, and it is approximate if a reduced number of normal modes are included. These are illustrated in three examples.

The main objective of the present report is to investigate how the component-mode procedure can be utilized to full advantage by including the smallest number of normal modes of the primary system in the analysis while still achieving the necessary accuracy in the results. For this purpose, numerical calculations are carried out for the frequency response of a single degree of freedom secondary system supported on an arbitrary floor in a multi-story building of shear-wall type construction. It is shown that when the secondary system is tuned to one of the natural frequencies of the primary system, sufficiently accurate results can usually be obtained by including the tuned primary mode, one immediately higher than the tuned primary mode, and all of those lower

than the tuned primary mode. Therefore, the calculation is relatively simple when the secondary system is tuned to a lower primary mode; however, this computational advantage is reduced progressively as the secondary system is tuned to higher and higher primary modes. In the latter case, a modified cascade approach is found to be more efficient in which the response near the natural frequencies of some selected primary modes is calculated on the basis of the component-mode approach including these primary modes, whereas the response for the remaining frequency region is calculated using the traditional cascade procedure. The selected primary modes normally include the one in tune with the secondary system and a few lowest primary modes. When damping in the primary system is sufficiently low, including only one primary mode, namely, the tuned primary mode, may be sufficient.

Table of Contents

1.0 INTRODUCTION . . . . .	1
2.0 ANALYSIS . . . . .	3
2.1 GENERAL FORMULATION . . . . .	3
2.1.1 EXAMPLE 1. A SIMPLE P-S SYSTEM . . . . .	10
2.1.2 EXAMPLE 2. MULTIPLE ATTACHMENTS . . . . .	15
2.1.3 EXAMPLE 3. BUILDING AND 1-D.O.F EQUIPMENT . . . . .	21
3.0 SOME NUMERICAL RESULTS . . . . .	25
3.1 EFFECT OF EQUIPMENT MASS . . . . .	33
3.2 EFFECT OF DAMPING IN BUILDING . . . . .	34
3.3 EFFECT OF EQUIPMENT LOCATION . . . . .	35
3.4 THE DETUNED CASE . . . . .	36
4.0 CONCLUDING REMARKS . . . . .	75
5.0 APPENDIX. EXACT TRANSFER MATRIX SOLUTIONS FOR AN EXAMPLE BUILDING-EQUIPMENT SYSTEM . . . . .	76
5.1 PRIMARY SYSTEM WITH IDENTICAL FLOORS . . . . .	78
5.2 CASCADE SOLUTION . . . . .	82
5.3 MODAL PROPERTIES OF PRIMARY SYSTEM . . . . .	82
6.0 ACKNOWLEDGEMENT . . . . .	85
7.0 REFERENCES . . . . .	86





## 1.0 INTRODUCTION

A secondary system is a lighter appendage to a more massive primary system. In a seismic event, it receives the excitation at the supports indirectly through the primary system. In theory, the combined primary-secondary system can be analyzed as a whole. However, the large difference between the mass of the secondary system and the mass of the primary system can sometimes lead to numerical problems. Even if such numerical difficulties can be circumvented, direct numerical integration of the equations of motion can be time consuming and expensive. As the size of the problem increases, the direct approach becomes more and more unattractive. For optimization studies, the dynamic properties of the combined system would have to be re-evaluated for each configuration.

In the present study, our emphasis is placed on the response of the secondary system to ground-motion excitations. When the mass of the secondary system is small in comparison to the mass of the primary system, methods based on perturbation [1,4,8,9,10,11,15] may be employed. Recently, an approach based on synthesizing the modal properties of the combined system from the properties of the subsystems [17,18,19,20] has been developed which is applicable even for relatively heavy secondary systems.

In this paper, we apply another approach based on component-mode substructuring techniques, [2,3,5,6,7], which allows considerable reduction in the order of the system

matrices. The accuracy and efficiency of this approach is evaluated by numerical examples, and alternative procedures are proposed when it is not sufficiently efficient.

## 2.0 ANALYSIS

### 2.1 GENERAL FORMULATION

Consider a combined system as shown in figure 1. The primary system, which we denote by  $P$ , is subjected to a base motion,  $G(t)$ . Connected to the primary system are  $q$  secondary subsystems  $S_1, \dots, S_q$ . For the primary system we can write the equations of motion in matrix form as follows

$$M \ddot{X} + C \dot{X} + K X = - M l \ddot{G} + R(t) \quad (1)$$

where  $M$ ,  $C$ , and  $K$ , are system matrices corresponding to a fixed base primary system,  $X$  is a column matrix of displacements relative to the ground,  $l$  is another column matrix in which all elements are unity, and  $R(t)$  is a vector of forces acting on the primary system by the  $q$  secondary systems. For each secondary system we can also write a matrix equation of motion in a form similar to equation (1). The generalized displacements selected for each secondary system include the degrees of freedom associated with the interfaces with the primary system. The forces acting at the interfaces must be equal and opposite to those in the  $R(t)$  vector in equation (1).

We denote the relative displacement vectors for the secondary systems by  $Y$ , to distinguish them from that of the primary system, and use subscripts 'u', and 'a' to denote the unattached and attached coordinates, respectively. By attached coordinates we mean those coordinates common to both

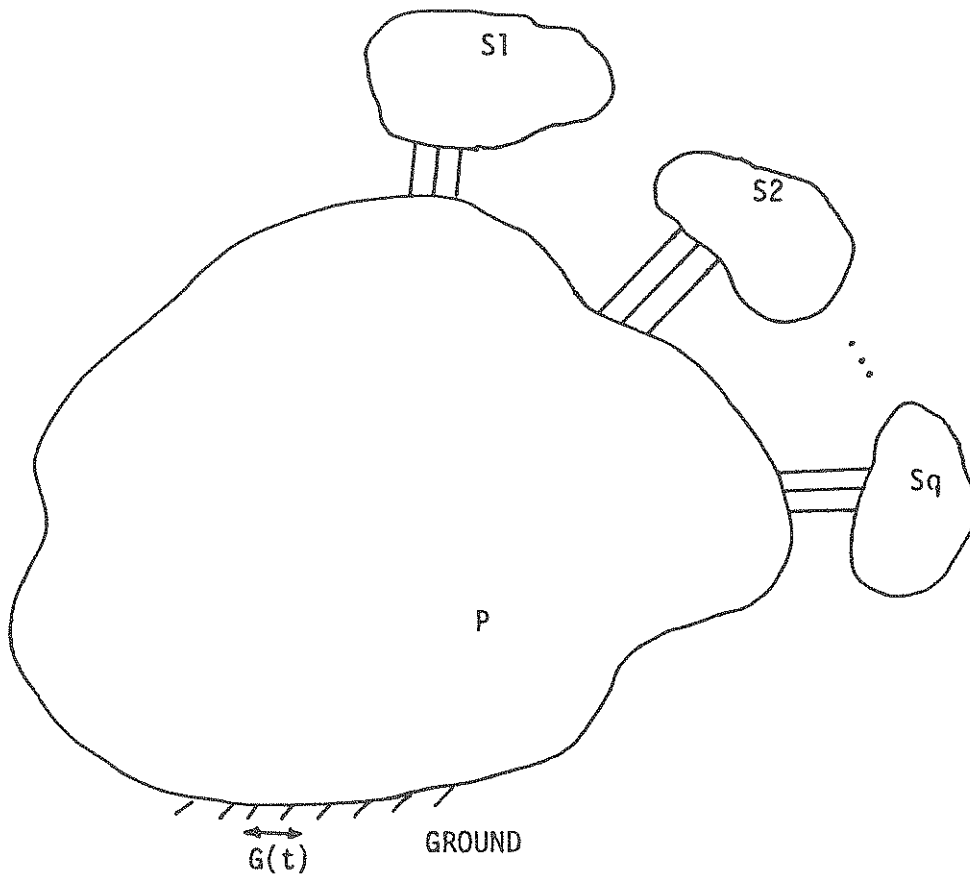


Figure 1. General model. Combined primary system and  $q$  attached secondary systems subject to seismic excitation  $G(t)$ .

the primary system and the connected secondary systems. With this notation, we rewrite equation (1) for the primary system as

$$\begin{aligned}
 \begin{bmatrix} M_u & 0 \\ 0 & M_a \end{bmatrix} \begin{bmatrix} \ddot{X}_u \\ \ddot{X}_a \end{bmatrix} + \begin{bmatrix} C_u & C_{ua} \\ C_{au} & C_a \end{bmatrix} \begin{bmatrix} \dot{X}_u \\ \dot{X}_a \end{bmatrix} + \begin{bmatrix} K_u & K_{ua} \\ K_{au} & K_a \end{bmatrix} \begin{bmatrix} X_u \\ X_a \end{bmatrix} \\
 = - \begin{bmatrix} M_u & 0 \\ 0 & M_a \end{bmatrix} \begin{bmatrix} 1 \\ 1 \end{bmatrix} \ddot{G} + \begin{bmatrix} 0 \\ R \end{bmatrix} \quad (2)
 \end{aligned}$$

Similarly, for the secondary systems we write

$$\begin{aligned}
 \begin{bmatrix} m_a & 0 \\ 0 & m_u \end{bmatrix}_j \begin{bmatrix} \ddot{Y}_a \\ \ddot{Y}_u \end{bmatrix}_j + \begin{bmatrix} c_a & c_{au} \\ c_{ua} & c_u \end{bmatrix}_j \begin{bmatrix} \dot{Y}_a \\ \dot{Y}_u \end{bmatrix}_j + \begin{bmatrix} k_a & k_{au} \\ k_{ua} & k_u \end{bmatrix}_j \begin{bmatrix} Y_a \\ Y_u \end{bmatrix}_j \\
 = - \begin{bmatrix} m_a & 0 \\ 0 & m_u \end{bmatrix}_j \begin{bmatrix} 1 \\ 1 \end{bmatrix} \ddot{G} - \begin{bmatrix} r \\ 0 \end{bmatrix}_j \quad (3)
 \end{aligned}$$

$$j = 1, \dots, q$$

The system matrices for all the secondary systems can be combined as follows:

$$\begin{aligned}
 & \begin{bmatrix} m_a^1 & & & & & \\ & \ddots & & & & \\ & & m_a^q & & & \\ \hline & & & m_u^1 & & \\ & & & & \ddots & \\ & & & & & m_u^q \end{bmatrix} \begin{bmatrix} \dot{y}_a \\ \vdots \\ \dot{y}_u \end{bmatrix} + \begin{bmatrix} c_a^1 & & & & & \\ & \ddots & & & & \\ & & c_a^q & & & \\ \hline c_{ua}^1 & & & & & \\ & \ddots & & & & \\ & & c_{ua}^q & & & \\ & & & c_u^1 & & \\ & & & & \ddots & \\ & & & & & c_u^q \end{bmatrix} \begin{bmatrix} \dot{y}_a \\ \vdots \\ \dot{y}_u \end{bmatrix} \\
 & + \begin{bmatrix} k_a^1 & & & & & \\ & \ddots & & & & \\ & & k_a^q & & & \\ \hline k_{ua}^1 & & & & & \\ & \ddots & & & & \\ & & k_{ua}^q & & & \\ & & & k_u^1 & & \\ & & & & \ddots & \\ & & & & & k_u^q \end{bmatrix} \begin{bmatrix} y_a \\ \vdots \\ y_u \end{bmatrix} \\
 & = - \begin{bmatrix} m_a^1 & & & & & \\ & \ddots & & & & \\ & & m_a^q & & & \\ \hline & & & m_u^1 & & \\ & & & & \ddots & \\ & & & & & m_u^q \end{bmatrix} \begin{bmatrix} 1 \\ \vdots \\ 1 \end{bmatrix} \ddot{G} - \begin{bmatrix} R \\ \vdots \\ 0 \end{bmatrix} \quad (4)
 \end{aligned}$$

In equation (4), the assembled force vector has been set equal and opposite to the vector R in equation (2), and all the null sub-matrices are omitted. Similar omissions will also be made when such omissions are obvious and will not cause confusion. For convenience we rewrite equation (4) more simply as

$$\begin{aligned}
 & \begin{bmatrix} m_a & 0 \\ 0 & m_u \end{bmatrix} \begin{bmatrix} \ddot{y}_a \\ \vdots \\ \ddot{y}_u \end{bmatrix} + \begin{bmatrix} c_a & c_{au} \\ c_{ua} & c_u \end{bmatrix} \begin{bmatrix} \dot{y}_a \\ \vdots \\ \dot{y}_u \end{bmatrix} + \begin{bmatrix} k_a & k_{au} \\ k_{ua} & k_u \end{bmatrix} \begin{bmatrix} y_a \\ \vdots \\ y_u \end{bmatrix} \\
 & = - \begin{bmatrix} m_a & 0 \\ 0 & m_u \end{bmatrix} \begin{bmatrix} 1 \\ \vdots \\ 1 \end{bmatrix} \ddot{G} - \begin{bmatrix} R \\ \vdots \\ 0 \end{bmatrix} \quad (5)
 \end{aligned}$$

which has the same form as equation (3) with the subscript j removed. The matrices in equation (5) represent the as-

sembled matrices for all the secondary systems and they should not be confused with those for the individual secondary systems. Further combining equations (2) and (5), we obtain

$$\begin{aligned}
 & \begin{bmatrix} M_u & & & & & \\ & M_a & & & & \\ & & m_a & & & \\ & & & m_u & & \\ & & & & & \end{bmatrix} \begin{bmatrix} \ddot{X}_u \\ \ddot{X}_a \\ \ddot{Y}_a \\ \ddot{Y}_u \end{bmatrix} + \begin{bmatrix} C_u & C_{ua} & & & & \\ & C_{au} & C_a & & & \\ \hline & & & c_a & c_{au} & \\ & & & c_{ua} & c_u & \end{bmatrix} \begin{bmatrix} \dot{X}_u \\ \dot{X}_a \\ \dot{Y}_a \\ \dot{Y}_u \end{bmatrix} \\
 & + \begin{bmatrix} K_u & K_{ua} & & & & \\ & K_{au} & K_a & & & \\ \hline & & & k_a & k_{au} & \\ & & & k_{ua} & k_u & \end{bmatrix} \begin{bmatrix} X_u \\ X_a \\ Y_a \\ Y_u \end{bmatrix} = - \begin{bmatrix} M_u & & & & & \\ & M_a & & & & \\ & & m_a & & & \\ & & & m_u & & \\ & & & & & \end{bmatrix} \begin{bmatrix} 1 \\ 1 \\ 1 \\ 1 \end{bmatrix} \ddot{G} + \begin{bmatrix} 0 \\ R \\ -R \\ 0 \end{bmatrix} \quad (6)
 \end{aligned}$$

We now impose the constraint at the common boundary,  $X_b = G_1 X_u$ ,  $X_a = G_2 Y_a$ , where  $G_1$  and  $G_2$  are conversion matrices depending on the interface geometry. In many cases,  $G_1$  and  $G_2$  are the identity matrices. Then

$$\begin{bmatrix} X_u \\ X_a \\ Y_a \\ Y_u \end{bmatrix} = \begin{bmatrix} I & 0 & 0 \\ 0 & I & 0 \\ 0 & I & 0 \\ 0 & 0 & I \end{bmatrix} \begin{bmatrix} X_u \\ X_b \\ Y_u \end{bmatrix} = [A] \begin{bmatrix} X_u \\ X_b \\ Y_u \end{bmatrix} \quad (7)$$

Substituting equation (7) into equation (6) and premultiply by  $[A]^T$ , we obtain for the coupled system

$$\begin{bmatrix} M_u & & & \\ & M_a + m_a & & \\ & & m_u & \\ & & & \end{bmatrix}
\begin{bmatrix} \ddot{X}_u \\ \ddot{X}_b \\ \ddot{Y}_u \end{bmatrix}
+
\begin{bmatrix} C_u & C_{ua} & 0 \\ C_{au} & C_a + c_a & c_{au} \\ 0 & c_{ua} & c_u \end{bmatrix}
\begin{bmatrix} \dot{X}_u \\ \dot{X}_b \\ \dot{Y}_u \end{bmatrix}
+
\begin{bmatrix} K_u & K_{ua} & 0 \\ K_{au} & K_a + k_a & k_{au} \\ 0 & k_{ua} & k_u \end{bmatrix}
\begin{bmatrix} X_u \\ X_b \\ Y_u \end{bmatrix}
= -
\begin{bmatrix} M_u & & \\ & M_a + m_a & \\ & & m_u \end{bmatrix}
\begin{bmatrix} 1 \\ 1 \\ 1 \end{bmatrix}
\ddot{G} \quad (8)$$

Note that the force vector 'R' does not appear in equation (8) after the geometric boundary conditions have been imposed. By combining  $X_u$  and  $X_b$  into  $X$ , equation (8) is condensed to the form

$$\begin{bmatrix} \tilde{M} & 0 \\ 0 & m_u \end{bmatrix}
\begin{bmatrix} \ddot{X} \\ \ddot{Y}_u \end{bmatrix}
+
\begin{bmatrix} \tilde{C} & \tilde{C}_{au} \\ \tilde{C}_{ua} & c_u \end{bmatrix}
\begin{bmatrix} \dot{X} \\ \dot{Y}_u \end{bmatrix}
+
\begin{bmatrix} \tilde{K} & \tilde{K}_{au} \\ \tilde{K}_{ua} & k_u \end{bmatrix}
\begin{bmatrix} X \\ Y_u \end{bmatrix}
= -
\begin{bmatrix} \tilde{M} & 0 \\ 0 & m_u \end{bmatrix}
\begin{bmatrix} 1 \\ 1 \end{bmatrix}
\ddot{G} \quad (9)$$

where the consolidated matrices are indicated by a tilde. Equation (9) is in a form similar to that usually given by other writers.

The development leading to the final coupled system of equations, equation (8) or (9), is useful because the contribution from the individual subsystems is clear, and the procedure can be directly coded in a numerical scheme. By separating the matrices for the subsystems, which we presume is available from other sources, we take advantage of information that may be more naturally available from a development process. For example, the design of the subsystems may have been carried out separately, or they may be the result of efforts carried out by different groups, and, perhaps at different times. The procedure also permits the



inclusion of protective devices for secondary systems, such as viscoelastic cushions, in the analysis with very little modification, which will be the subject of a future report. Furthermore, whereas ground motion has been taken to be the input excitation in the present report one can accommodate other external excitations such as wind loads, by including them in the forcing vector on the RHS of the preceding equations in a straightforward manner.

The number of degrees of freedom for the primary system is usually large in comparison to those of the secondary subsystems. Correspondingly, the order of the system matrices in the final assembled system equations can be very large. However, we shall take advantage of component-mode substructuring techniques, using a reduced number of modes of the primary system in a Rayleigh-Ritz type analysis to reduce the order of the matrices. Let  $N$  be the number of degrees of freedom of the primary system. Denoting the  $i$ -th normal mode of the primary system by  $\phi_i$ , we consider a Ritz vector

$$\begin{bmatrix} X \\ \bar{X} \end{bmatrix} = \begin{bmatrix} \phi_1 & \dots & \phi_n \\ N \times n \end{bmatrix} \begin{bmatrix} q_1 \\ \vdots \\ q_n \\ n \times 1 \end{bmatrix} = \begin{bmatrix} \phi \end{bmatrix} \begin{bmatrix} q \end{bmatrix} \quad (10)$$

where  $n < N$ , and 'q' is the corresponding vector of generalized coordinates. In general, the accuracy of the approximation expressed by equation (10) will be good provided that the discarded modes do not contribute significantly to the response. The selection of appropriate modes will be explored later. We can partition equation (10) as follows:

$$\begin{bmatrix} X_u \\ -\bar{X}_a \end{bmatrix} = \begin{bmatrix} \phi_u \\ -\phi_a \end{bmatrix} \begin{bmatrix} q \end{bmatrix} \quad (11)$$

The response vector for the disjoint systems is related to that of the coupled system through the compatibility condi-

tion, say  $X_a = Y_a$ . With equation (11), this relation is written as

$$\begin{bmatrix} X_u \\ X_a \\ Y_a \\ Y_u \end{bmatrix} = \begin{bmatrix} \phi_u & 0 \\ \phi_a & 0 \\ \phi_a & 0 \\ 0 & I \end{bmatrix} \begin{bmatrix} q \\ Y_u \end{bmatrix} = [B] \begin{bmatrix} q \\ Y_u \end{bmatrix} \quad (12)$$

Upon substituting equation (12) into equation (6) and premultiplying by  $[B]^T$ , we obtain the reduced equation of motion in the form

$$\begin{bmatrix} M \\ r \end{bmatrix} \begin{bmatrix} \ddot{q} \\ \ddot{Y} \end{bmatrix} + \begin{bmatrix} C \\ r \end{bmatrix} \begin{bmatrix} \dot{q} \\ \dot{Y} \end{bmatrix} + \begin{bmatrix} K \\ r \end{bmatrix} \begin{bmatrix} q \\ Y \end{bmatrix} = - \begin{bmatrix} M \\ r \end{bmatrix} \begin{bmatrix} 1 \\ 1 \end{bmatrix} \ddot{G} \quad (13)$$

where

$$\begin{aligned} [M_r] &= [B]^T [M] [B] \\ [C_r] &= [B]^T [C] [B] \\ [K_r] &= [B]^T [K] [B] \end{aligned} \quad (14)$$

### 2.1.1 EXAMPLE 1. A SIMPLE P-S SYSTEM

As the first example to illustrate the assemblage of the coupled equations of motion, consider a 2-d.o.f primary system with an attached 2-d.o.f secondary system, as sketched in figure 2. The p-s system has four degrees of freedom. As a first step, we separate the primary system and the secondary system as shown in figure 2b. In the process, we introduce an additional degree of freedom,  $Z_3$ , representing the motion at the common boundary together with the force

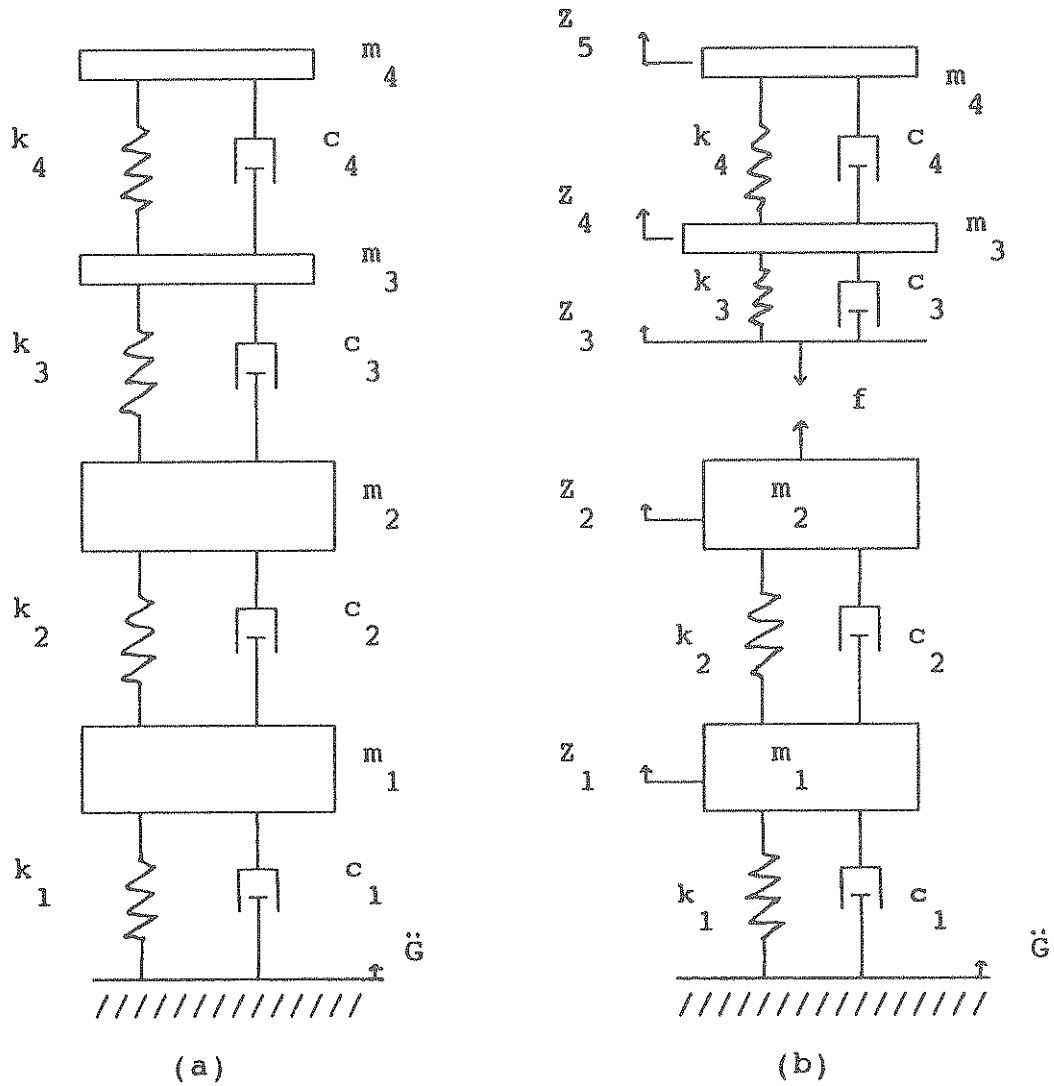


Figure 2. (a) A 4 degree-of-freedom combined p-s system, (b) separated subsystems

vector 'f', as shown. The equations of motion for the primary system can be written as

$$\begin{bmatrix} m_1 & 0 \\ 0 & m_2 \end{bmatrix} \begin{bmatrix} \ddot{X}_u \\ \ddot{X}_a \end{bmatrix} + \begin{bmatrix} c_1+c_2 & -c_2 \\ -c_2 & c_2 \end{bmatrix} \begin{bmatrix} \dot{X}_u \\ \dot{X}_a \end{bmatrix} + \begin{bmatrix} k_1+k_2 & -k_2 \\ -k_2 & k_2 \end{bmatrix} \begin{bmatrix} X_u \\ X_a \end{bmatrix} \\ = - \begin{bmatrix} m_1 & 0 \\ 0 & m_2 \end{bmatrix} \begin{bmatrix} 1 \\ 1 \end{bmatrix} \ddot{G} + \begin{bmatrix} 0 \\ f \end{bmatrix} \quad (15)$$

where

$$\begin{aligned} X_u &= Z_1 - G \\ X_a &= Z_2 - G \end{aligned} \quad (16)$$

Similarly, for the secondary system we have

$$\begin{bmatrix} 0 & 0 & 0 \\ 0 & m_3 & 0 \\ 0 & 0 & m_4 \end{bmatrix} \begin{bmatrix} \ddot{Y}_a \\ \ddot{Y}_1 \\ \ddot{Y}_2 \end{bmatrix} + \begin{bmatrix} c_3 & -c_3 & 0 \\ -c_3 & c_3+c_4 & -c_4 \\ 0 & -c_4 & c_4 \end{bmatrix} \begin{bmatrix} \dot{Y}_a \\ \dot{Y}_1 \\ \dot{Y}_2 \end{bmatrix} \\ + \begin{bmatrix} k_3 & -k_3 & 0 \\ -k_3 & k_3+k_4 & -k_4 \\ 0 & -k_4 & k_4 \end{bmatrix} \begin{bmatrix} Y_a \\ Y_1 \\ Y_2 \end{bmatrix} = - \begin{bmatrix} 0 & 0 & 0 \\ 0 & m_3 & 0 \\ 0 & 0 & m_4 \end{bmatrix} \begin{bmatrix} 1 \\ 1 \\ 1 \end{bmatrix} \ddot{G} - \begin{bmatrix} f \\ 0 \\ 0 \end{bmatrix} \quad (17)$$

where

$$\begin{aligned} Y_a &= Z_3 - G \\ Y_1 &= Z_4 - G \\ Y_2 &= Z_5 - G \end{aligned} \quad (18)$$

Comparing equations (17) and (5), the various submatrices are easily identified; we have

$$\begin{aligned}
 m_u &= \begin{bmatrix} m_3 & 0 \\ 0 & m_4 \end{bmatrix}, & c_a &= c_3, & c_{au} &= [-c_3 \quad 0], \\
 m_a &= 0, & c_{ua} &= [c_{au}]^T, & c_u &= \begin{bmatrix} c_3+c_4 & -c_4 \\ -c_4 & c_4 \end{bmatrix}, \\
 & & k_a &= k_3, & k_{au} &= [-k_3 \quad 0], \\
 & & k_{ua} &= [k_{au}]^T, & k_u &= \begin{bmatrix} k_3+k_4 & -k_4 \\ -k_4 & k_4 \end{bmatrix}.
 \end{aligned} \tag{19}$$

Similarly, comparing equations (15) and (2), we have

$$\begin{aligned}
 M_u &= m_1, & M_a &= m_2, & C_u &= c_1 + c_2, & C_{ua} &= -c_2, \\
 C_{au} &= -c_2, & C_a &= c_2, & K_u &= k_1 + k_2, & K_{ua} &= -k_2, \\
 K_{au} &= -k_2, & K_a &= k_2.
 \end{aligned} \tag{20}$$

With equations (19) and (20), the assembled equations of motion for the coupled system can be written according to equation (8). The result is

$$\begin{bmatrix} m_1 & & & \\ & m_2 & & \\ & & m_3 & \\ & & & m_4 \end{bmatrix} \begin{bmatrix} \ddot{X}_u \\ \ddot{X}_a \\ \ddot{Y}_1 \\ \ddot{Y}_2 \end{bmatrix} + \begin{bmatrix} c_1+c_2 & -c_2 & 0 & 0 \\ -c_2 & c_2+c_3 & -c_3 & 0 \\ 0 & -c_3 & c_3+c_4 & -c_4 \\ 0 & 0 & -c_4 & c_4 \end{bmatrix} \begin{bmatrix} \dot{X}_u \\ \dot{X}_a \\ \dot{Y}_1 \\ \dot{Y}_2 \end{bmatrix} + \begin{bmatrix} k_1+k_2 & -k_2 & 0 & 0 \\ -k_2 & k_2+k_3 & -k_3 & 0 \\ 0 & -k_3 & k_3+k_4 & -k_4 \\ 0 & 0 & -k_4 & k_4 \end{bmatrix} \begin{bmatrix} X_u \\ X_a \\ Y_1 \\ Y_2 \end{bmatrix} = - \begin{bmatrix} m_1 & & & \\ & m_2 & & \\ & & m_3 & \\ & & & m_4 \end{bmatrix} \begin{bmatrix} 1 \\ 1 \\ 1 \\ 1 \end{bmatrix} \ddot{G} \quad (21)$$

It should be noted that since every possible degree of freedom is included in equation (21), the analysis represented by this equation is exact. Approximation is introduced only if "mathematical" constraints are imposed by restricting the motions of the primary system, or the secondary system, or both to fewer modes than the original degrees of freedom. Note also that the interactive forces between the primary and secondary systems do not appear in equation (21) as expected.

### 2.1.2 EXAMPLE 2. MULTIPLE ATTACHMENTS

As a second example, we consider a more general case as indicated in figure 3. Attached to the 2-d.o.f primary system are two secondary subsystems; one system being a simple oscillator attached to the second coordinate of the primary system and the second, a 2-d.o.f system attached to both coordinates of the primary system. Again, we separate the subsystems as indicated in figure 3b. Following the same procedure as before, we have for the primary system

$$\begin{bmatrix} m_1 & 0 \\ 0 & m_2 \end{bmatrix} \begin{bmatrix} \ddot{X}_{a1} \\ \ddot{X}_{a2} \end{bmatrix} + \begin{bmatrix} c_1+c_2 & -c_2 \\ -c_2 & c_2 \end{bmatrix} \begin{bmatrix} \dot{X}_{a1} \\ \dot{X}_{a2} \end{bmatrix} + \begin{bmatrix} k_1+k_2 & -k_2 \\ -k_2 & k_2 \end{bmatrix} \begin{bmatrix} X_{a1} \\ X_{a2} \end{bmatrix} \\ = - \begin{bmatrix} m_1 & 0 \\ 0 & m_2 \end{bmatrix} \begin{bmatrix} 1 \\ 1 \end{bmatrix} \ddot{G} + \begin{bmatrix} f_2 \\ f_1+f_3 \end{bmatrix} \quad (22)$$

where

$$\begin{aligned} X_{a1} &= Z_1 - G \\ X_{a2} &= Z_2 - G \end{aligned} \quad (23)$$

and for the secondary subsystems

$$\begin{bmatrix} 0 & 0 & 0 & 0 \\ 0 & 0 & 0 & 0 \\ 0 & 0 & m_3 & 0 \\ 0 & 0 & 0 & m_4 \end{bmatrix} \begin{bmatrix} \ddot{Y}_{1a} \\ \ddot{Y}_{2a} \\ \ddot{Y}_1 \\ \ddot{Y}_2 \end{bmatrix} + \begin{bmatrix} c_4 & 0 & -c_4 & 0 \\ 0 & c_6 & 0 & -c_6 \\ -c_4 & 0 & c_4+c_5 & -c_5 \\ 0 & -c_6 & -c_5 & c_5+c_6 \end{bmatrix} \begin{bmatrix} \dot{Y}_{1a} \\ \dot{Y}_{2a} \\ \dot{Y}_1 \\ \dot{Y}_2 \end{bmatrix} \\ + \begin{bmatrix} k_4 & 0 & -k_4 & 0 \\ 0 & k_6 & 0 & -k_6 \\ -k_4 & 0 & k_4+k_5 & -k_5 \\ 0 & -k_6 & -k_5 & k_5+k_6 \end{bmatrix} \begin{bmatrix} Y_{1a} \\ Y_{2a} \\ Y_1 \\ Y_2 \end{bmatrix} = - \begin{bmatrix} 0 & 0 & 0 & 0 \\ 0 & 0 & 0 & 0 \\ 0 & 0 & m_3 & 0 \\ 0 & 0 & 0 & m_4 \end{bmatrix} \begin{bmatrix} 1 \\ 1 \\ 1 \\ 1 \end{bmatrix} \ddot{G} - \begin{bmatrix} f_2 \\ f_3 \\ 0 \\ 0 \end{bmatrix} \quad (24)$$

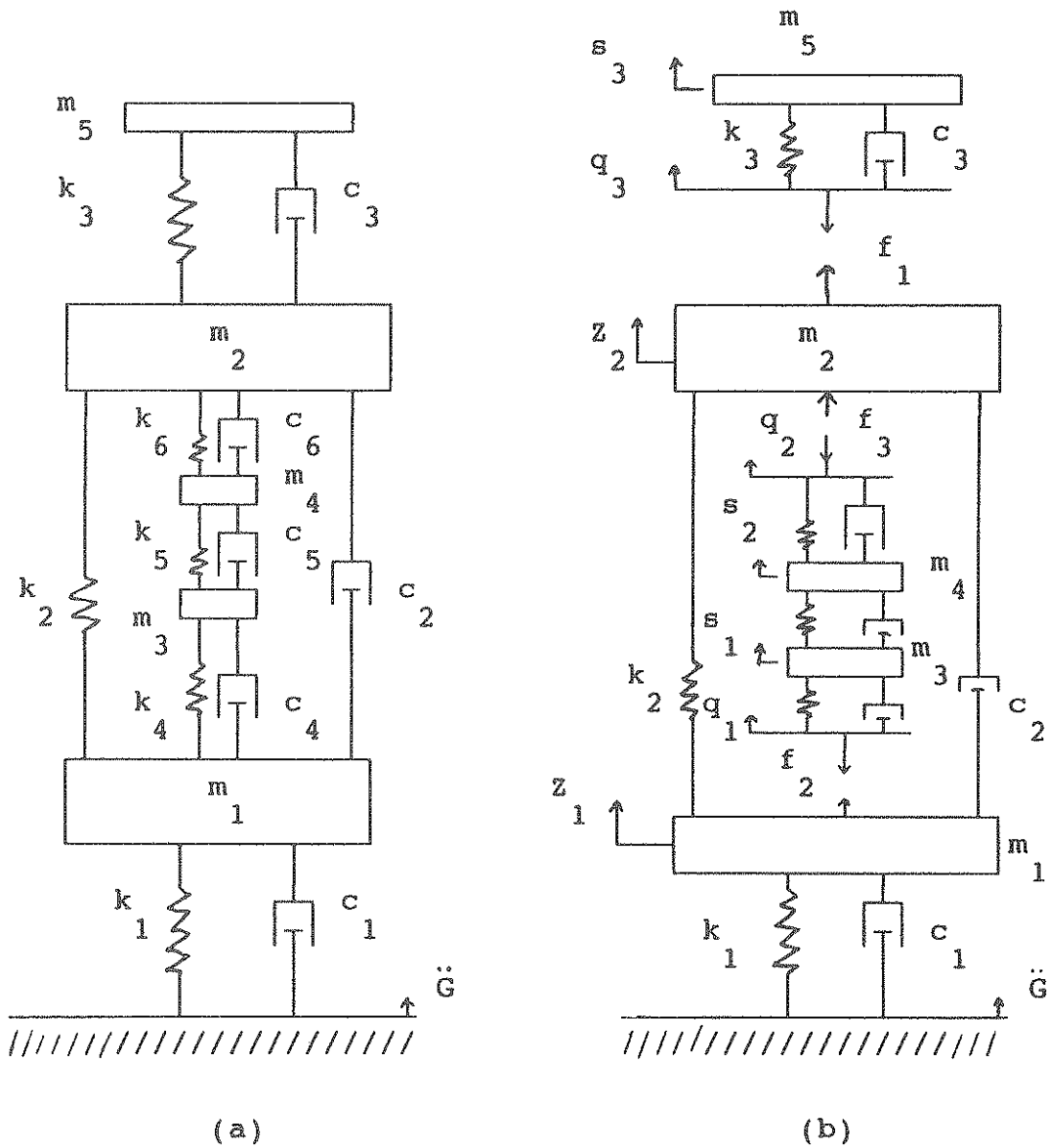


Figure 3. (a) Multiple secondary systems attached to a primary system, (b) separated subsystems



and

$$\begin{aligned} \begin{bmatrix} 0 & 0 \\ 0 & m_5 \end{bmatrix} \begin{bmatrix} \ddot{Y}_{3a} \\ \ddot{Y}_3 \end{bmatrix} + \begin{bmatrix} c_3 & -c_3 \\ -c_3 & c_3 \end{bmatrix} \begin{bmatrix} \dot{Y}_{3a} \\ \dot{Y}_3 \end{bmatrix} + \begin{bmatrix} k_3 & -k_3 \\ -k_3 & k_3 \end{bmatrix} \begin{bmatrix} Y_{3a} \\ Y_3 \end{bmatrix} \\ = - \begin{bmatrix} 0 & 0 \\ 0 & m_5 \end{bmatrix} \begin{bmatrix} 1 \\ 1 \end{bmatrix} \ddot{G} - \begin{bmatrix} f_1 \\ 0 \end{bmatrix} \end{aligned} \quad (25)$$

where

$$\begin{aligned} Y_{1a} &= q_1 - G \\ Y_{2a} &= q_2 - G \\ Y_{3a} &= q_3 - G \\ Y_1 &= s_1 - G \\ Y_2 &= s_2 - G \\ Y_3 &= s_3 - G \end{aligned} \quad (26)$$

By imposing the compatibility condition at the common coordinate for the two secondary systems, ie.,  $Y_{2a} = Y_{3a}$ , and following a procedure similar to that indicated by equation (7), equations (24) and (25) can be combined in the form indicated by equation (4). The result is

$$\begin{aligned}
 & \begin{bmatrix} 0 & 0 & 0 & 0 & 0 \\ 0 & 0 & 0 & 0 & 0 \\ 0 & 0 & m_3 & 0 & 0 \\ 0 & 0 & 0 & m_4 & 0 \\ 0 & 0 & 0 & 0 & m_5 \end{bmatrix} \begin{bmatrix} \ddot{Y}_{1a} \\ \ddot{Y}_{2a} \\ \ddot{Y}_1 \\ \ddot{Y}_2 \\ \ddot{Y}_3 \end{bmatrix} + \begin{bmatrix} c_4 & 0 & -c_4 & 0 & 0 \\ 0 & c_3+c_6 & 0 & -c_6 & -c_3 \\ -c_4 & 0 & c_4+c_5 & -c_5 & 0 \\ 0 & -c_6 & -c_5 & c_5+c_6 & 0 \\ 0 & -c_3 & 0 & 0 & c_3 \end{bmatrix} \begin{bmatrix} \dot{Y}_{1a} \\ \dot{Y}_{2a} \\ \dot{Y}_1 \\ \dot{Y}_2 \\ \dot{Y}_3 \end{bmatrix} \\
 & + \begin{bmatrix} k_4 & 0 & -k_4 & 0 & 0 \\ 0 & k_3+k_6 & 0 & -k_6 & -k_3 \\ -k_4 & 0 & k_4+k_5 & -k_5 & 0 \\ 0 & -k_6 & -k_5 & k_5+k_6 & 0 \\ 0 & -k_3 & 0 & 0 & k_3 \end{bmatrix} \begin{bmatrix} Y_{1a} \\ Y_{2a} \\ Y_1 \\ Y_2 \\ Y_3 \end{bmatrix} \\
 & = - \begin{bmatrix} 0 & 0 & 0 & 0 & 0 \\ 0 & 0 & 0 & 0 & 0 \\ 0 & 0 & m_3 & 0 & 0 \\ 0 & 0 & 0 & m_4 & 0 \\ 0 & 0 & 0 & 0 & m_5 \end{bmatrix} \begin{bmatrix} 1 \\ 1 \\ 1 \\ 1 \\ 1 \end{bmatrix} \ddot{G} - \begin{bmatrix} f_2 \\ f_1+f_3 \\ 0 \\ 0 \\ 0 \end{bmatrix} \quad (27)
 \end{aligned}$$

Comparing equation (27) with equation (5), and equation (22) with equation (2), the following matrices are identified:

$$\begin{aligned}
 m_u &= \begin{bmatrix} m_3 & 0 & 0 \\ 0 & m_4 & 0 \\ 0 & 0 & m_5 \end{bmatrix}, & c_a &= \begin{bmatrix} c_4 & 0 \\ 0 & c_3+c_6 \end{bmatrix}, & c_{au} &= \begin{bmatrix} -c_4 & 0 & 0 \\ 0 & -c_6 & -c_3 \end{bmatrix}, \\
 m_a &= \begin{bmatrix} 0 & 0 \\ 0 & 0 \end{bmatrix}, & c_{ua} &= [c_{au}]^T, & c_u &= \begin{bmatrix} c_4+c_5 & -c_5 & 0 \\ -c_5 & c_5+c_6 & 0 \\ 0 & 0 & c_3 \end{bmatrix}, \\
 k_a &= \begin{bmatrix} k_4 & 0 \\ 0 & k_3+k_6 \end{bmatrix}, & k_{au} &= \begin{bmatrix} -k_4 & 0 & 0 \\ 0 & -k_6 & -k_3 \end{bmatrix}, \\
 k_{ua} &= [k_{au}]^T, & k_u &= \begin{bmatrix} k_4+k_5 & -k_5 & 0 \\ -k_5 & k_5+k_6 & 0 \\ 0 & 0 & k_3 \end{bmatrix}, \\
 M_a &= \begin{bmatrix} m_1 & 0 \\ 0 & m_2 \end{bmatrix}, & C_a &= \begin{bmatrix} c_1+c_2 & -c_2 \\ -c_2 & c_2 \end{bmatrix}, & K_a &= \begin{bmatrix} k_1+k_2 & -k_2 \\ -k_2 & k_2 \end{bmatrix}.
 \end{aligned} \tag{28}$$

The final assembled equations for the combined system can then be written directly from equation (8). The result is

$$\begin{bmatrix} m_1 & 0 & 0 & 0 & 0 \\ 0 & m_2 & 0 & 0 & 0 \\ 0 & 0 & m_3 & 0 & 0 \\ 0 & 0 & 0 & m_4 & 0 \\ 0 & 0 & 0 & 0 & m_5 \end{bmatrix} \begin{bmatrix} \ddot{X}_{a1} \\ \ddot{X}_{a2} \\ \ddot{Y}_1 \\ \ddot{Y}_2 \\ \ddot{Y}_3 \end{bmatrix} + \begin{bmatrix} (c_1+c_2) & -c_2 & -c_4 & 0 & 0 \\ (c_1+c_2+c_4) & (c_2+c_3+c_6) & 0 & -c_6 & -c_3 \\ -c_2 & 0 & c_4+c_5 & -c_5 & 0 \\ -c_4 & 0 & 0 & c_5+c_6 & 0 \\ 0 & -c_6 & -c_5 & 0 & c_3 \\ 0 & -c_3 & 0 & 0 & c_3 \end{bmatrix} \begin{bmatrix} \dot{X}_{a1} \\ \dot{X}_{a2} \\ \dot{Y}_1 \\ \dot{Y}_2 \\ \dot{Y}_3 \end{bmatrix} \\
 + \begin{bmatrix} (k_1+k_2) & -k_2 & -k_4 & 0 & 0 \\ (k_1+k_2+k_4) & (k_2+k_3+k_6) & 0 & -k_6 & -k_3 \\ -k_2 & 0 & k_4+k_5 & -k_5 & 0 \\ -k_4 & 0 & k_4+k_5 & -k_5 & 0 \\ 0 & -k_6 & -k_5 & k_5+k_6 & 0 \\ 0 & -k_3 & 0 & 0 & k_3 \end{bmatrix} \begin{bmatrix} X_{a1} \\ X_{a2} \\ Y_1 \\ Y_2 \\ Y_3 \end{bmatrix} \\
 = - \begin{bmatrix} m_1 & 0 & 0 & 0 & 0 \\ 0 & m_2 & 0 & 0 & 0 \\ 0 & 0 & m_3 & 0 & 0 \\ 0 & 0 & 0 & m_4 & 0 \\ 0 & 0 & 0 & 0 & m_5 \end{bmatrix} \begin{bmatrix} 1 \\ 1 \\ 1 \\ 1 \\ 1 \end{bmatrix} \ddot{r} \quad (29)$$

Equation (29) is exact, similar to equation (21).

### 2.1.3 EXAMPLE 3. BUILDING AND 1-D.O.F EQUIPMENT

The general theory will now be applied to a building equipment system. Figure 4(a) shows the structural model for the combined primary-secondary system. The primary system is an N-story building with an equipment located at some arbitrary floor which we denote as the s-th floor.

The combined system is assumed to be linear. For the primary system, it is further assumed that:

1. the mass of each story unit is concentrated at the floor level,
2. the deformation of the system is characterized by the horizontal translations of individual floors,
3. linear elasticity is provided by massless columns or shear walls between neighboring floors, and
4. linear viscous damping is generated by the relative motion between neighboring floors.

For the secondary system, it is further assumed that:

5. the equipment is a simple linear oscillator with mass  $M_e$ , stiffness,  $K_e$ , and viscous damping coefficient  $C_e$ , and
6. the equipment is firmly attached to its supporting floor.

Referring to figures 4(a-d), the equation of motion for each floor  $j$ , is given by

$$\begin{aligned}
 M_j \ddot{X}_j - C_{j+1} \dot{X}_{j+1} + (C_j + C_{j+1}) \dot{X}_j - C_j \dot{X}_{j-1} - K_{j+1} X_{j+1} \\
 + (K_j + K_{j+1}) X_j - K_j X_{j-1} - U_e \delta_{js} = - M_j \ddot{G} \quad (30)
 \end{aligned}$$

$j=1, \dots, N$

where  $X_j$  denotes the horizontal translation of the  $j$ -th floor, relative to the ground, and  $U_e$  represent the shear force acting on the primary system by the equipment. For dynamic equilibrium at the primary-secondary interface we have

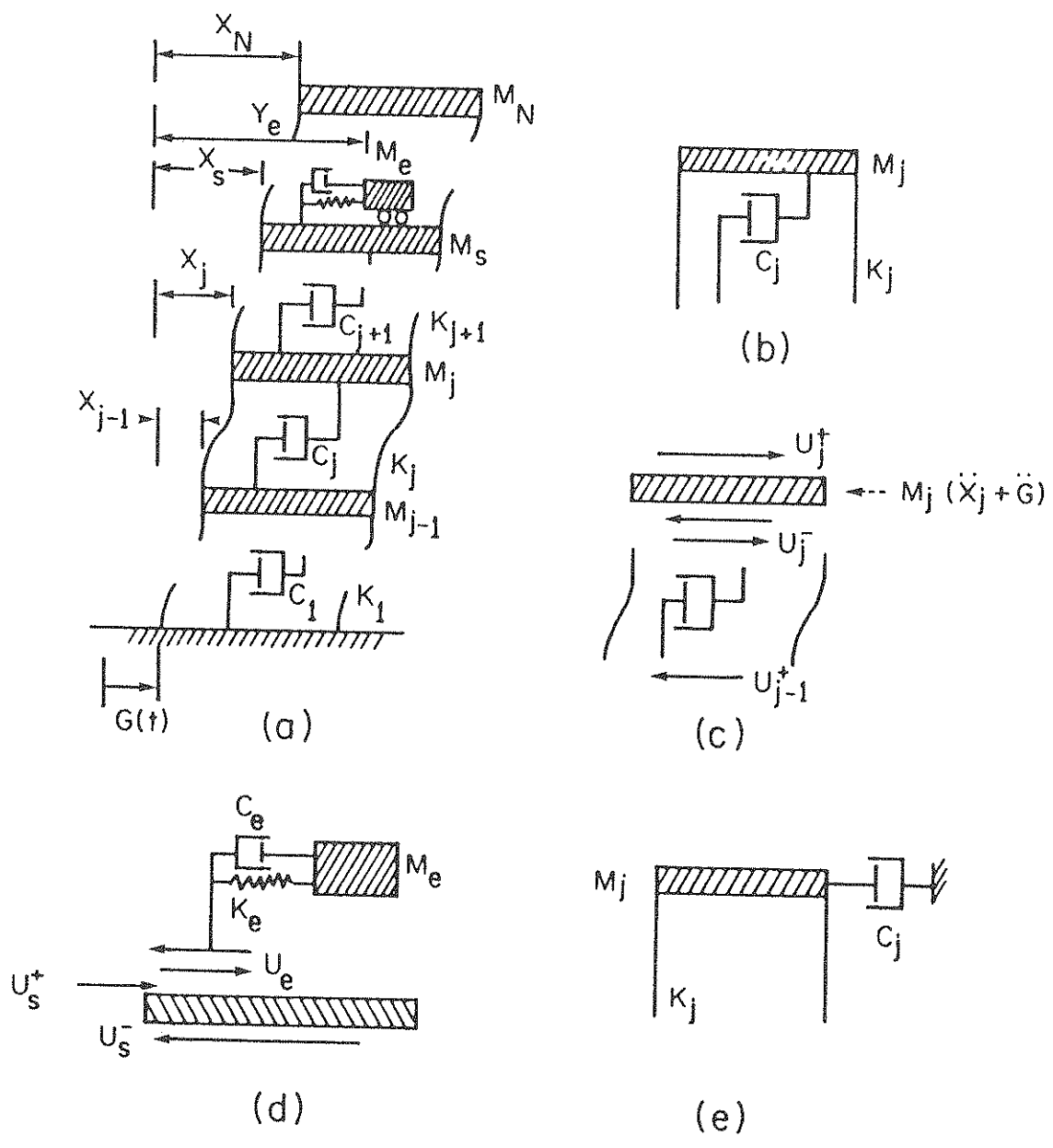


Figure 4. Structural model: (a) N+1 degree-of-freedom combined p-s system, (b) the j-th story unit, (c) forces in the j-th story unit, (d) forces on the s-th floor, (e) alternate model for story unit.

$$-K_e ( Y_e - Z_{N+1} ) - C_e ( \dot{Y}_e - \dot{Z}_{N+1} ) = - U_e \quad (31)$$

where we have denoted the translation at the base of the equipment by  $Z$  and considered it as an additional, the  $N+1$ -st, degree of freedom. For the equipment we have

$$M_e \ddot{Y}_e + C_e ( \dot{Y}_e - \dot{Z}_{N+1} ) + K_e ( Y_e - Z_{N+1} ) = - M_e \ddot{G} \quad (32)$$

For compatibility, we have at the common boundary

$$Z_{N+1} = X_s \quad (33)$$

The above equations can be combined and written in matrix form similar to equation (9). Introduce the approximation

$$\begin{bmatrix} X_1 \\ \vdots \\ X_N \end{bmatrix} = \begin{bmatrix} \varphi_1 & \dots & \varphi_n \end{bmatrix} \begin{bmatrix} q_1 \\ \vdots \\ q_n \end{bmatrix} \quad (34)$$

where  $n < N$ , denote the  $n$  normal modes chosen to approximate the general motion of the primary system, and the  $q$ 's are the corresponding generalized coordinates. From equations (33) and (34), the compatibility condition becomes

$$Z_{N+1} = X_s = \varphi_1(s) q_1 + \dots + \varphi_n(s) q_n \quad (35)$$

The response vector of the combined system is therefore related to the reduced response vector as follows:

$$\begin{bmatrix} X_1 \\ \vdots \\ X_N \\ \hline Z_{N+1} \\ \hline Y_e \end{bmatrix} = \begin{bmatrix} \varphi_1 & \dots & \varphi_n & 0 \\ \vdots & & & \vdots \\ \vdots & & & 0 \\ \hline \varphi_1(s) & \dots & \varphi_n(s) & 0 \\ \hline 0 & \dots & 0 & -I \end{bmatrix} \begin{bmatrix} q_1 \\ \vdots \\ q_n \\ \hline Y_e \end{bmatrix} = [B] \{q\} \quad (36)$$

With matrix [B] defined, the reduced system matrices can be obtained as indicated by equation (14), and any suitable technique used to solve the resulting system of equations.



### 3.0 SOME NUMERICAL RESULTS

Examples 1 and 2 in the preceding section were selected to demonstrate the general procedure of the component-mode synthesis and show that without modal reduction the procedure leads to exact results. In example 3 however, the idea of modal reduction was actually implemented. It remains to be shown how we can preserve the numerical accuracy and, at the same time, simplify the analysis through modal reduction. We shall now present some numerical results obtained for the last example in the preceding section.

For convenience, we assume that each floor of the building is identically constructed. This simplification permits the exact frequency response function of the equipment (as well as the frequency response functions of the building itself at various floors) to be obtained in closed form, using a transfer matrix approach. The details of the exact solution are summarized in the Appendix. The approximate frequency response of the equipment obtained from a modal reduction scheme can then be compared to the exact results.

Numerical calculations were performed for a 20 story building with floor mass  $m = 3.456 \times 10^6$  kg, and interstory stiffness  $K = 3.404 \times 10^9$  N/m. Two different values of damping coefficient  $c = 1.0 \times 10^6$  N/m/s, and  $c = 1.0 \times 10^7$  N/m/s were used to model a lightly damped and a moderately damped building, respectively. The equipment was assumed to have a damping ratio of 0.03.

To investigate the important primary modes that should be included in the analysis, three different cases were considered, in which the equipment was assumed to be perfectly tuned to a low, an intermediate, and a high modal frequency of the building, respectively. Specifically, the second, ninth, and eighteenth modes of the building were selected in the computation. The corresponding natural frequencies and modal damping ratios corresponding to  $c = 1.0 \times 10^6$  N/m/s computed from equations (A-31) and (A-33) in the Appendix, are shown in Table 1. The modal damping ratios corresponding

TABLE 1. NATURAL FREQUENCIES AND DAMPING RATIOS  
OF AN EXAMPLE 20-STORY BUILDING

Mode	Frequency (rad/s.)	Damping ratio ( $c=1 \times 10^6$ N/m/s)
1	2.40418	0.00035
2	7.19844	0.00106
3	11.95046	0.00176
4	16.63235	0.00244
5	21.21662	0.00312
6	25.67640	0.00377
7	29.98550	0.00440
8	34.11862	0.00501
9	38.05153	0.00559
10	41.76113	0.00613
11	45.22567	0.00664
12	48.42479	0.00713
13	51.33975	0.00754
14	53.95342	0.00793
15	56.25048	0.00826
16	58.21743	0.00855
17	59.84274	0.00879
18	61.11687	0.00898
19	62.03234	0.00911
20	62.58378	0.00919

to the higher  $c$  value of  $1 \times 10^7$  N/m/s can be obtained from Table 1 by multiplying the values by ten. The corresponding eigenvectors, calculated from equation (A-39) and normalized with respect to the mass matrix, are given in Table 2. For the purpose of computing the frequency response due to seismic input, the ground excitation was taken as a unit sinusoidal acceleration, and the induced force in the equipment was taken as the output.

Figures 5 through 16 show the results for a moderately heavy equipment (mass ratio  $M_e/M = 0.01$ ) located on the 4-th floor of a lightly damped building. The exact solution, obtained from equation (A-27), is shown in figure 5, which indicates that when the equipment is perfectly tuned to the second building mode, the equipment response is dominated by the first two primary modes. In figure 6 we show the result obtained by keeping only a single primary mode, namely the tuned second mode. This approximate frequency response is obtained as the solution to a 2-d.o.f combined system, rather than solving the full 21-d.o.f coupled system. Comparing figures 6 and 5, it is clear that the approximate equipment response in the neighborhood of the tuned frequency is reproduced almost exactly, whereas the response outside this region is essentially zero.

Next, in figure 7 we compare the exact solution with a cascade solution (see Appendix), i.e., the solution obtained if one uses the motion of the 4-th floor, calculated without including the effect of the equipment, as the input excitation to the equipment. It can be seen that in the neighborhood of the tuned equipment frequency the cascade solution overestimates the equipment response, however, it is quite accurate outside of the tuned region. This suggests that a modified cascade approach might be feasible; namely a combination of the component-mode approach, using only the tuned second primary mode to calculate the response of the secondary system in the vicinity of tuning, and the cascade approach for the solution outside this region. In figure 8 we compare this modified cascade solution with the exact solution. It is difficult to distinguish between the two

TABLE 2. ORTHONORMAL MODES OF AN EXAMPLE 20-STORY BUILDING

Mode Number				
1	2	3	4	5
0.12861E-04	0.38283E-04	0.62807E-04	0.85859E-04	0.10690E-03
0.25648E-04	0.74552E-04	0.11651E-03	0.14760E-03	0.16494E-03
0.38283E-04	0.10690E-03	0.15332E-03	0.16789E-03	0.14760E-03
0.50694E-04	0.13362E-03	0.16789E-03	0.14103E-03	0.62807E-04
0.62807E-04	0.15332E-03	0.15813E-03	0.74552E-04	-.50694E-04
0.74552E-04	0.16494E-03	0.12543E-03	-.12861E-04	-.14103E-03
0.85859E-04	0.16789E-03	0.74552E-04	-.96663E-04	-.16691E-03
0.96663E-04	0.16201E-03	0.12862E-04	-.15332E-03	-.11651E-03
0.10690E-03	0.14760E-03	-.50694E-04	-.16691E-03	-.12861E-04
0.11651E-03	0.12543E-03	-.10690E-03	-.13362E-03	0.96663E-04
0.12543E-03	0.96663E-04	-.14760E-03	-.62807E-04	0.16201E-03
0.13362E-03	0.62807E-04	-.16691E-03	0.25648E-04	0.15332E-03
0.14103E-03	0.25648E-04	-.16201E-03	0.10690E-03	0.74552E-04
0.14760E-03	-.12862E-04	-.13362E-03	0.15813E-03	-.38283E-04
0.15332E-03	-.50694E-04	-.85859E-04	0.16494E-03	-.13362E-03
0.15813E-03	-.85859E-04	-.25648E-04	0.12543E-03	-.16789E-03
0.16201E-03	-.11651E-03	0.38283E-04	0.50694E-04	-.12543E-03
0.16494E-03	-.14103E-03	0.96663E-04	-.38283E-04	-.25648E-04
0.16691E-03	-.15813E-03	0.14103E-03	-.11651E-03	0.85859E-04
0.16789E-03	-.16691E-03	0.16494E-03	-.16201E-03	0.15813E-03

TABLE 2 CONTINUED

Mode Number				
6	7	8	9	10
0.12543E-03	0.14103E-03	0.15332E-03	0.16201E-03	0.16691E-03
0.16691E-03	0.15332E-03	0.12543E-03	0.85859E-04	0.38283E-04
0.96663E-04	0.25648E-04	-.50694E-04	-.11651E-03	-.15813E-03
-.38283E-04	-.12543E-03	-.16691E-03	-.14760E-03	-.74552E-04
-.14760E-03	-.16201E-03	-.85859E-04	0.38283E-04	0.14103E-03
-.15813E-03	-.50694E-04	0.96663E-04	0.16789E-03	0.10690E-03
-.62807E-04	0.10690E-03	0.16494E-03	0.50694E-04	-.11651E-03
0.74552E-04	0.16691E-03	0.38283E-04	-.14103E-03	-.13362E-03
0.16201E-03	0.74552E-04	-.13362E-03	-.12543E-03	0.85859E-04
0.14103E-03	-.85859E-04	-.14760E-03	0.74552E-04	0.15332E-03
0.25648E-04	-.16789E-03	0.12862E-04	0.16494E-03	-.50694E-04
-.10690E-03	-.96663E-04	0.15813E-03	0.12862E-04	-.16494E-03
-.16789E-03	0.62807E-04	0.11651E-03	-.15813E-03	0.12862E-04
-.11651E-03	0.16494E-03	-.62807E-04	-.96663E-04	0.16789E-03
0.12862E-04	0.11651E-03	-.16789E-03	0.10690E-03	0.25648E-04
0.13362E-03	-.38283E-04	-.74552E-04	0.15332E-03	-.16201E-03
0.16494E-03	-.15813E-03	0.10690E-03	-.25648E-04	-.62807E-04
0.85859E-04	-.13362E-03	0.16201E-03	-.16691E-03	0.14760E-03
-.50694E-04	0.12861E-04	0.25648E-04	-.62807E-04	0.96663E-04
-.15332E-03	0.14760E-03	-.14103E-03	0.13362E-03	-.12543E-03

TABLE 2 -CONTINUED

Mode Number

11	12	13	14	15
0.16789E-03	0.16494E-03	0.15813E-03	0.14760E-03	0.13362E-03
-.12861E-04	-.62808E-04	-.10690E-03	-.14103E-03	-.16201E-03
-.16691E-03	-.14103E-03	-.85860E-04	-.12862E-04	0.62807E-04
0.25647E-04	0.11651E-03	0.16494E-03	0.15332E-03	0.85859E-04
0.16494E-03	0.96663E-04	-.25647E-04	-.13362E-03	-.16691E-03
-.38283E-04	-.15332E-03	-.14760E-03	-.25648E-04	0.11651E-03
-.16201E-03	-.38283E-04	0.12543E-03	0.15813E-03	0.25648E-04
0.50694E-04	0.16789E-03	0.62807E-04	-.12543E-03	-.14760E-03
0.15813E-03	-.25648E-04	-.16789E-03	-.38283E-04	0.15332E-03
-.62807E-04	-.15813E-03	0.50694E-04	0.16201E-03	-.38283E-04
-.15332E-03	0.85859E-04	0.13362E-03	-.11651E-03	-.10690E-03
0.74552E-04	0.12543E-03	-.14103E-03	-.50694E-04	0.16789E-03
0.14760E-03	-.13362E-03	-.38283E-04	0.16494E-03	-.96663E-04
-.85859E-04	-.74552E-04	0.16691E-03	-.10690E-03	-.50694E-04
-.14103E-03	0.16201E-03	-.74552E-04	-.62807E-04	0.15813E-03
0.96663E-04	0.12861E-04	-.11651E-03	0.16691E-03	-.14103E-03
0.13362E-03	-.16691E-03	0.15332E-03	-.96663E-04	0.12861E-04
-.10690E-03	0.50694E-04	0.12862E-04	-.74552E-04	0.12543E-03
-.12543E-03	0.14760E-03	-.16201E-03	0.16789E-03	-.16494E-03
0.11651E-03	-.10690E-03	0.96663E-04	-.85859E-04	0.74552E-04

TABLE 2 CONTINUED

Mode Number

16	17	18	19	20
0.11651E-03	0.96663E-04	0.74553E-04	0.50694E-04	0.25648E-04
-.16789E-03	-.15813E-03	-.13362E-03	-.96663E-04	-.50694E-04
0.12543E-03	0.16201E-03	0.16494E-03	0.13362E-03	0.74552E-04
-.12862E-04	-.10690E-03	-.16201E-03	-.15813E-03	-.96663E-04
-.10690E-03	0.12862E-04	0.12543E-03	0.16789E-03	0.11651E-03
0.16691E-03	0.85859E-04	-.62807E-04	-.16201E-03	-.13362E-03
-.13362E-03	-.15332E-03	-.12862E-04	0.14103E-03	0.14760E-03
0.25648E-04	0.16494E-03	0.85860E-04	-.10690E-03	-.15813E-03
0.96663E-04	-.11651E-03	-.14103E-03	0.62807E-04	0.16494E-03
-.16494E-03	0.25648E-04	0.16691E-03	-.12861E-04	-.16789E-03
0.14103E-03	0.74552E-04	-.15813E-03	-.38283E-04	0.16691E-03
-.38283E-04	-.14760E-03	0.11651E-03	0.85859E-04	-.16201E-03
-.85859E-04	0.16691E-03	-.50694E-04	-.12543E-03	0.15332E-03
0.16201E-03	-.12543E-03	-.25648E-04	0.15332E-03	-.14103E-03
-.14760E-03	0.38283E-04	0.96663E-04	-.16691E-03	0.12543E-03
0.50694E-04	0.62807E-04	-.14760E-03	0.16494E-03	-.10690E-03
0.74552E-04	-.14103E-03	0.16789E-03	-.14760E-03	0.85859E-04
-.15813E-03	0.16789E-03	-.15332E-03	0.11651E-03	-.62807E-04
0.15332E-03	-.13362E-03	0.10690E-03	-.74552E-04	0.38283E-04
-.62807E-04	0.50694E-04	-.38283E-04	0.25648E-04	-.12862E-04

solutions. When the equipment is tuned to a low primary mode, such as the present case, a component-mode approach which utilizes all the lower modes as well as the tuned mode and possibly the next higher primary mode, may be just as efficient. In figure 9, for example, we show the component-mode approximation using the first three primary modes.

In figures 10 through 14, we show corresponding results when the equipment is tuned to the ninth building mode. It is clear from figure 10 that not only the tuned primary mode, or modes in the neighborhood of tuning, contribute to the response, but all the lower modes contribute as well. In figure 11 we show the approximate results obtained by keeping only the tuned (the ninth) primary mode. This one mode approximation for the primary system is accurate (note the change in scale between figures 10 and 11) only in the vicinity of tuning, but is incapable of capturing the significant contributions from the lower primary modes. In figure 12 we see once again that the cascade solution is reasonably accurate away from the tuned region, but it grossly overestimates the response in the neighborhood of tuning and slightly overestimates the response in the vicinity of the second primary mode frequency. The modified cascade solution, obtained from superimposing these two solutions, are once again compared with the exact solution in figure 13. It can be seen that the modified cascade solution is reasonably accurate both near and away from the tuning region. Increased accuracy may be obtained by using the first two primary modes as well as the ninth primary mode in the component-mode approximation. The modified cascade solution for this case is shown in figure 14, where we use the three-primary-mode approximation in the vicinity of the three selected primary modes, and the cascade solution everywhere else.

For the equipment tuned to a high (the 18-th) building mode, we compare in figure 15 the exact result with the modified cascade approximation obtained by keeping only the tuned primary mode in the component-mode synthesis. Again, all the primary modes lower than the tuned mode contribute sig-



nificantly to the equipment response. It can also be seen that the peaks corresponding to the higher primary modes ( starting with about mode 15 ) appear to coalesce indicating a higher degree of modal interaction. This may be attributed to two different factors. Firstly, the higher natural frequencies of the primary system are closer to each other as can be seen from equation (A-31). Secondly, the modal damping ratios are higher for the higher modes, as seen from equation (A-33).

The error represented by the difference between the dotted and solid lines in the higher frequency region can be reduced by including the first primary mode in addition to the tuned eighteenth primary mode in the component-mode approximation. This is shown in figure 16.

### 3.1 EFFECT OF EQUIPMENT MASS

Next, it was of interest to investigate the effect of the equipment mass on the preceding results. In figures 17 through 19 we show the results obtained for a light equipment ( mass ratio = 0.001 ). For brevity, we only show the comparison between the modified cascade solutions and the exact solutions. In these figures only the single tuned primary mode was used in the approximate analysis since it was found to yield sufficiently accurate results.

Comparing figures 8 and 17, it can be seen that as the equipment mass decreases, the magnitude of the response (the interacting force at the interface between the primary and secondary system) is reduced. The response is still dominated by the tuned (second) mode, and the response at the first mode is still greater than the third mode in both cases, but the ratios between the dominant peak at the second primary mode frequency and its neighboring peaks are different in figures 8 and 17. A comparison between figures 13 and 18 for the equipment tuned to the ninth mode, and figures 15 and 19 for the equipment tuned to the eighteenth mode, indicate these same trends.

### 3.2 EFFECT OF DAMPING IN BUILDING

To investigate the effect of damping in the building, which is perhaps the least known parameter in actual structures, we increase the modal damping ratios by a factor of ten in all the modes. This is easily done by increasing the value of  $c$ , the damping constant for each story of the building by ten. The resulting damping ratios (ten times the values listed in Table 1) might be more indicative of a moderately damped structure. The results, for a mass ratio of 0.01, are shown in figures 20 through 26.

Comparing figures 8 and 20, it can be seen that the force transmitted to the equipment at its support is reduced as the damping in the supporting structure is increased. The shape of the response curve is not radically changed because the damping in the second mode is still relatively light ( see Table 1 ). By comparing figures 14 and 21, however, it can be seen that when the equipment is tuned to the ninth building mode, the increased modal damping of the structure radically changes the shape of the equipment response curve. The highest peak shifts from the second primary mode frequency to the first primary mode frequency. Greater modal interaction as well as greater error from the one primary-mode approximation in a modified cascade approach is also evident from figure 21. As before, improved accuracy can be obtained by including a number of lower modes in the analysis. In figure 22, for example, we show the improvement obtained by including the first primary mode in addition to the tuned primary mode. The equipment response at the higher frequencies is diminished by the increased damping of the higher modes. This is true even when the equipment is tuned to the eighteenth mode. In figure 23 we show the comparison between the modified cascade solution, obtained by using the single tuned primary mode only, and the exact solution. In figure 24 we show the improvement obtained by including the first primary mode. The error is still large. Acceptable results are obtained by including the first three primary modes in addition to the tuned mode, as shown in figure 25. In figure 26 we show the corresponding results obtained by

using primary modes thirteen through twenty. It is interesting to note that the solution is not as accurate as the results obtained in figure 25. This comparison, together with additional calculations, indicate that an optimum selection for the primary modes should include the tuned primary mode and if necessary, the lower primary modes. In figures 27 through 29 we show the corresponding results for a light equipment (mass ratio = 0.001). Comparison of these figures with figures 20, 22, and 25, reveals that the response is lower with the lighter equipment but the shape of the response curves are not significantly changed.

### 3.3 EFFECT OF EQUIPMENT LOCATION

To investigate the effect of equipment location, calculations were repeated for an equipment located on the 17-th floor of the building. In the following figures it is even more difficult to distinguish between the exact and the approximate solutions. In figures 30 through 32, we show the corresponding results for a moderately heavy equipment on a lightly damped building. Comparison of these figures with figures 8, 12, and 15 reveals that the response curves are substantially different. The peak equipment response shifts from the second primary-mode frequency to the first, and the participation of the higher modes are reduced.

In figures 33 through 35 we show the corresponding results for a light equipment. The trend is the same as that observed previously. That is, the forces are reduced, and the peak at the first primary mode frequency is the highest, except when the equipment is tuned to a low primary mode (figure 33).

In figures 36 through 38, we repeat the calculations for a moderately heavy equipment placed on the 17-th floor of a moderately damped structure. Again, not only are the response curves very different, but their magnitudes are insignificant at higher primary-mode frequencies compared

with the corresponding results obtained for the fourth floor equipment location.

In figures 39 through 41, we show the corresponding results for a light equipment. Whereas the forces are diminished as before, the shape of the curves for the equipment tuned to the second primary mode is different.

Specifically, the response at the second mode frequency is greater than that at the first mode frequency.

### 3.4 THE DETUNED CASE

Finally, we consider a case where the equipment is not tuned to any mode of the building. Specifically, we consider a moderately heavy equipment located on the fourth floor of a moderately damped building. The natural frequency of the equipment is chosen to lie mid-way between the first and second modes of the building. The component-mode approximation was calculated by using the first two primary modes. The result is shown in figure 42, which is indistinguishable from the exact solution. It is clear that the modified cascade approach can be applied to both the tuned and detuned cases, and for any equipment frequency. However, when the equipment frequency is low, the large reduction in the size of the matrices make the component-mode approach especially attractive.

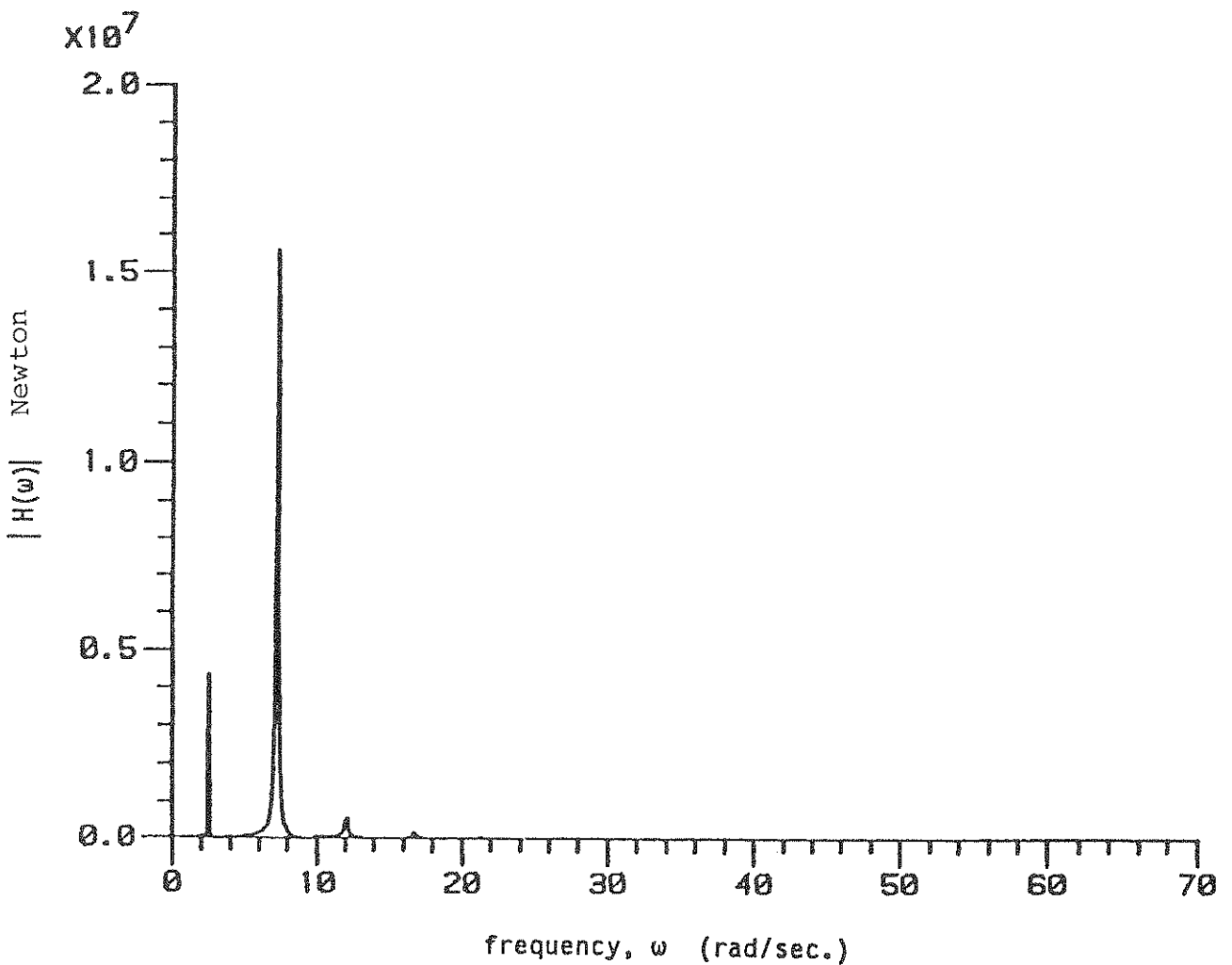


Figure 5. Modulus of frequency response function for interactive force at the equipment-building interface: exact solution. Equipment on 4-th floor tuned to second mode of building. (mass ratio = 0.01,  $c = 1.0 \times 10^6$  N/m/s).

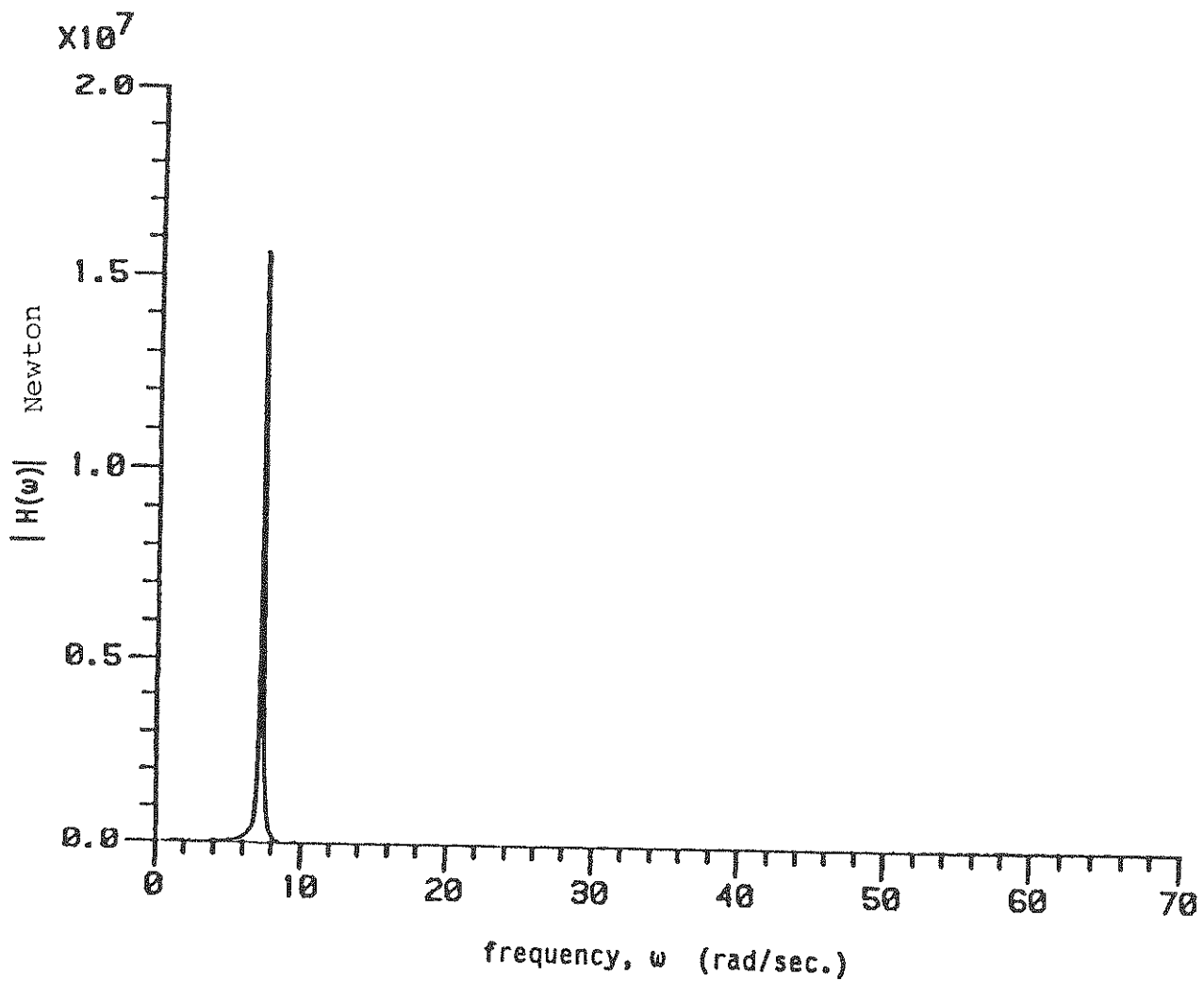


Figure 6. Modulus of frequency response function for interactive force acting at the equipment-building interface: single tuned primary mode approximation. Equipment on 4-th floor tuned to second mode of building. ( Mass ratio = 0.01,  $c = 1.0 \times 10^6$  N/m/s).

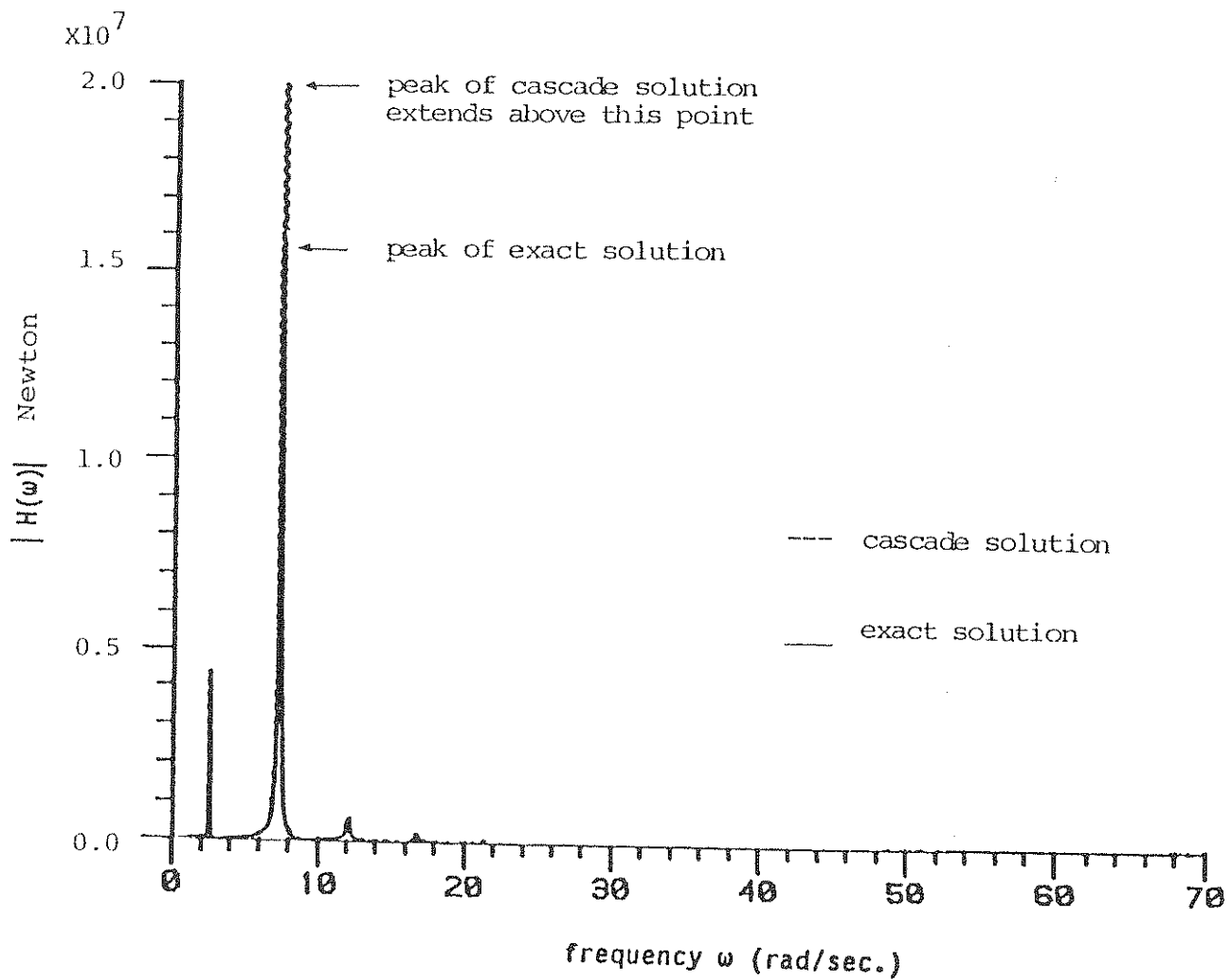


Figure 7. Modulus of frequency response function for interactive force acting at the equipment-building interface: cascade .vs. exact solutions. Equipment on 4-th floor tuned to second mode of building. ( Mass ratio = 0.01,  $c = 1.0 \times 10^6$  N/m/s).

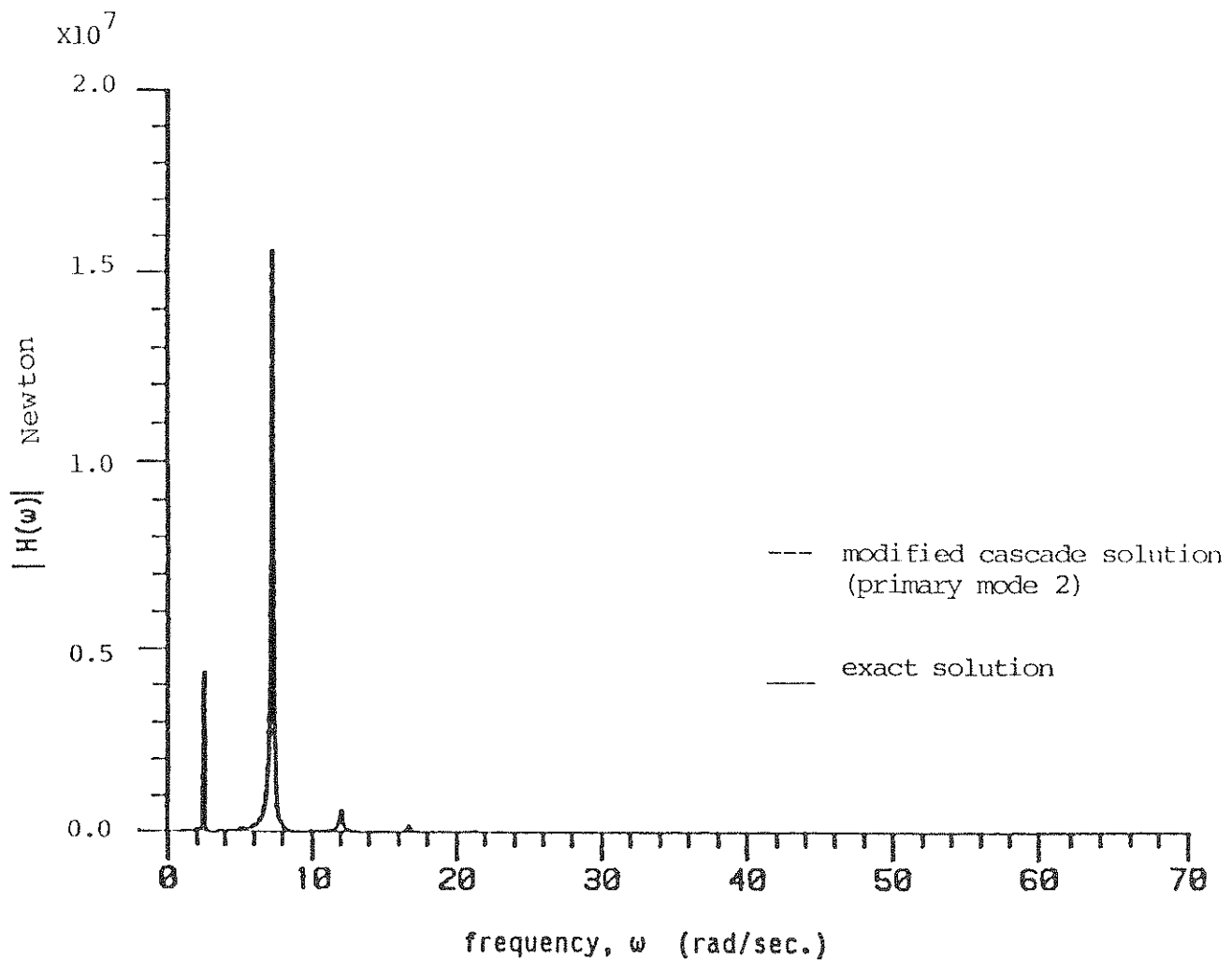


Figure 8. Modulus of frequency response function for interactive force at the equipment-building interface: modified cascade .vs. exact solutions. Equipment on 4-th floor tuned to second mode of building. ( Mass ratio = 0.01,  $c = 1.0 \times 10^6$  N/m/s).



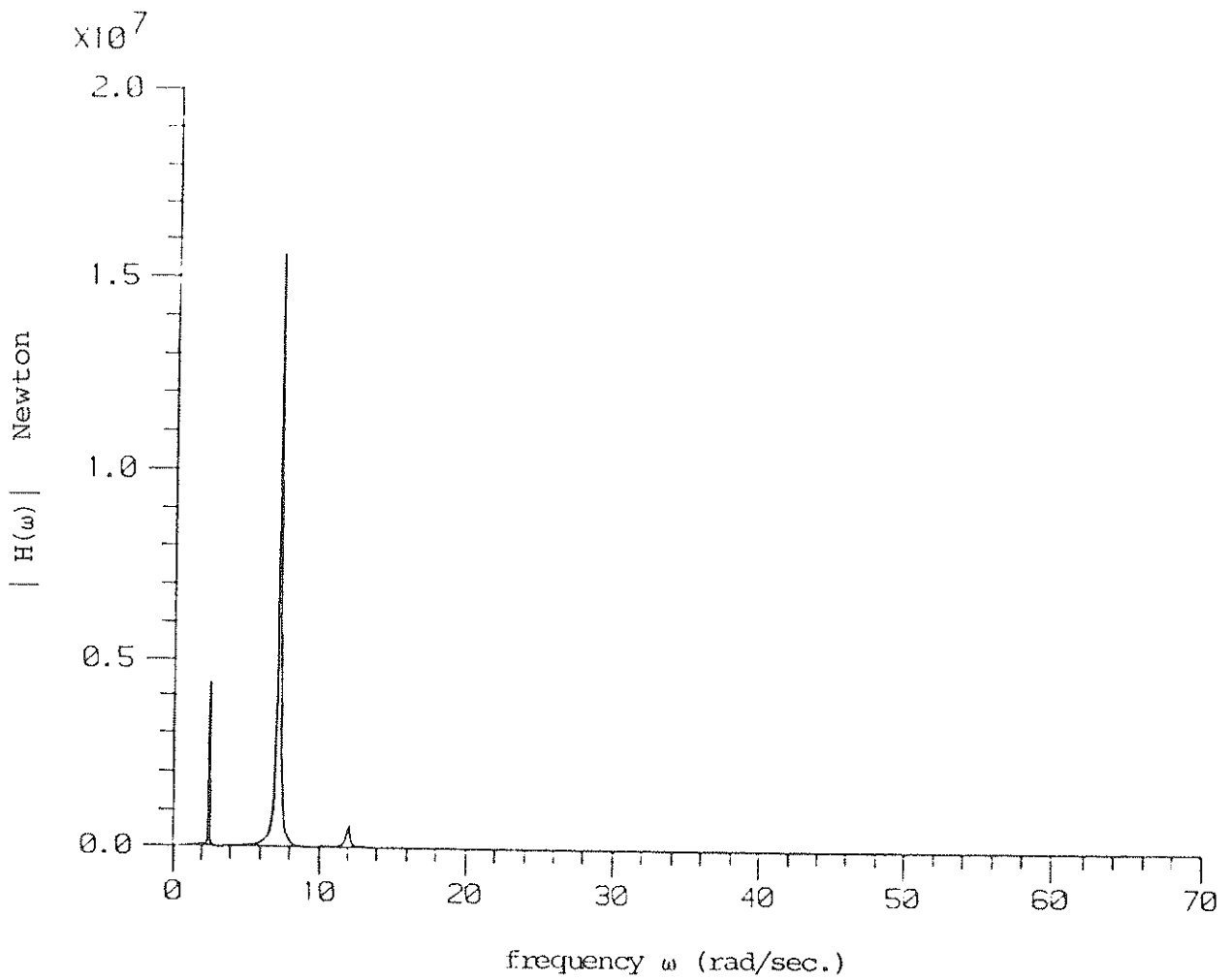


Figure 9. Modulus of frequency response function for interactive force acting at the equipment-building interface: component-mode approximation using the first three primary modes. Equipment on 4-th floor tuned to second mode of building. ( Mass ratio = 0.01,  $c = 1.0 \times 10^6$  N/m/s).

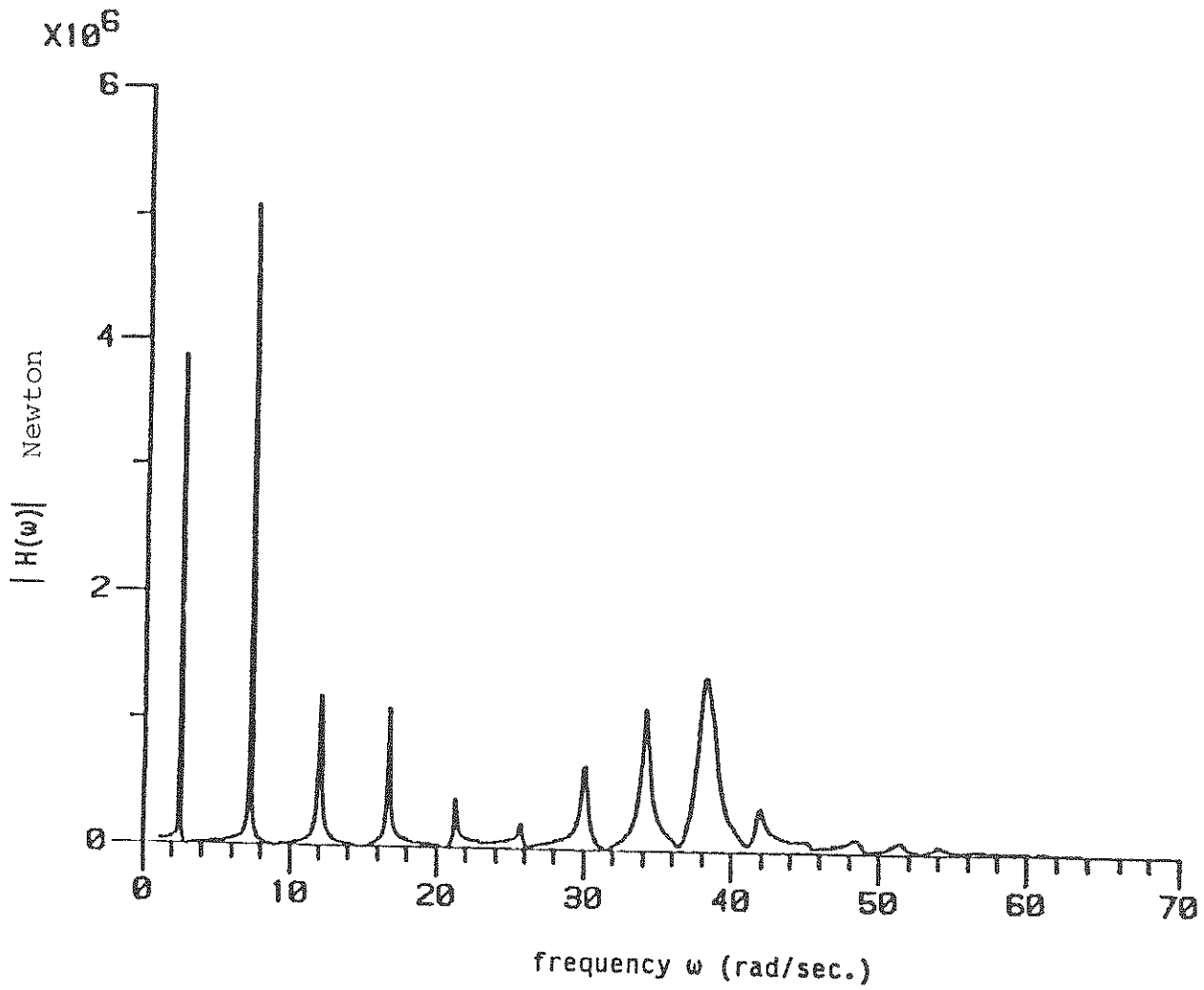


Figure 10. Modulus of frequency response function for interactive force acting at the equipment-building interface: exact solution. Equipment on 4-th floor tuned to ninth mode of building. ( Mass ratio = 0.01,  $c = 1.0 \times 10^6$  N/m/s).

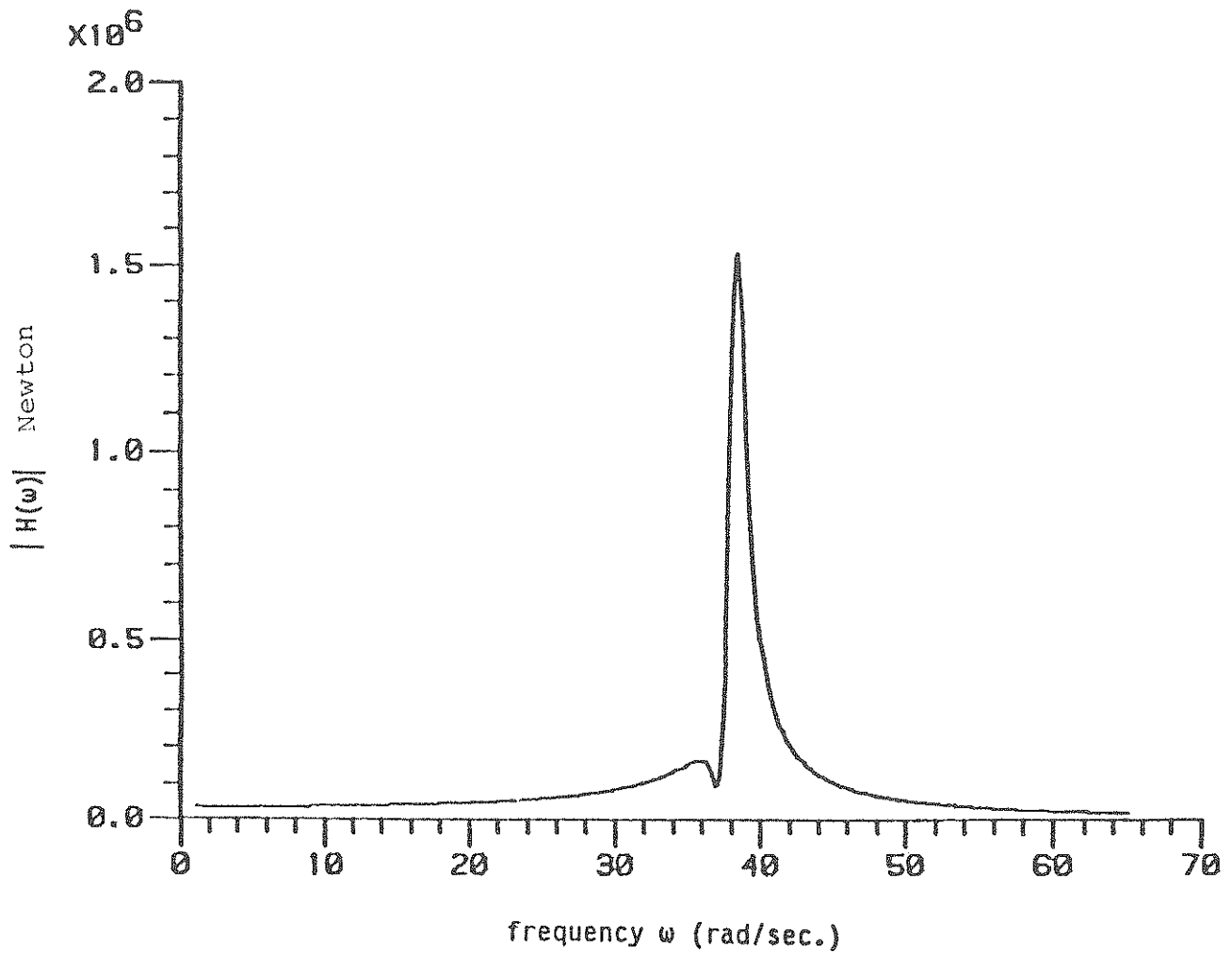


Figure 11. Modulus of frequency response function for interactive force acting at the equipment-building interface: single tuned primary mode approximation. Equipment on 4-th floor tuned to ninth mode of building. (Mass ratio = 0.01,  $c = 1.0 \times 10^6$  N/m/s).

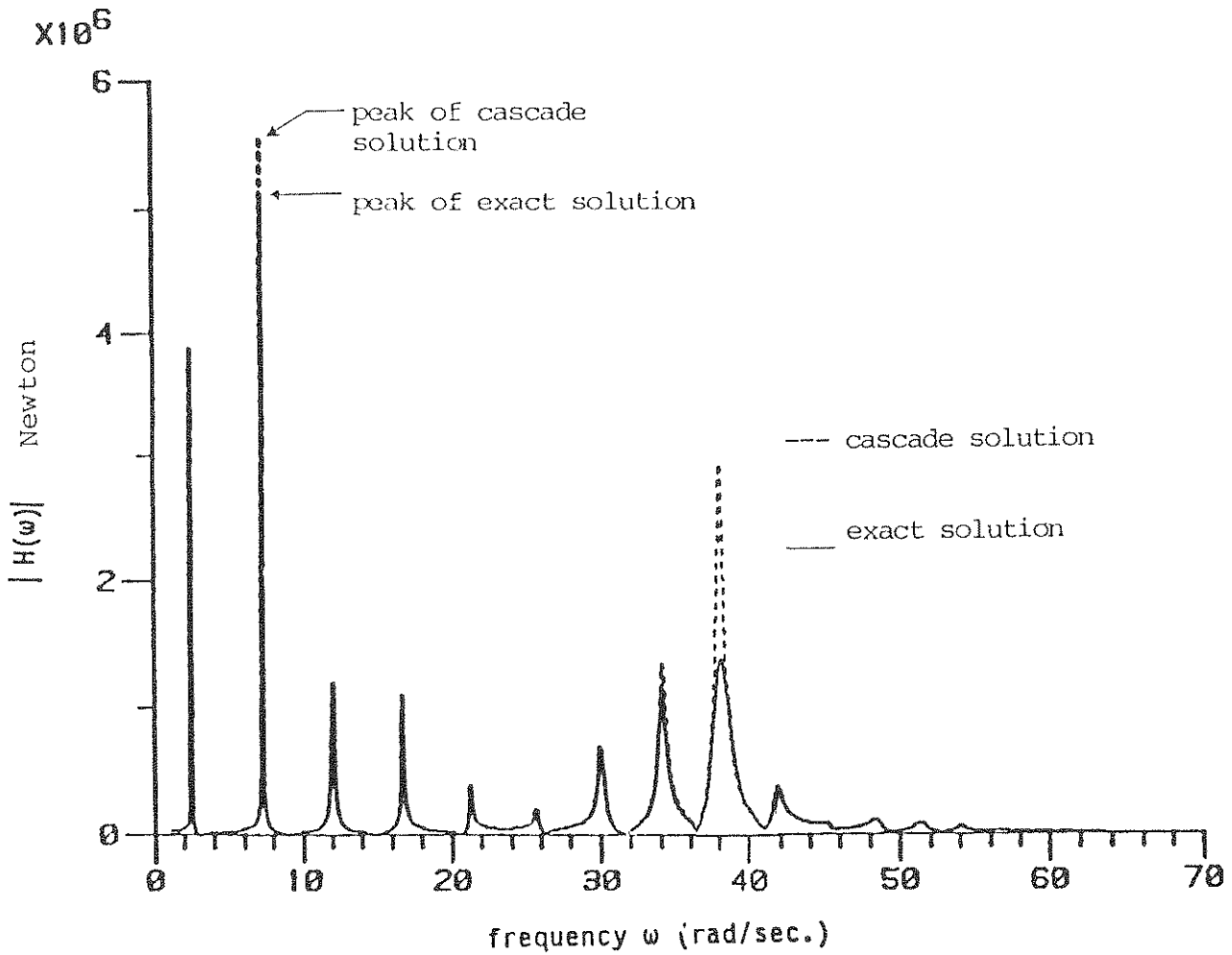


Figure 12. Modulus of frequency response function for interactive force acting at the equipment-building interface: cascade .vs. exact solutions. Equipment on 4-th floor tuned to ninth mode of building. ( Mass ratio = 0.01,  $c = 1.0 \times 10^6$  N/m/s).

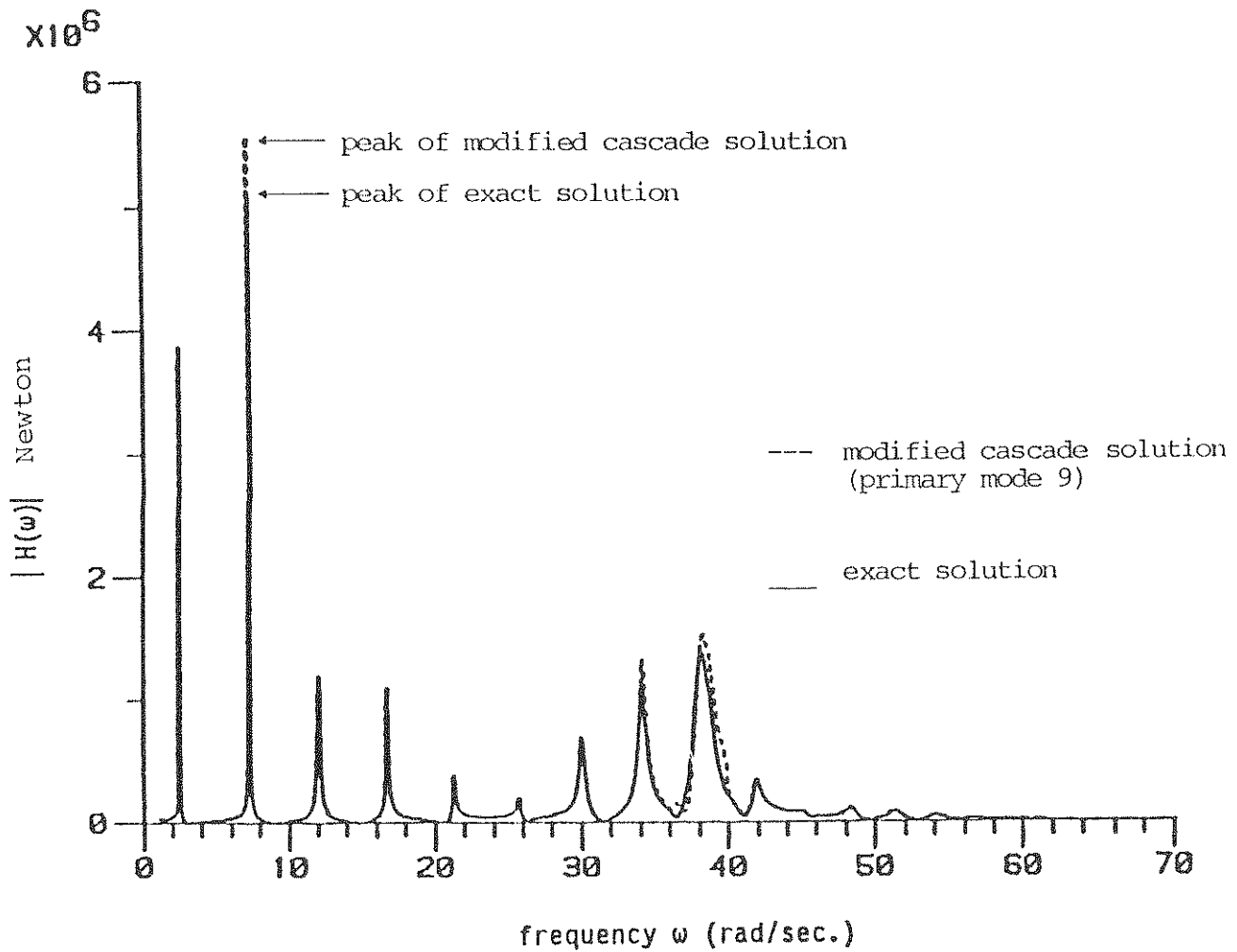


Figure 13. Modulus of frequency response function for interactive force acting at the equipment-building interface: modified cascade .vs. exact solutions. Equipment on 4-th floor tuned to ninth mode of building. ( Mass ratio = 0.01,  $c = 1.0 \times 10^6$  N/m/s).

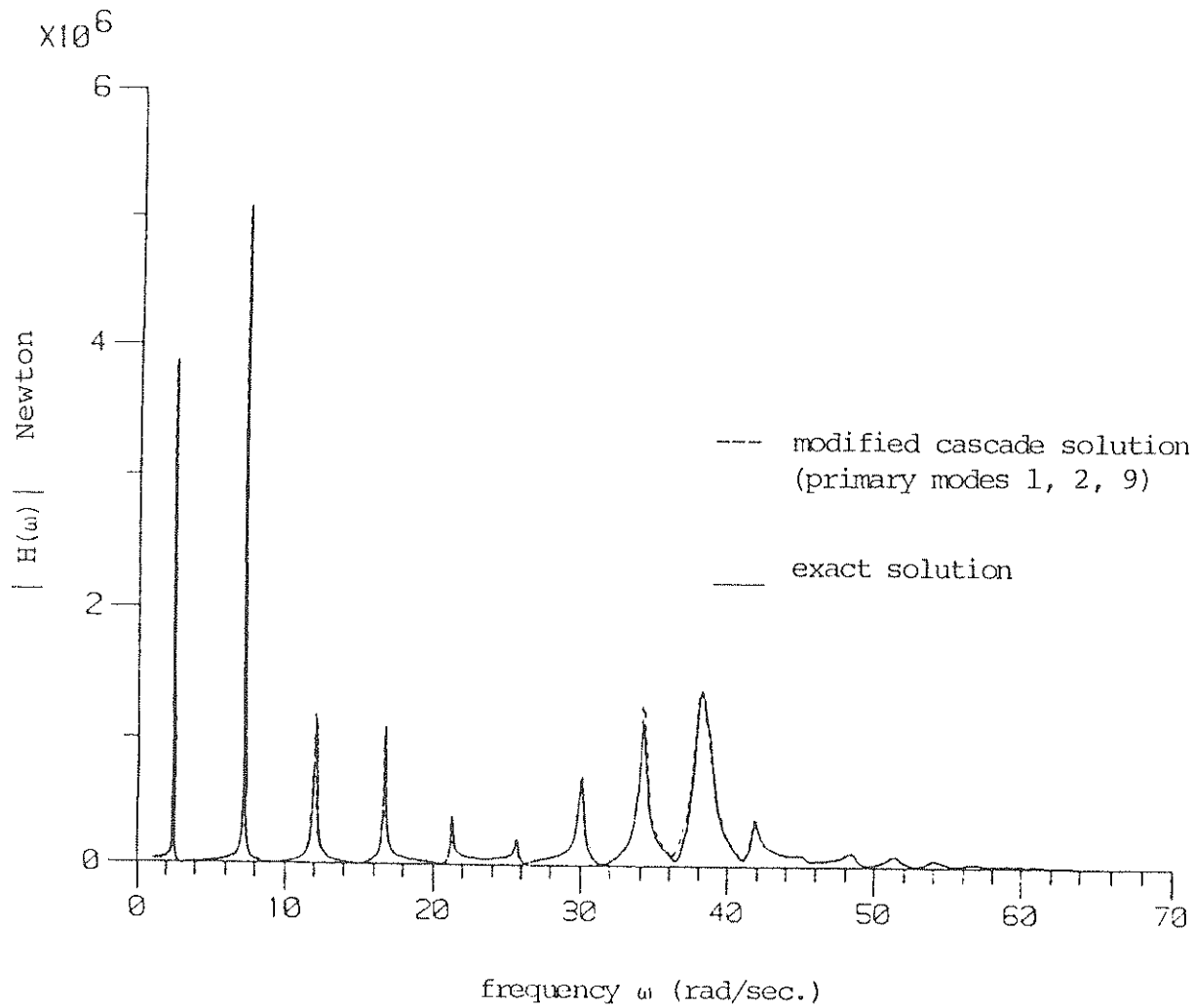


Figure 14. Modulus of frequency response function for interactive force acting at the equipment-building interface: modified cascade .vs. exact solutions. Equipment on 4-th floor tuned to ninth mode of building. ( Mass ratio = 0.01,  $c = 1.0 \times 10^6$  N/m/s).

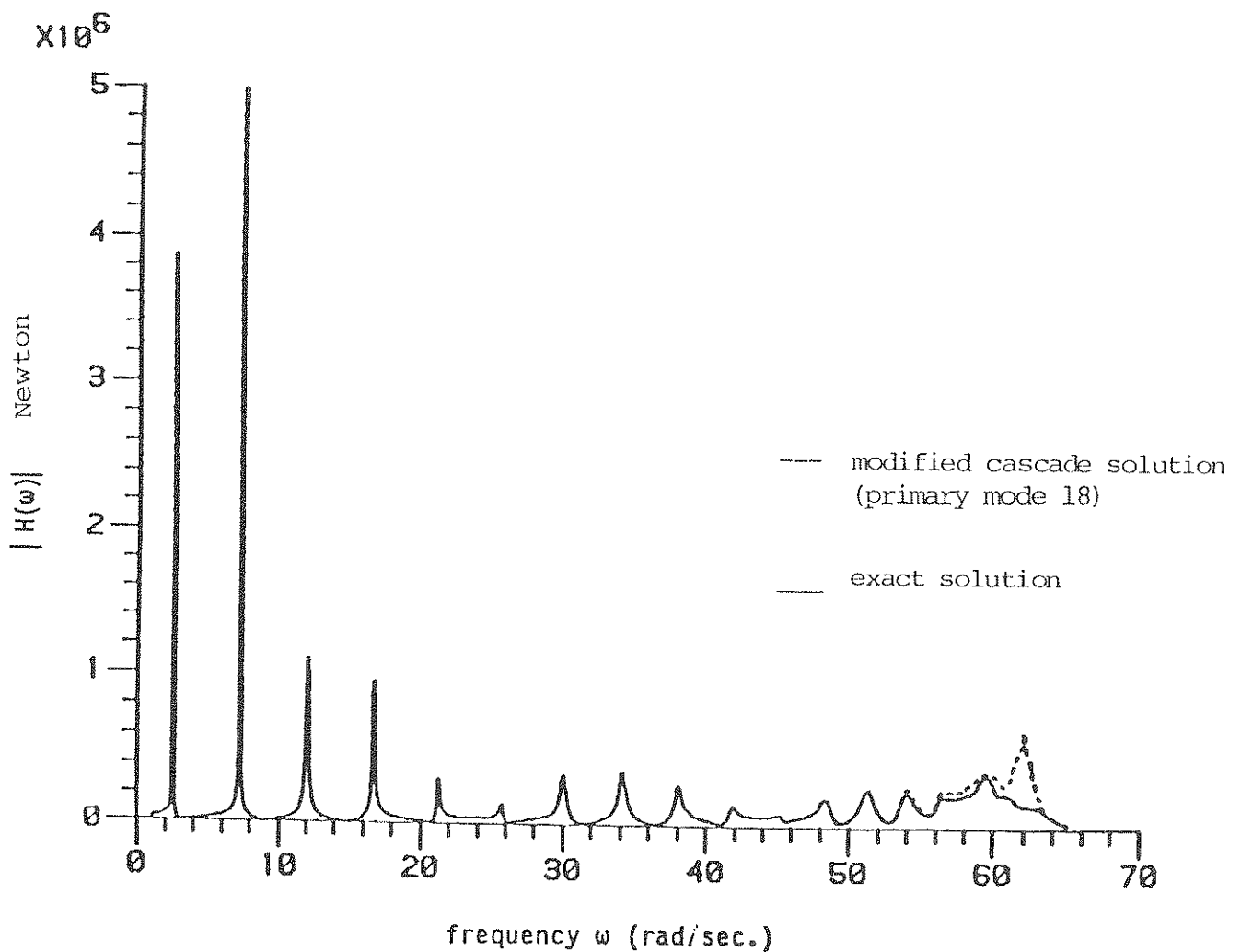


Figure 15. Modulus of frequency response function for interactive force acting at the equipment-building interface: modified cascade .vs. exact solutions. Equipment on 4-th floor tuned to eighteenth mode of building. ( Mass ratio = 0.01,  $c = 1.0 \times 10^6$  N/m/s).

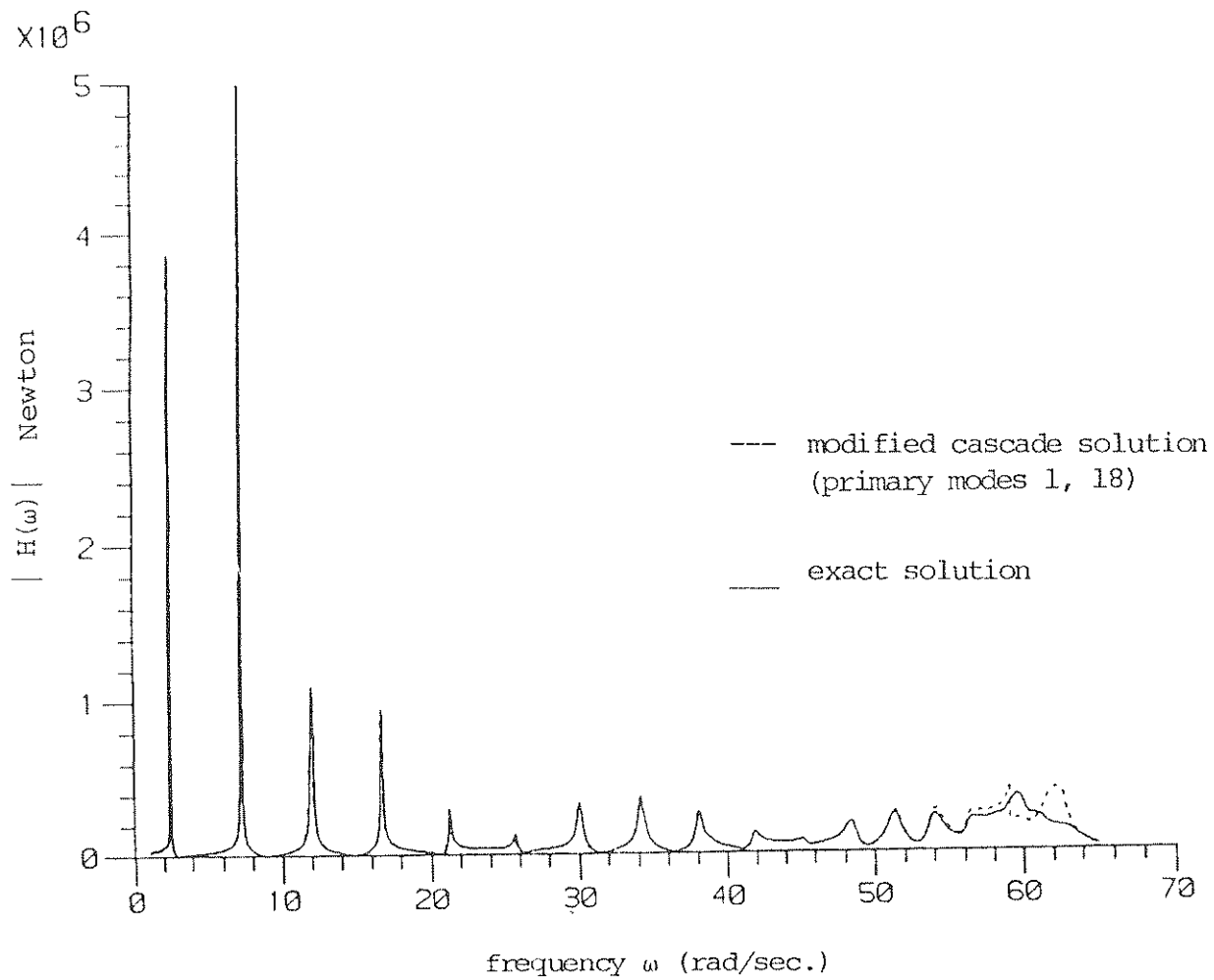


Figure 16. Modulus of frequency response function for interactive force acting at the equipment-building interface: modified cascade .vs. exact solutions. Equipment on 4-th floor tuned to eighteenth mode of building. (Mass ratio = 0.01,  $c = 1.0 \times 10^6$  N/m/s).



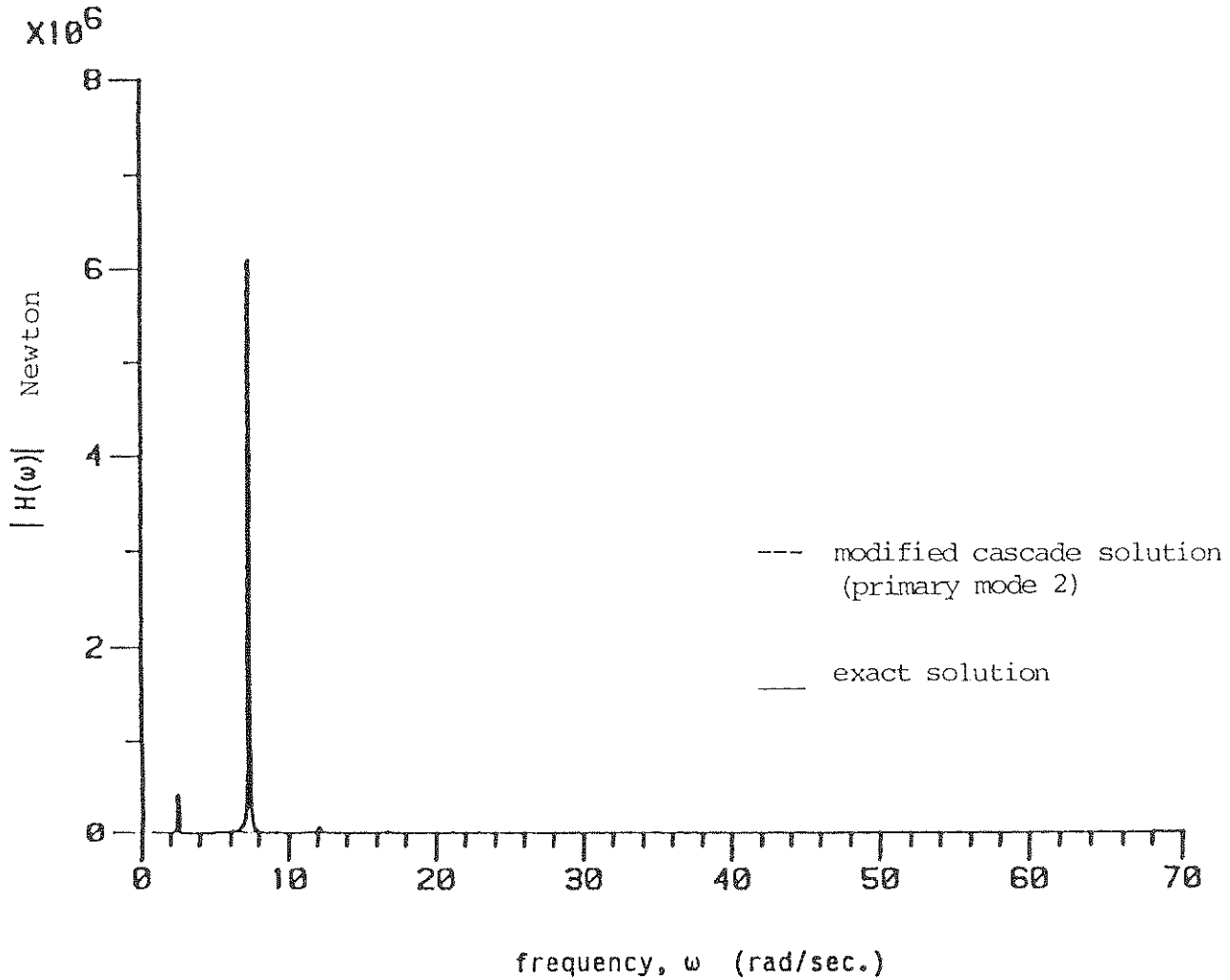


Figure 17. Modulus of frequency response function for interactive force acting at the equipment-building interface: modified cascade .vs. exact solutions. Equipment on 4-th floor tuned to second mode of building. ( Mass ratio = 0.001,  $c = 1.0 \times 10^6$  N/m/s).

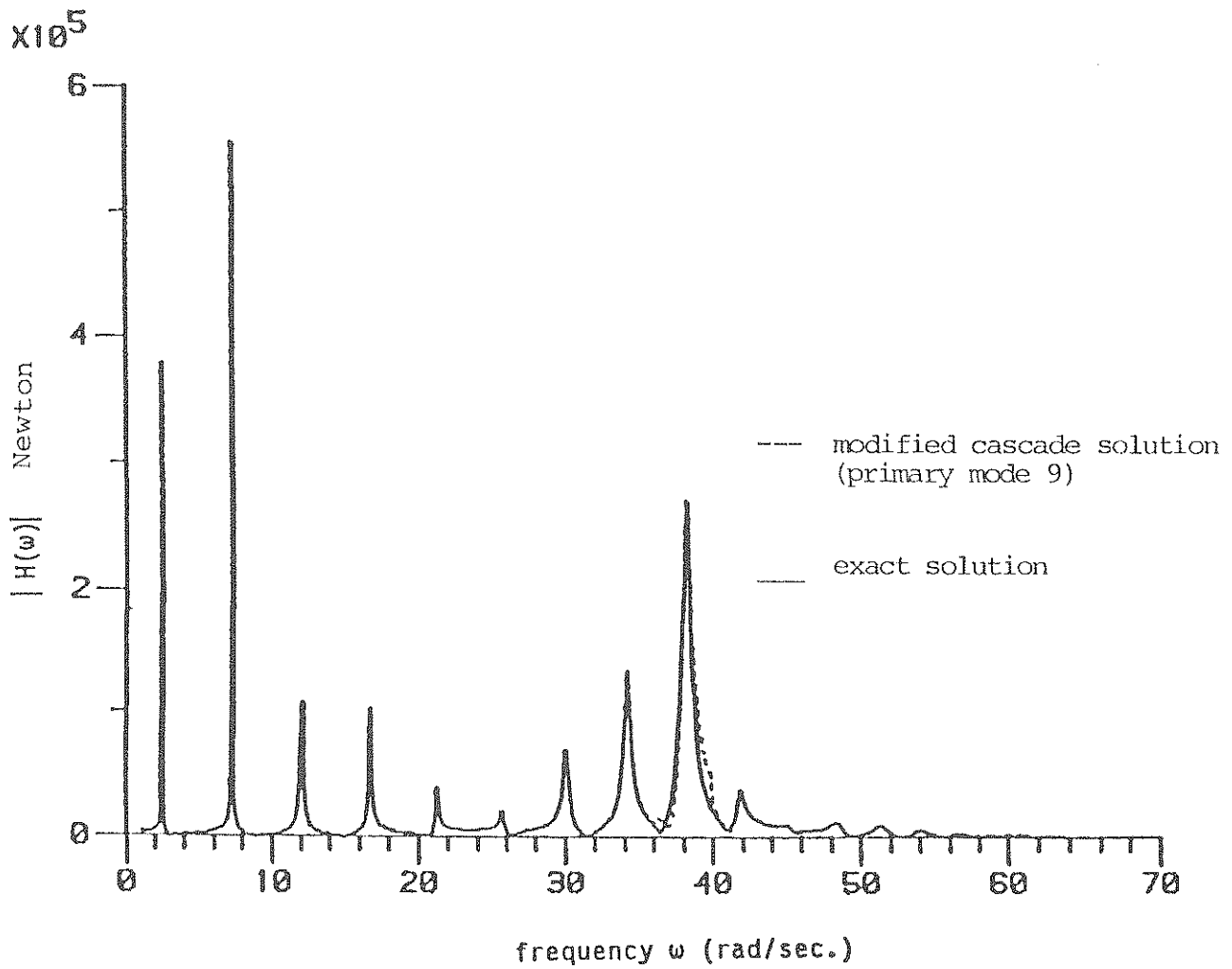


Figure 18. Modulus of frequency response function for interactive force acting at the equipment-building interface: modified cascade .vs. exact solutions. Equipment on 4-th floor tuned to ninth mode of building. ( Mass ratio = 0.001,  $c = 1.0 \times 10^6$  N/m/s).

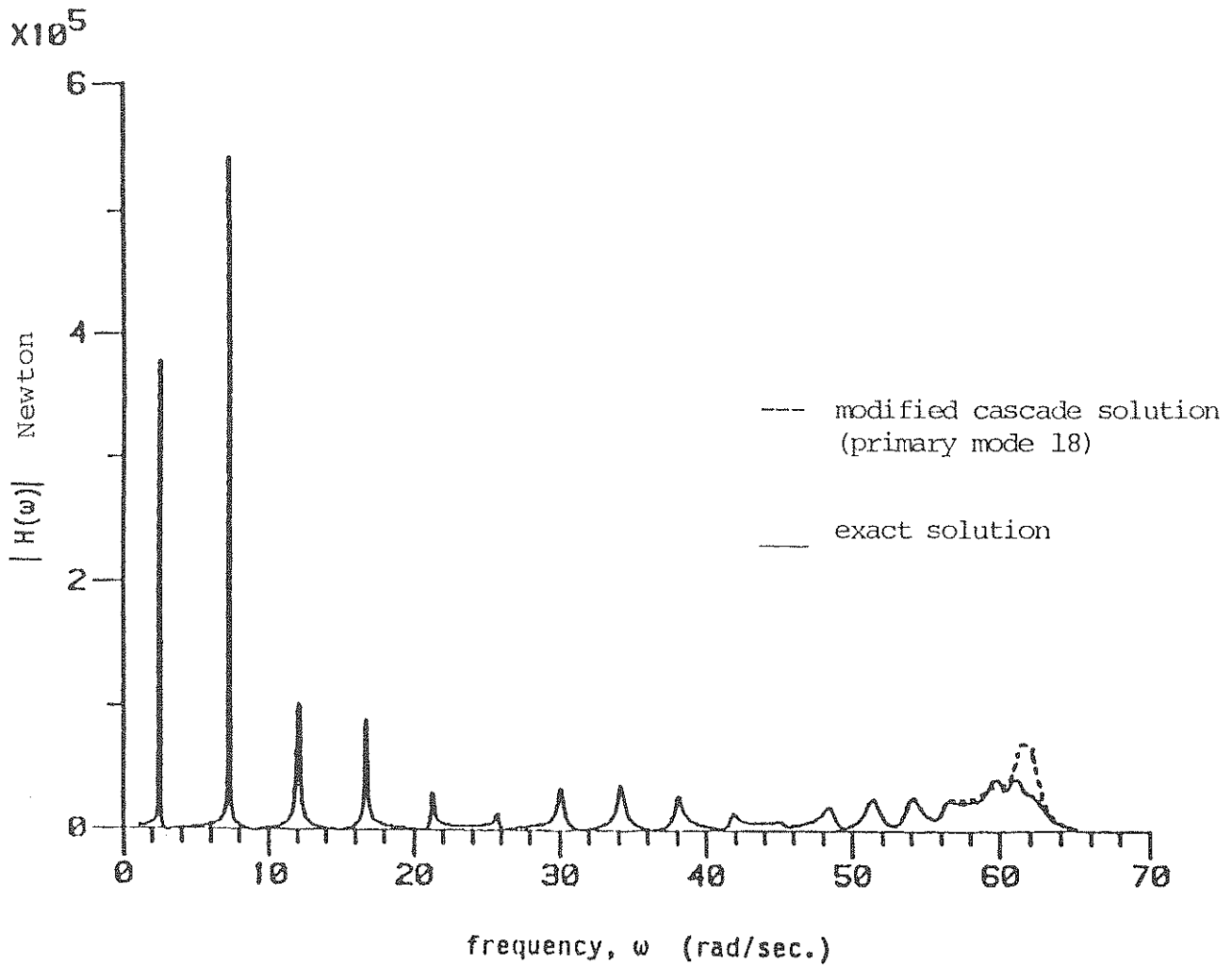


Figure 19. Modulus of frequency response function for interactive force acting at the equipment-building interface: modified cascade .vs. exact solutions. Equipment on 4-th floor tuned to eighteenth mode of building. (Mass ratio = 0.001,  $c = 1.0 \times 10^6$  N/m/s).

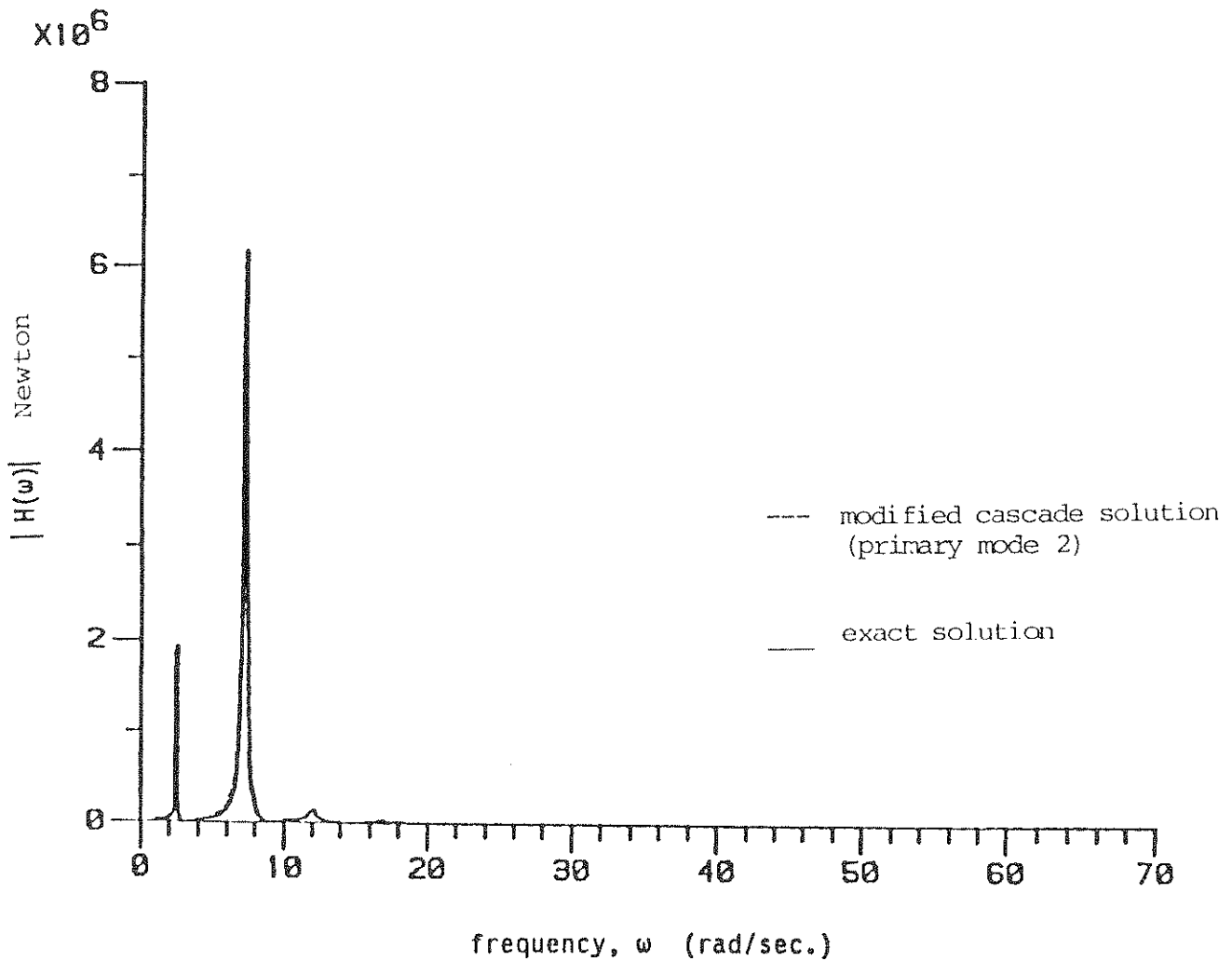


Figure 20. Modulus of frequency response function for interactive force acting at the equipment-building interface: modified cascade .vs. exact solutions. Equipment on 4-th floor tuned to second mode of building. ( Mass ratio = .01,  $c = 1.0 \times 10^7$  N/m/s).

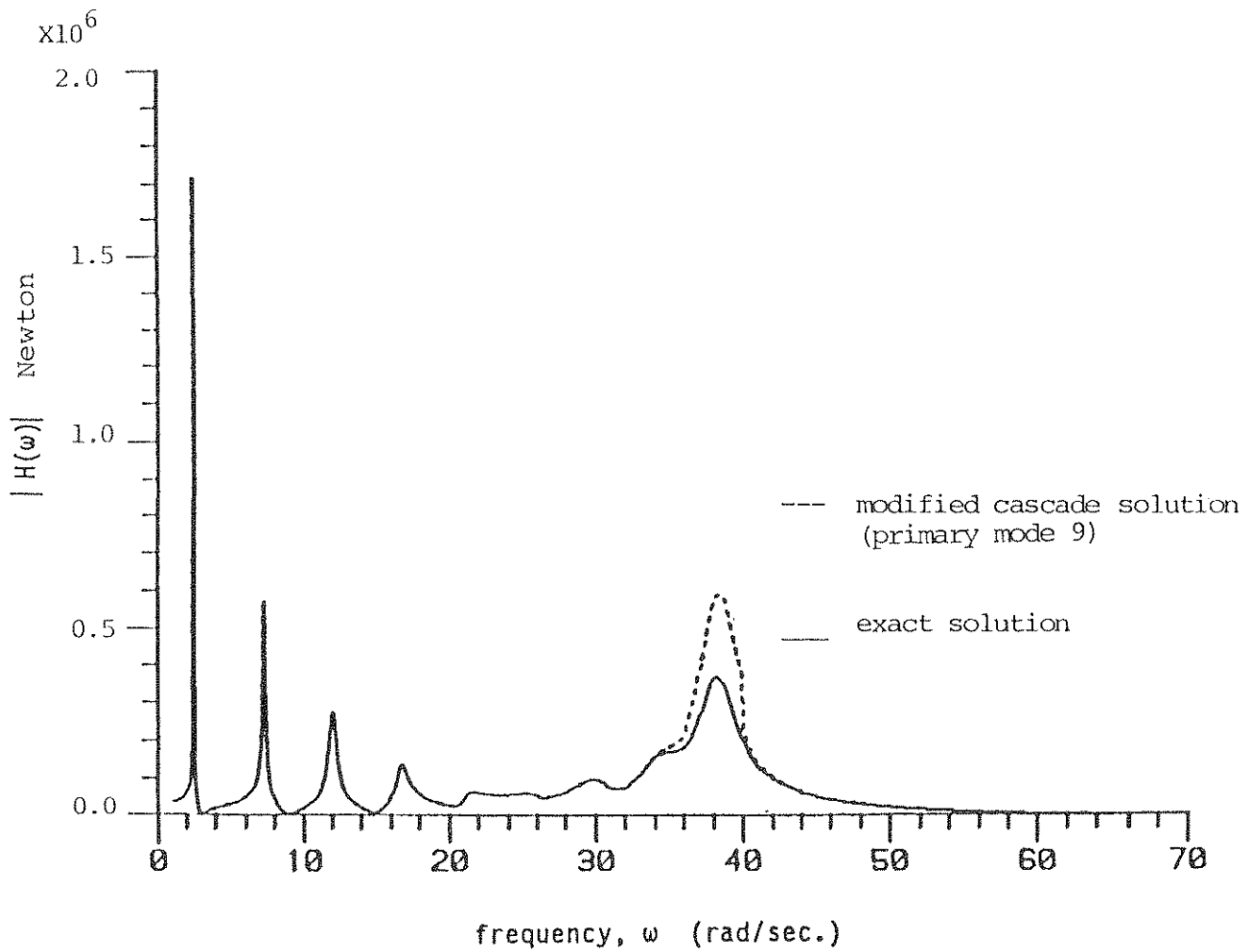


Figure 21. Modulus of frequency response function for interactive force acting at the equipment-building interface: modified cascade .vs. exact solutions. Equipment on 4-th floor tuned to ninth mode of building. ( Mass ratio = .01,  $c = 1.0 \times 10^7$  N/m/s).

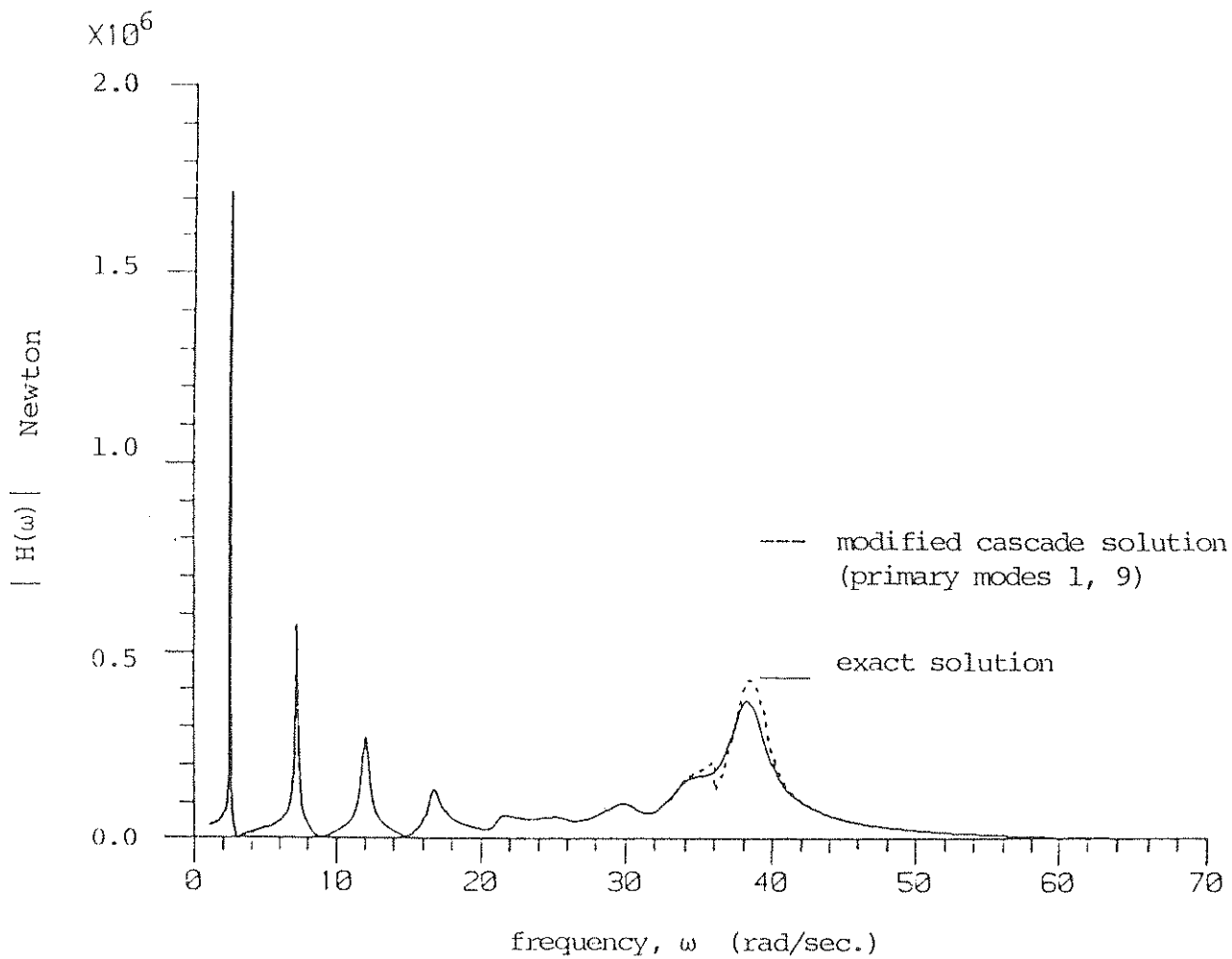


Figure 22. Modulus of frequency response function for interactive force acting at the equipment-building interface: modified cascade .vs. exact solutions. Equipment on 4-th floor tuned to ninth mode of building. ( Mass ratio = .01,  $c = 1.0 \times 10^7$  N/m/s).

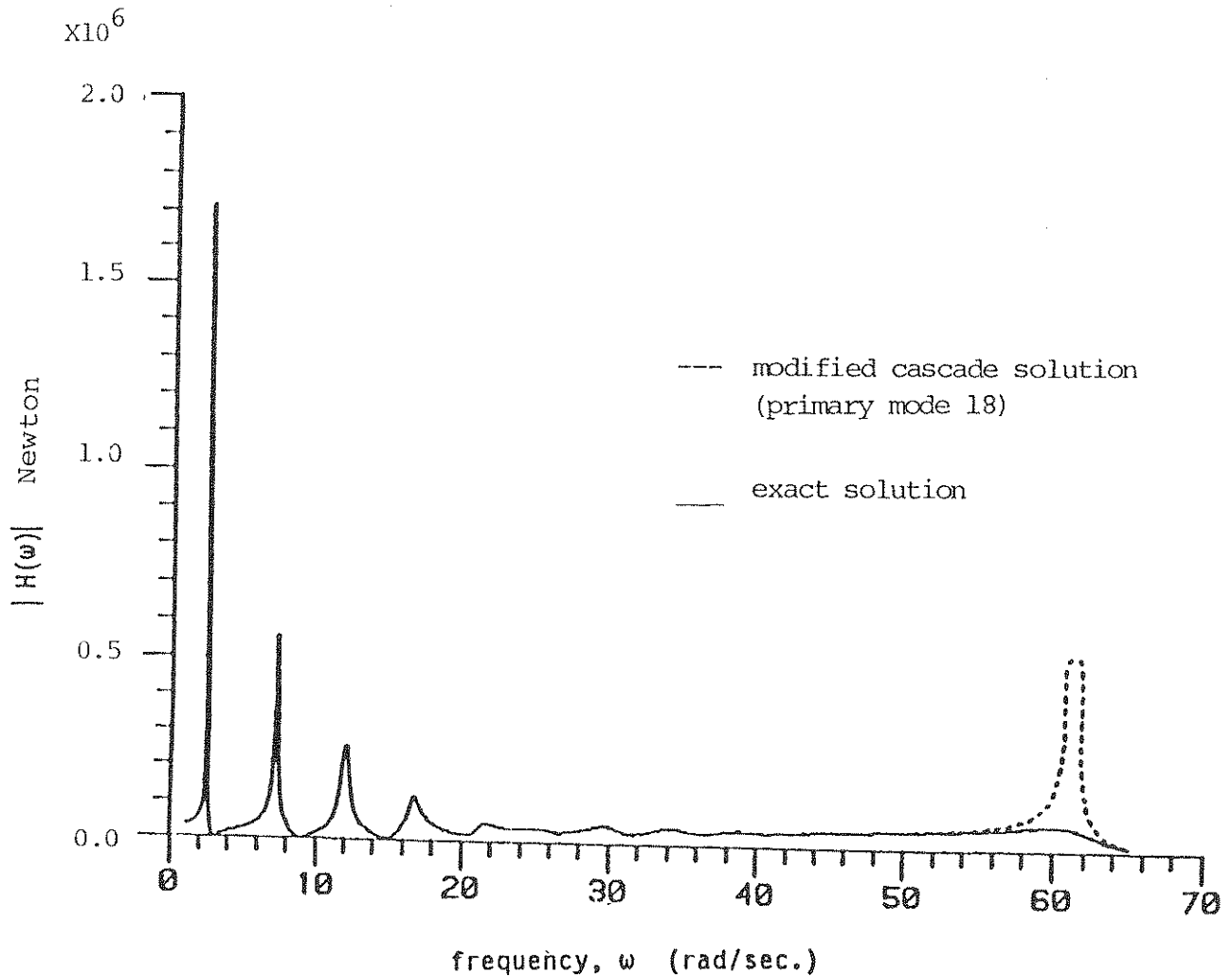


Figure 23. Modulus of frequency response function for interactive force acting at the equipment-building interface: modified cascade .vs. exact solutions. Equipment on 4-th floor tuned to eighteenth mode of building. ( Mass ratio = .01,  $c = 1.0 \times 10^7$  N/m/s).

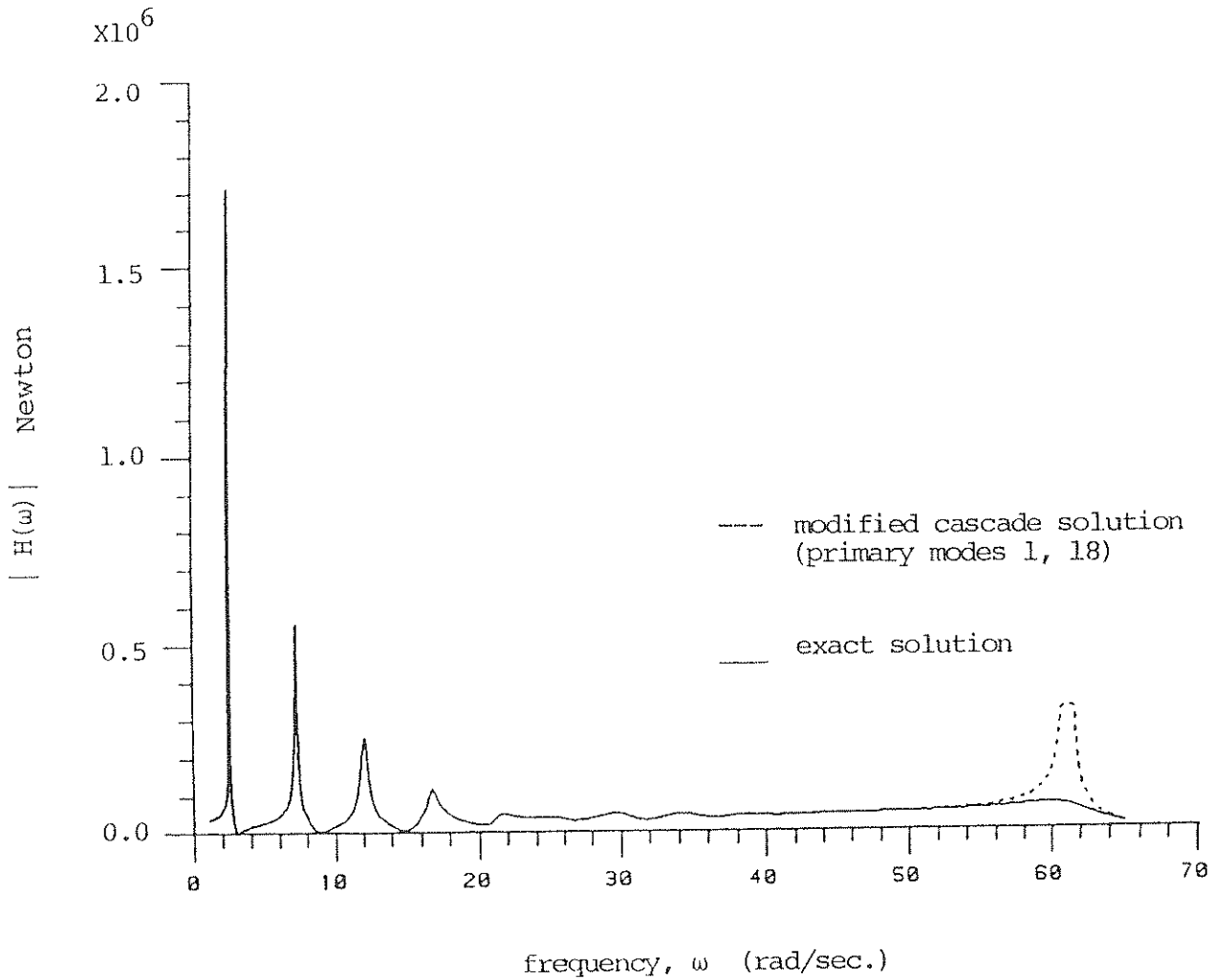


Figure 24. Modulus of frequency response function for interactive force acting at the equipment-building interface: modified cascade .vs. exact solutions. Equipment on 4-th floor tuned to eighteenth mode of building. ( Mass ratio = .01,  $c = 1.0 \times 10^7$  N/m/s).



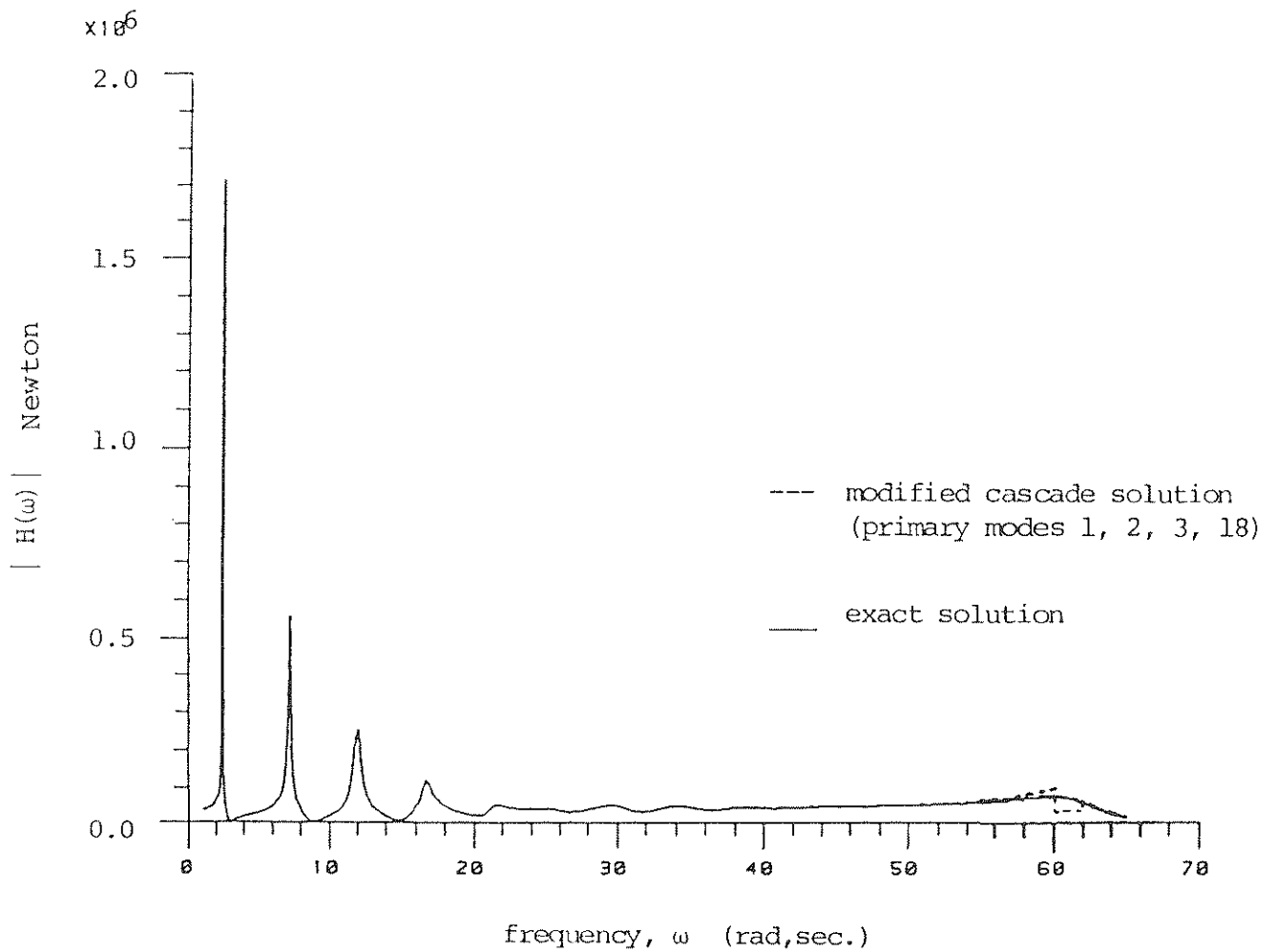


Figure 25. Modulus of frequency response function for interactive force acting at the equipment-building interface: modified cascade .vs. exact solutions. Equipment on 4-th floor tuned to eighteenth mode of building. ( Mass ratio = .01,  $c = 1.0 \times 10^7$  N/m/s).

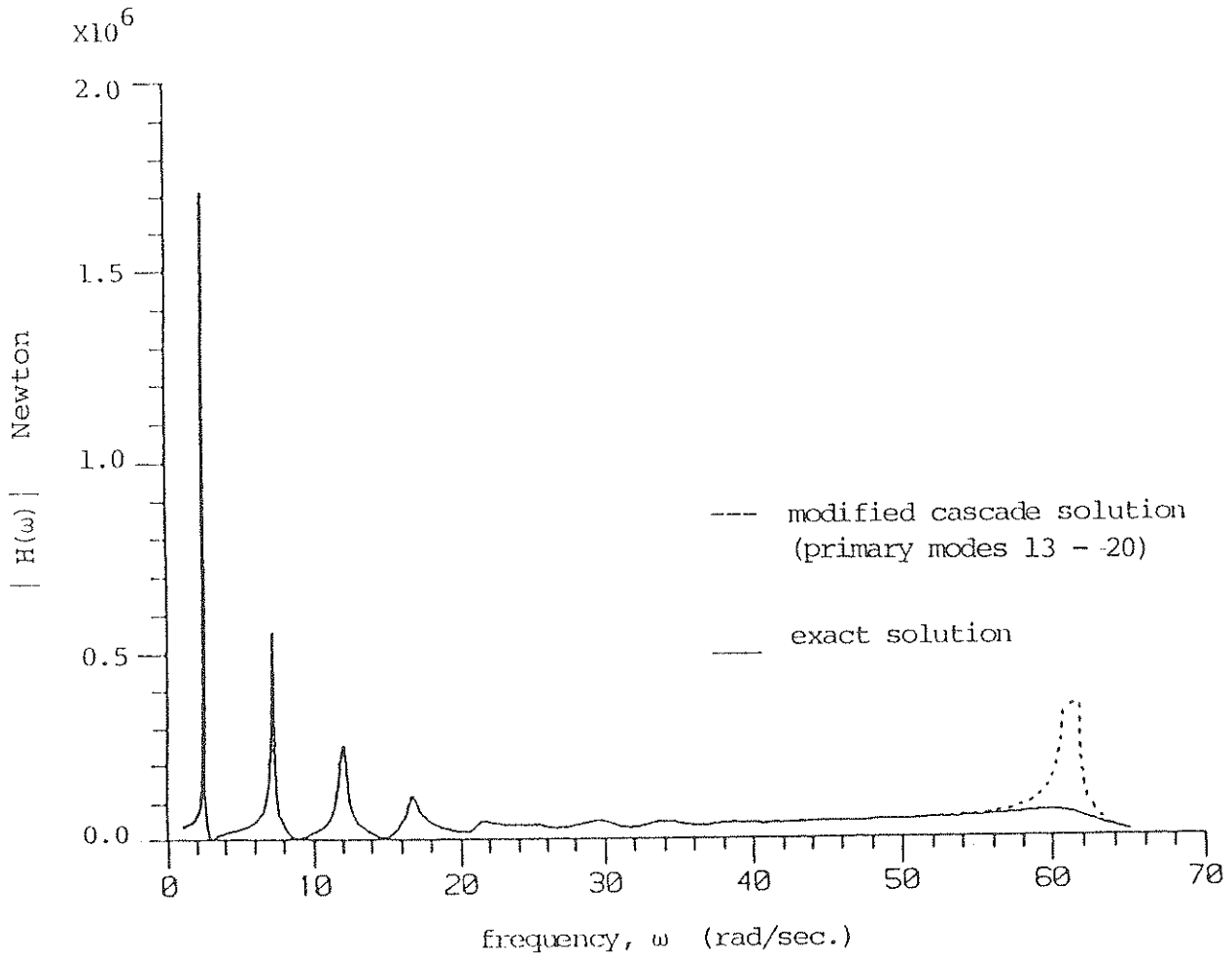


Figure 26. Modulus of frequency response function for interactive force acting at the equipment-building interface: modified cascade .vs. exact solutions. Equipment on 4-th floor tuned to eighteenth mode of building. ( Mass ratio = .01,  $c = 1.0 \times 10^7$  N/m/s).

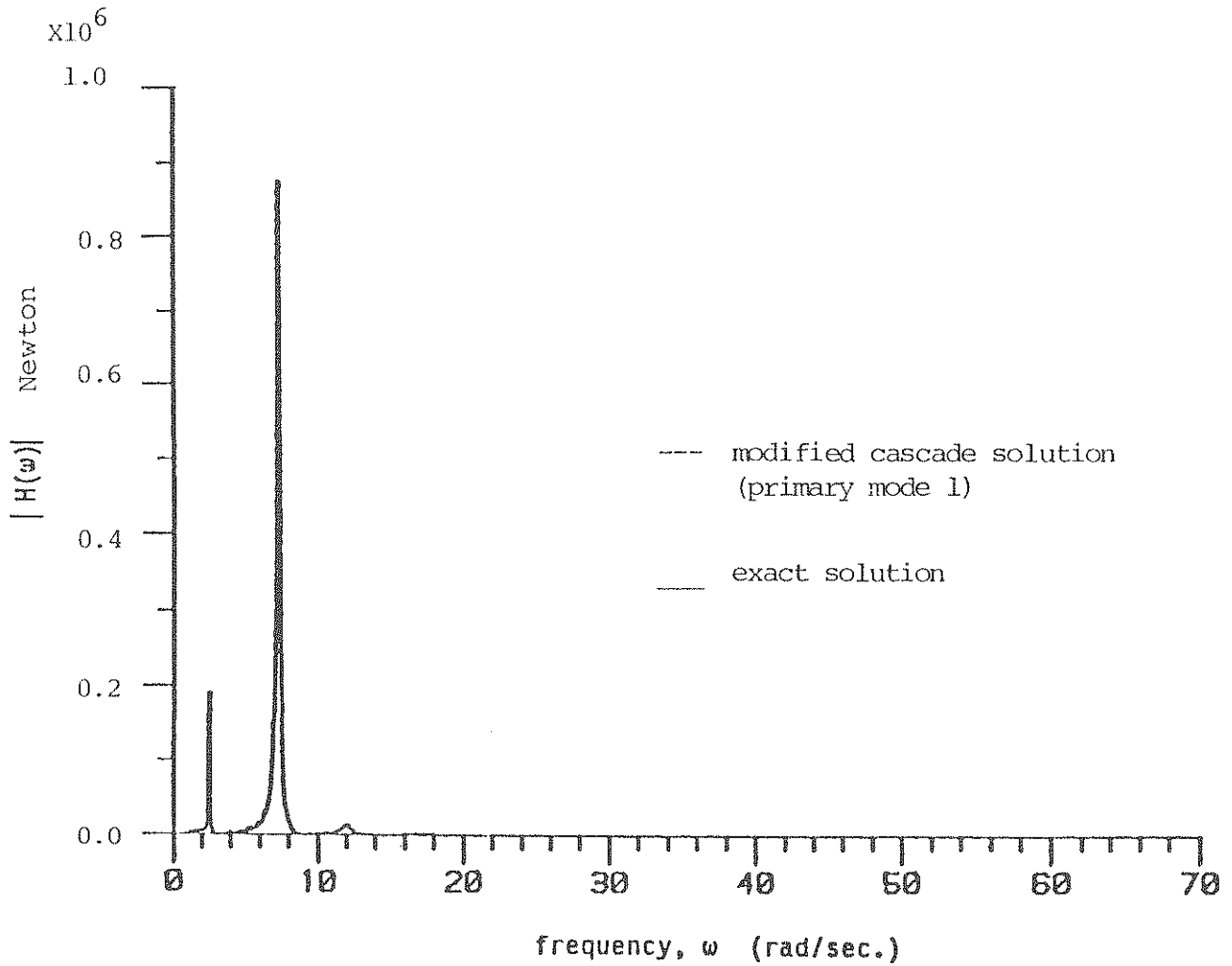


Figure 27. Modulus of frequency response function for interactive force acting at the equipment-building interface: modified cascade .vs. exact solutions. Equipment on 4-th floor tuned to second mode of building. ( Mass ratio = .001,  $c = 1.0 \times 10^7$  N/m/s).

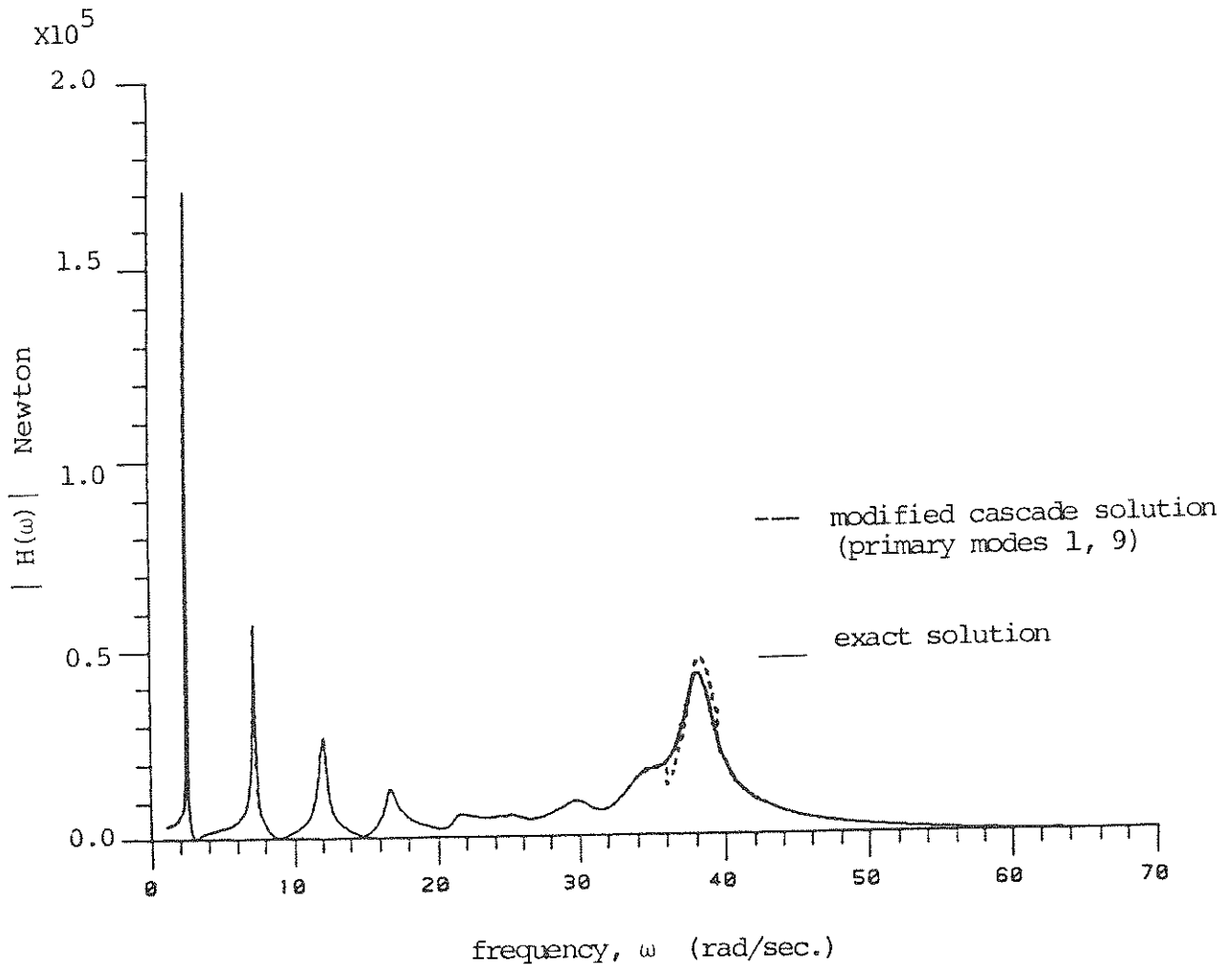


Figure 28. Modulus of frequency response function for interactive force acting at the equipment-building interface: modified cascade .vs. exact solutions. Equipment on 4-th floor tuned to ninth mode of building. ( Mass ratio = .001,  $c = 1.0 \times 10^7$  N/m/s).

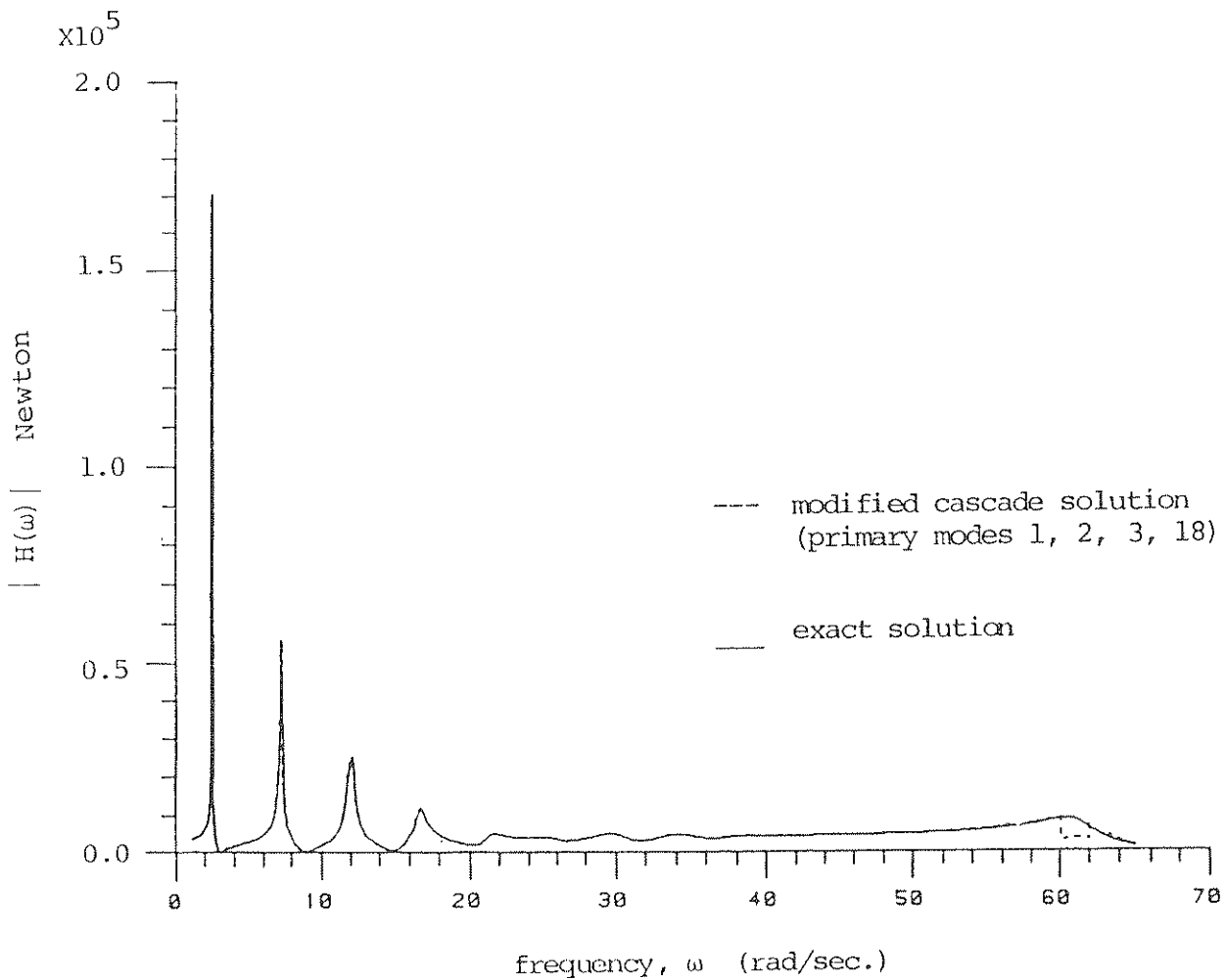


Figure 29. Modulus of frequency response function for interactive force acting at the equipment-building interface: modified cascade .vs. exact solutions. Equipment on 4-th floor tuned to eighteenth mode of building. ( Mass ratio = .001,  $c = 1.0 \times 10^7$  N/m/s).

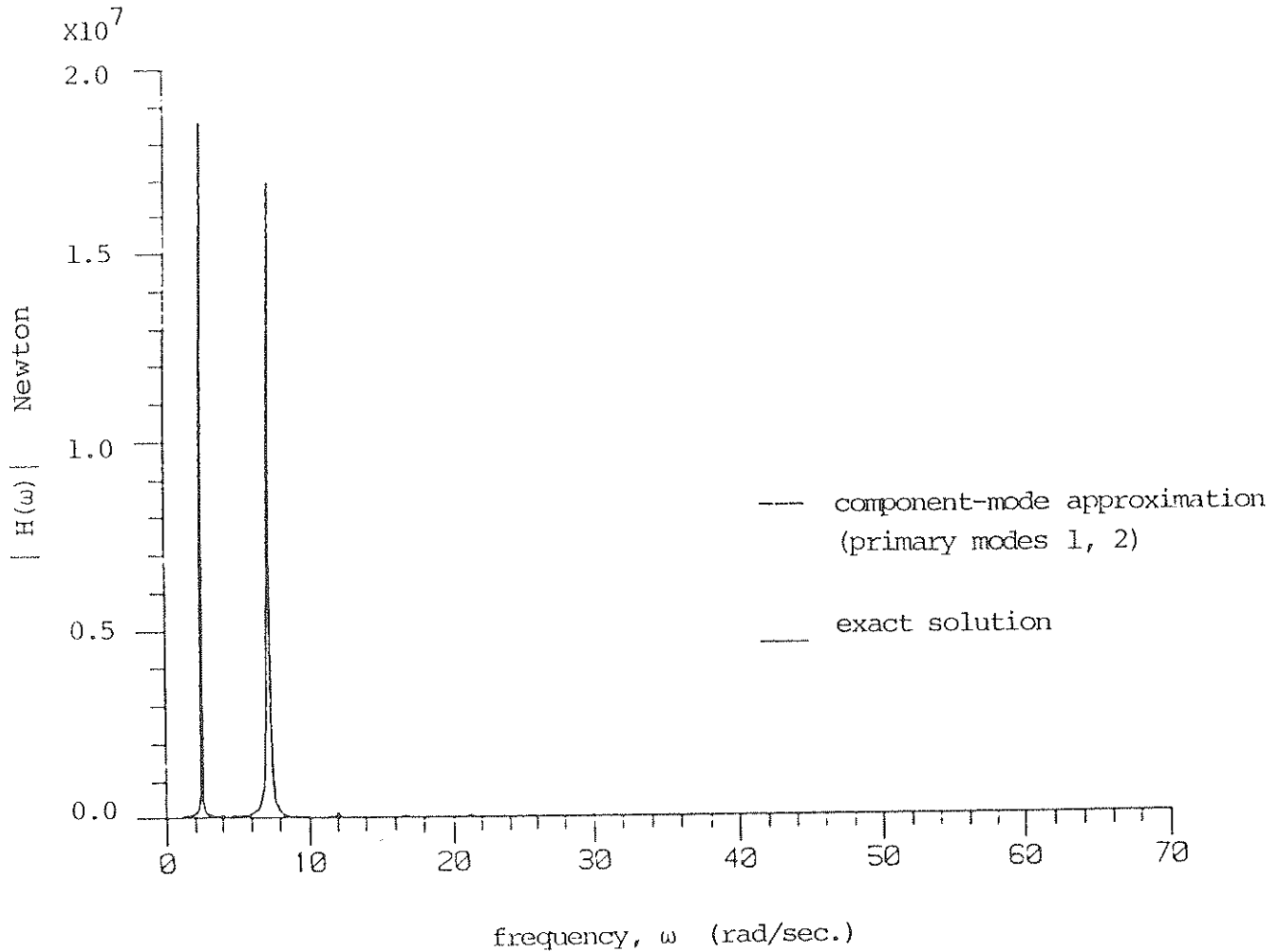


Figure 30. Modulus of frequency response function for interactive force acting at the equipment-building interface: component-mode approximation .vs. exact solutions. Equipment on 17-th floor tuned to second mode of building. ( Mass ratio = .01,  $c = 1.0 \times 10^6$  N/m/s).

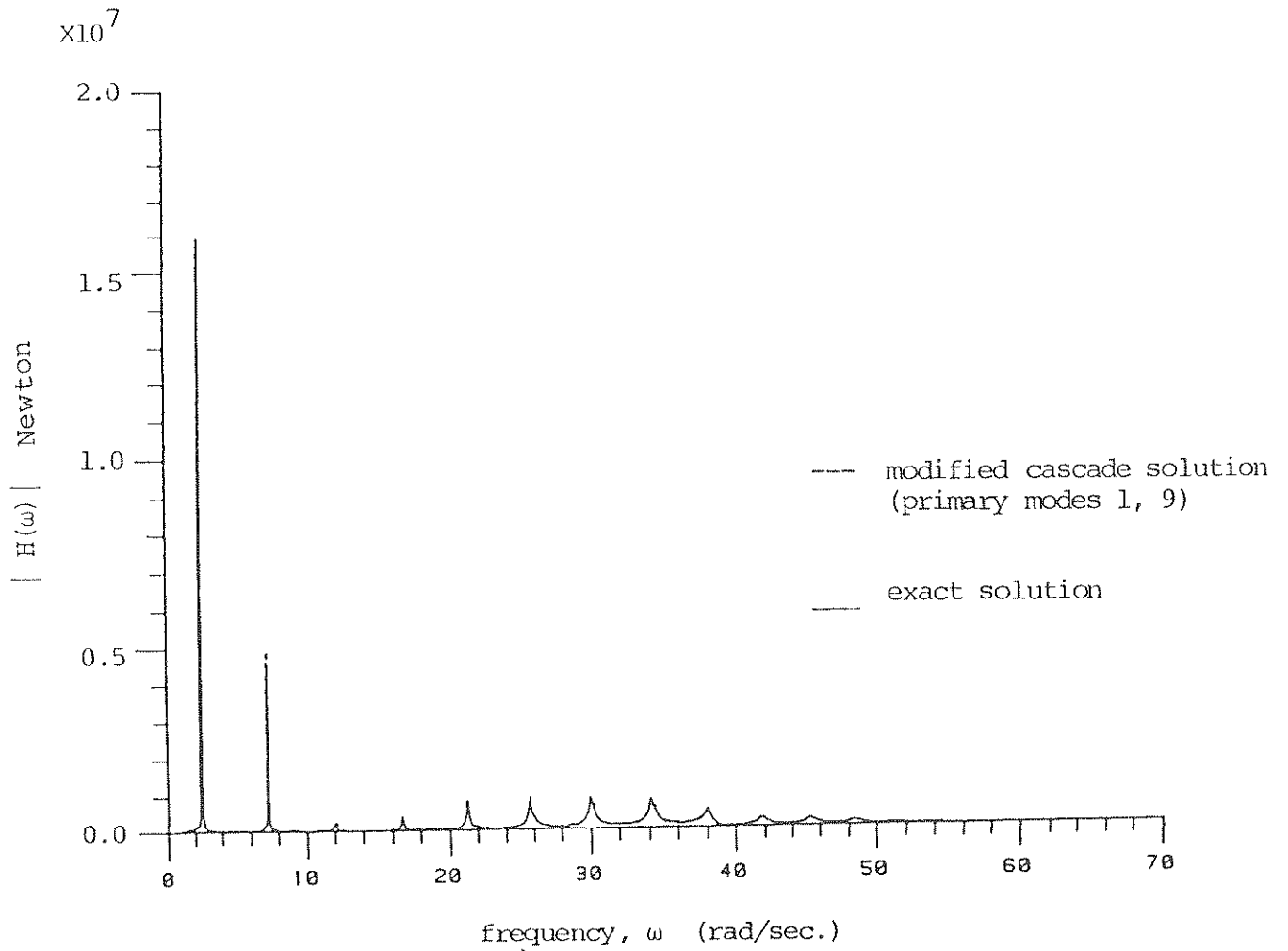


Figure 31. Modulus of frequency response function for interactive force acting at the equipment-building interface: modified cascade .vs. exact solutions. Equipment on 17-th floor tuned to ninth mode of building. ( Mass ratio = .01,  $c = 1.0 \times 10^6$  N/m/s).

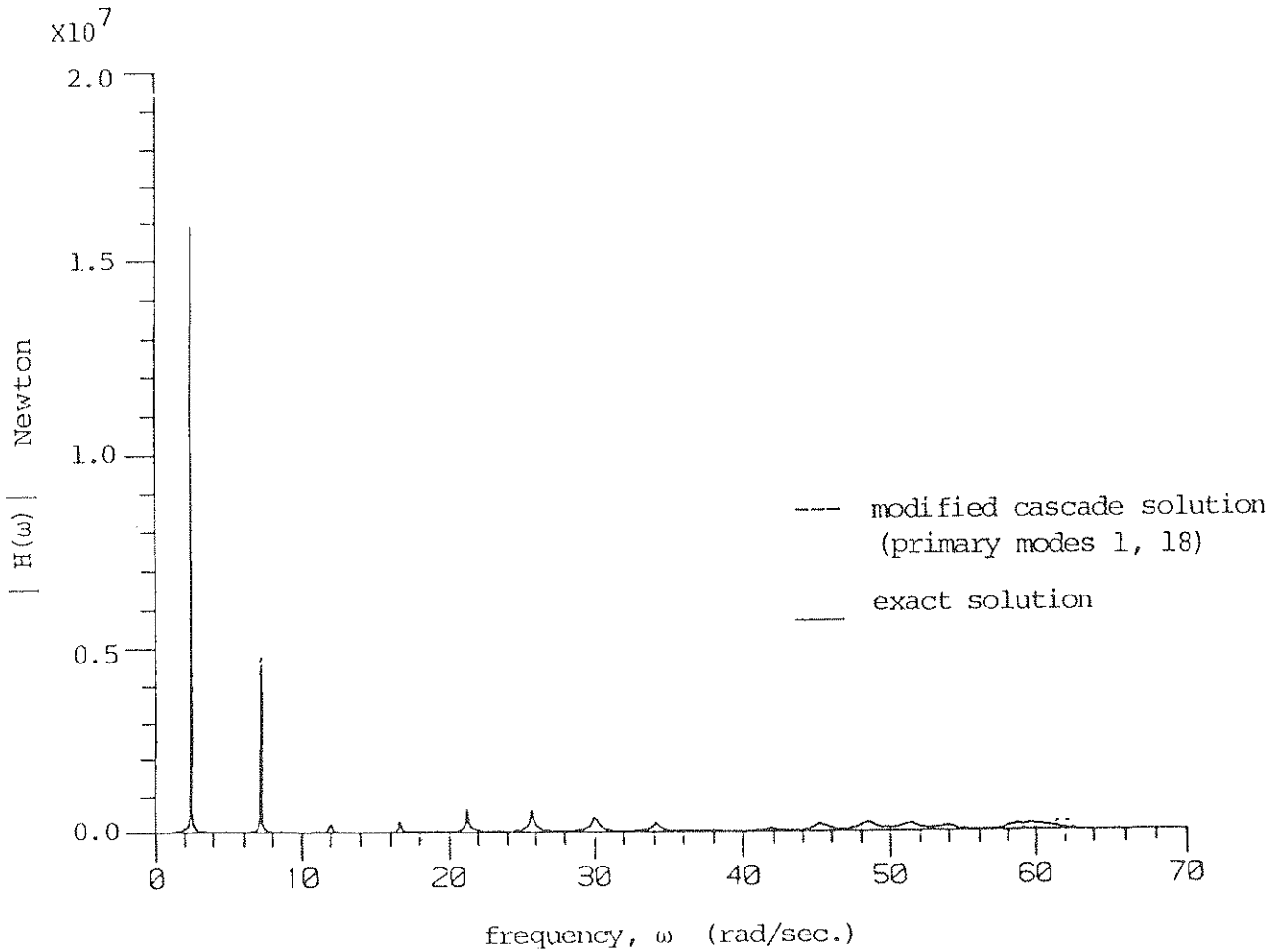


Figure 32. Modulus of frequency response function for interactive force acting at the equipment-building interface: modified cascade .vs. exact solutions. Equipment on 17-th floor tuned to eighteenth mode of building. ( Mass ratio = .01,  $c = 1.0 \times 10^6$  N/m/s).



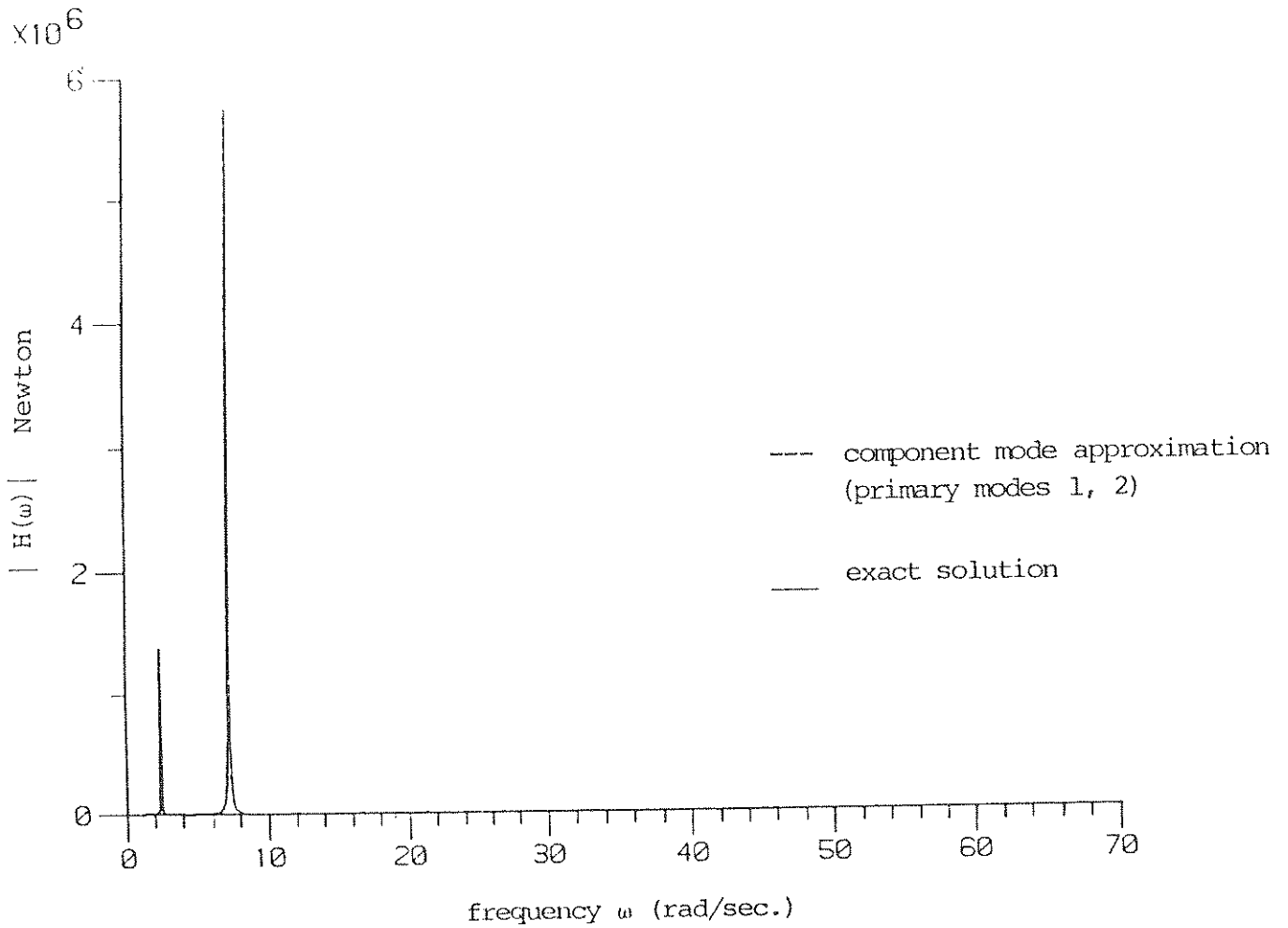


Figure 33. Modulus of frequency response function for interactive force acting at the equipment-building interface: component-mode approximation .vs. exact solutions. Equipment on 17-th floor tuned to second mode of building. ( Mass ratio = .001,  $c = 1.0 \times 10^6$  N/m/s).

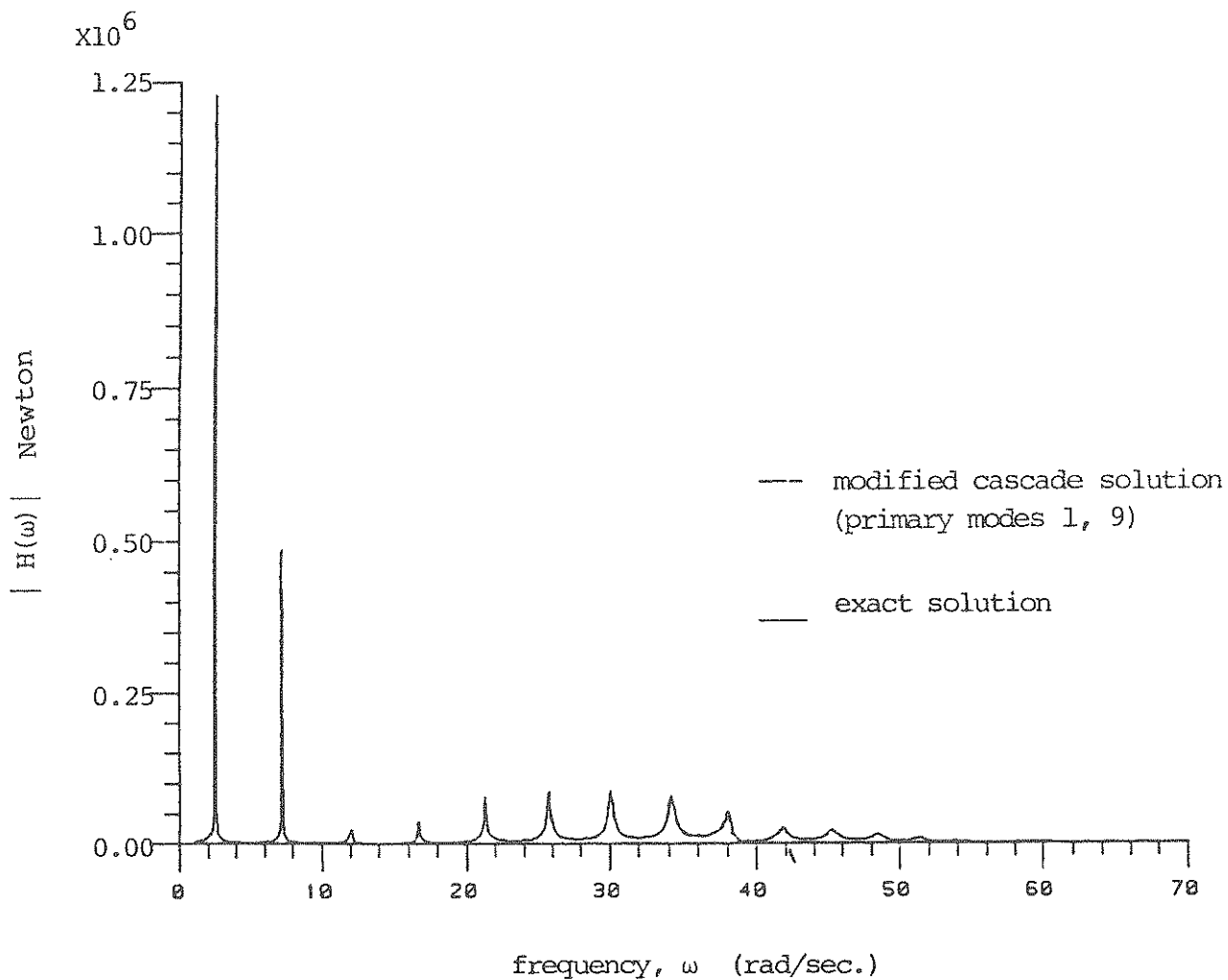


Figure 34. Modulus of frequency response function for interactive force acting at the equipment-building interface: modified cascade .vs. exact solutions. Equipment on 17-th floor tuned to ninth mode of building. ( Mass ratio = .001,  $c = 1.0 \times 10^6$  N/m/s).

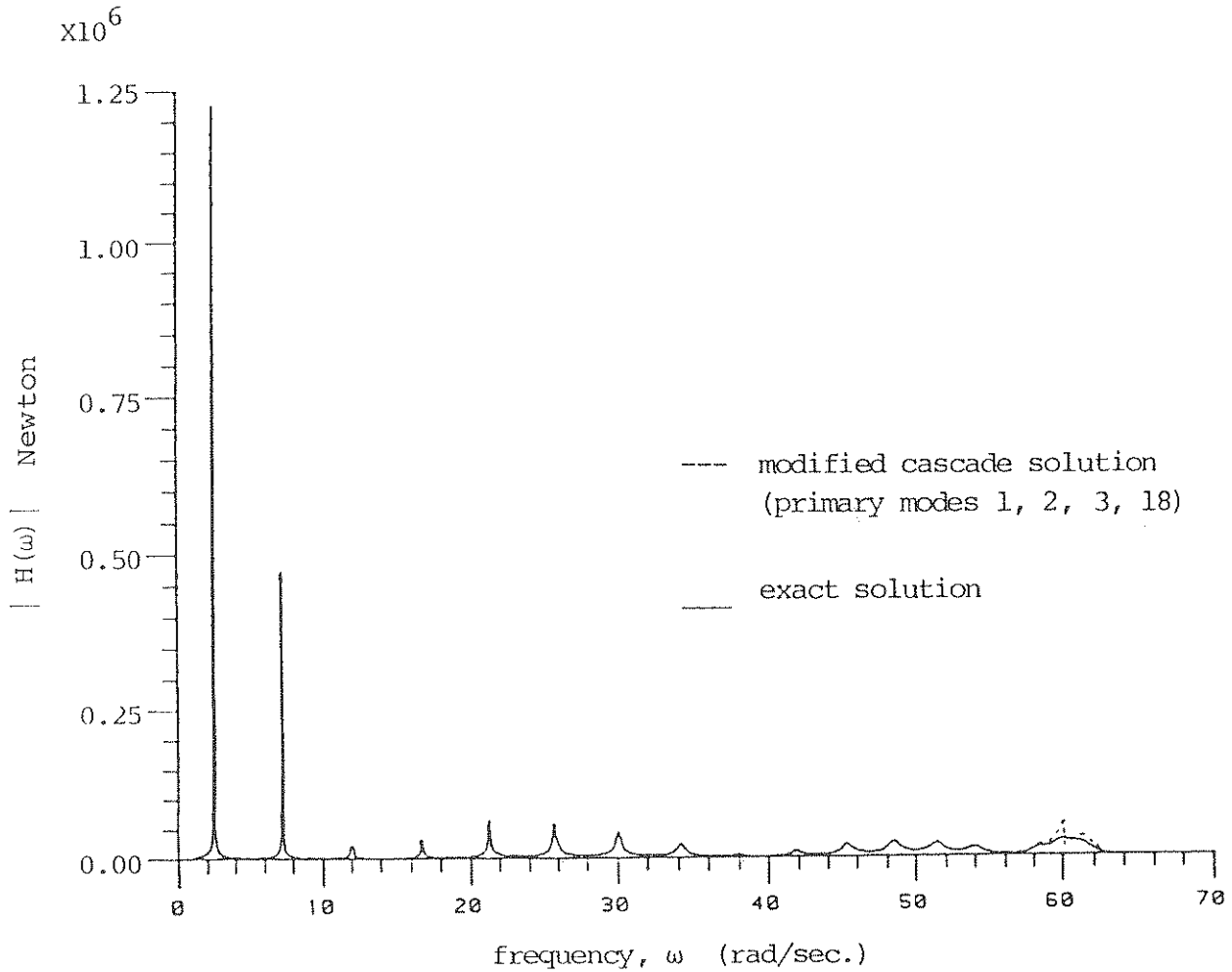


Figure 35. Modulus of frequency response function for interactive force acting at the equipment-building interface: modified cascade .vs. exact solutions. Equipment on 17-th floor tuned to eighteenth mode of building. ( Mass ratio = .001,  $c = 1.0 \times 10^6$  N/m/s).

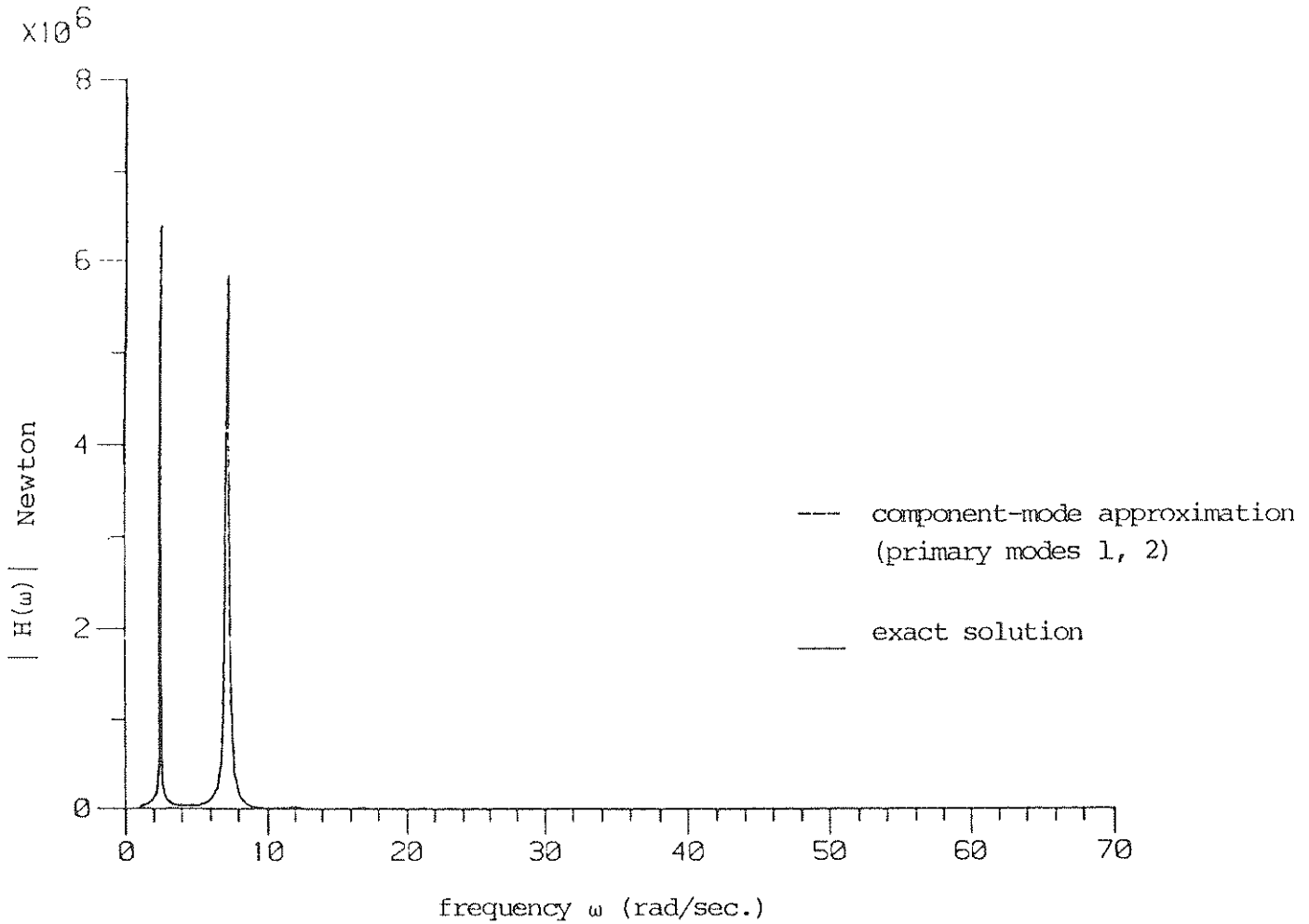


Figure 36. Modulus of frequency response function for interactive force acting at the equipment-building interface: component-mode approximation .vs. exact solutions. Equipment on 17-th floor tuned to second mode of building. ( Mass ratio = .01,  $c = 1.0 \times 10^7$  N/m/s).

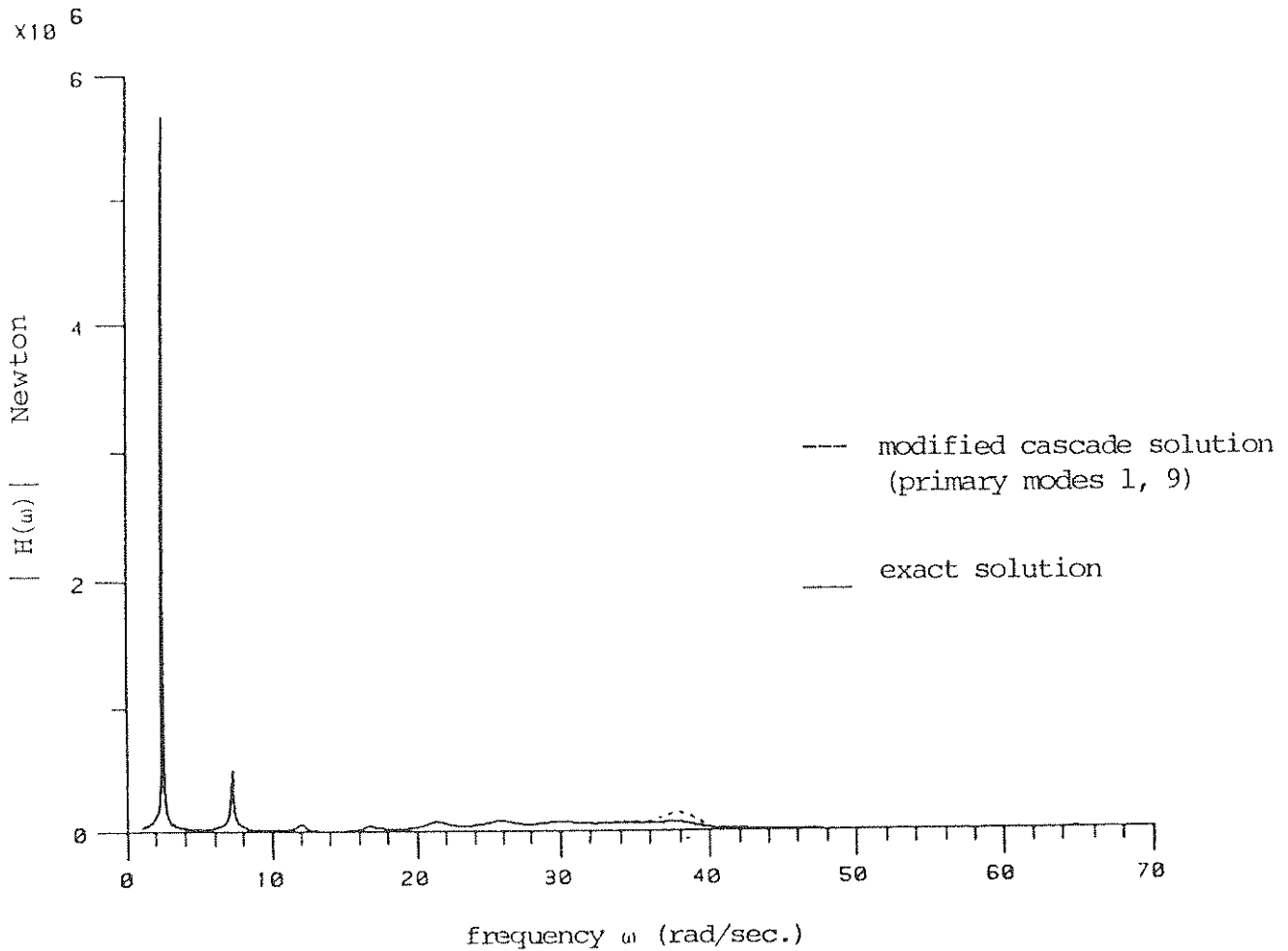


Figure 37. Modulus of frequency response function for interactive force acting at the equipment-building interface: modified cascade .vs. exact solutions. Equipment on 17-th floor tuned to ninth mode of building. ( Mass ratio = .01,  $c = 1.0 \times 10^7$  N/m/s).

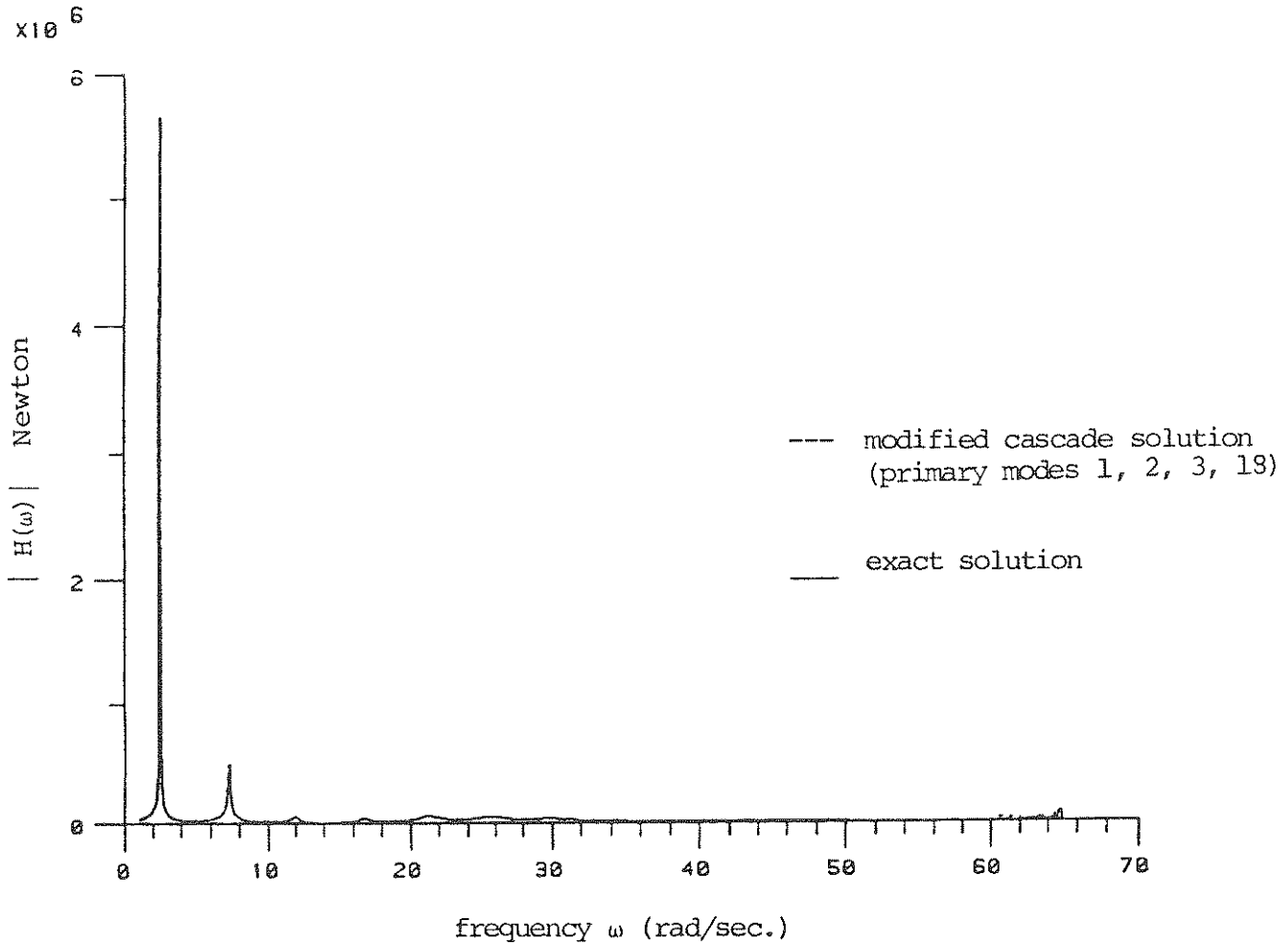


Figure 38. Modulus of frequency response function for interactive force acting at the equipment-building interface: modified cascade .vs. exact solutions. Equipment on 17-th floor tuned to eighteenth mode of building. ( Mass ratio = .01,  $c = 1.0 \times 10^7$  N/m/s).

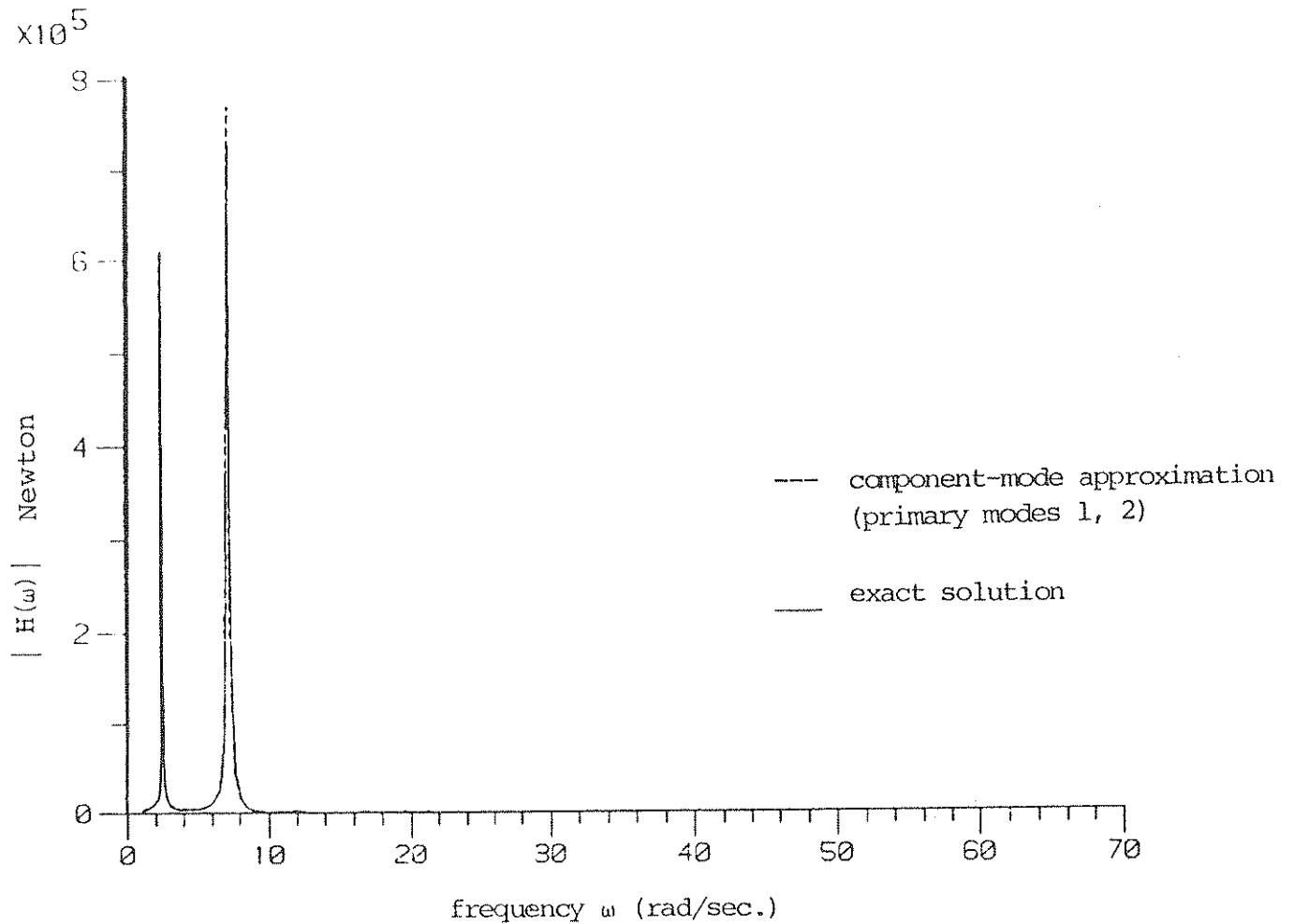


Figure 39. Modulus of frequency response function for interactive force acting at the equipment-building interface: component-mode approximation .vs. exact solutions. Equipment on 17-th floor tuned to second mode of building. ( Mass ratio = 0.001,  $c = 1.0 \times 10^7$  N/m/s).

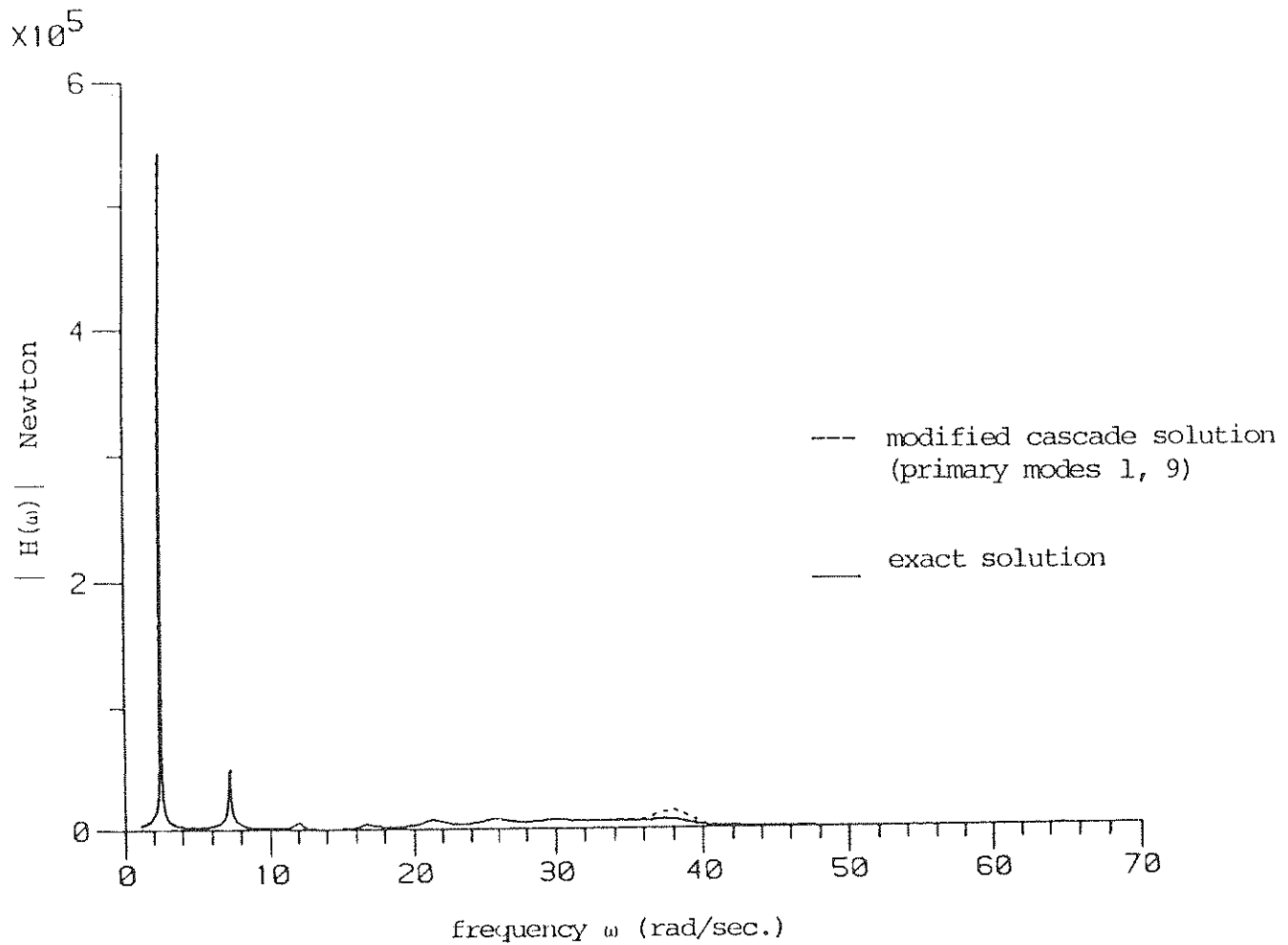


Figure 40. Modulus of frequency response function for interactive force acting at the equipment-building interface: modified cascade .vs. exact solutions. Equipment on 17-th floor tuned to ninth mode of building. ( Mass ratio = 0.001,  $c = 1.0 \times 10^7$  N/m/s).



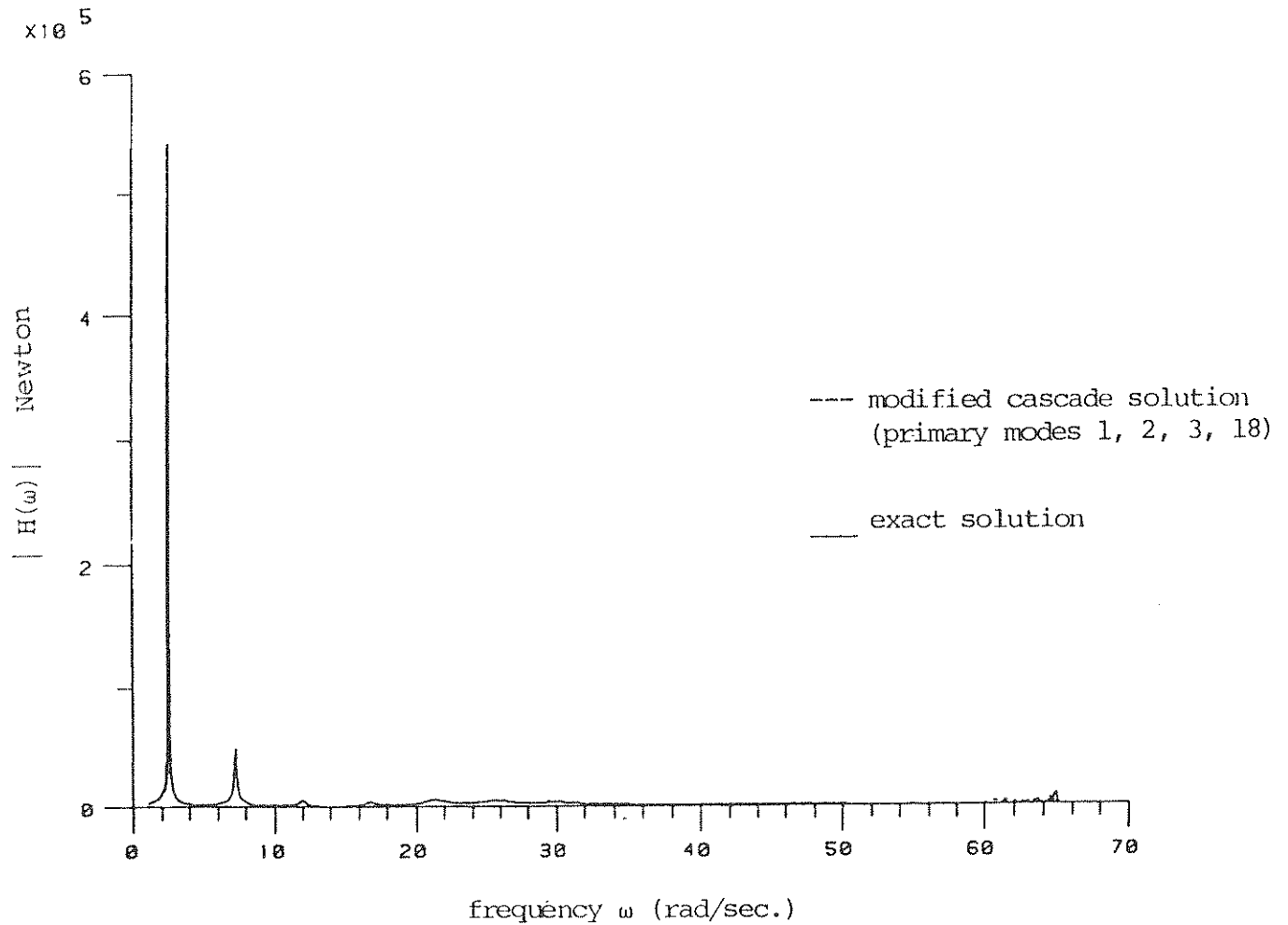


Figure 41. Modulus of frequency response function for interactive force acting at the equipment-building interface: modified cascade .vs. exact solutions. Equipment on 17-th floor tuned to eighteenth mode of building. ( Mass ratio = 0.001,  $c = 1.0 \times 10^7$  N/m/s).

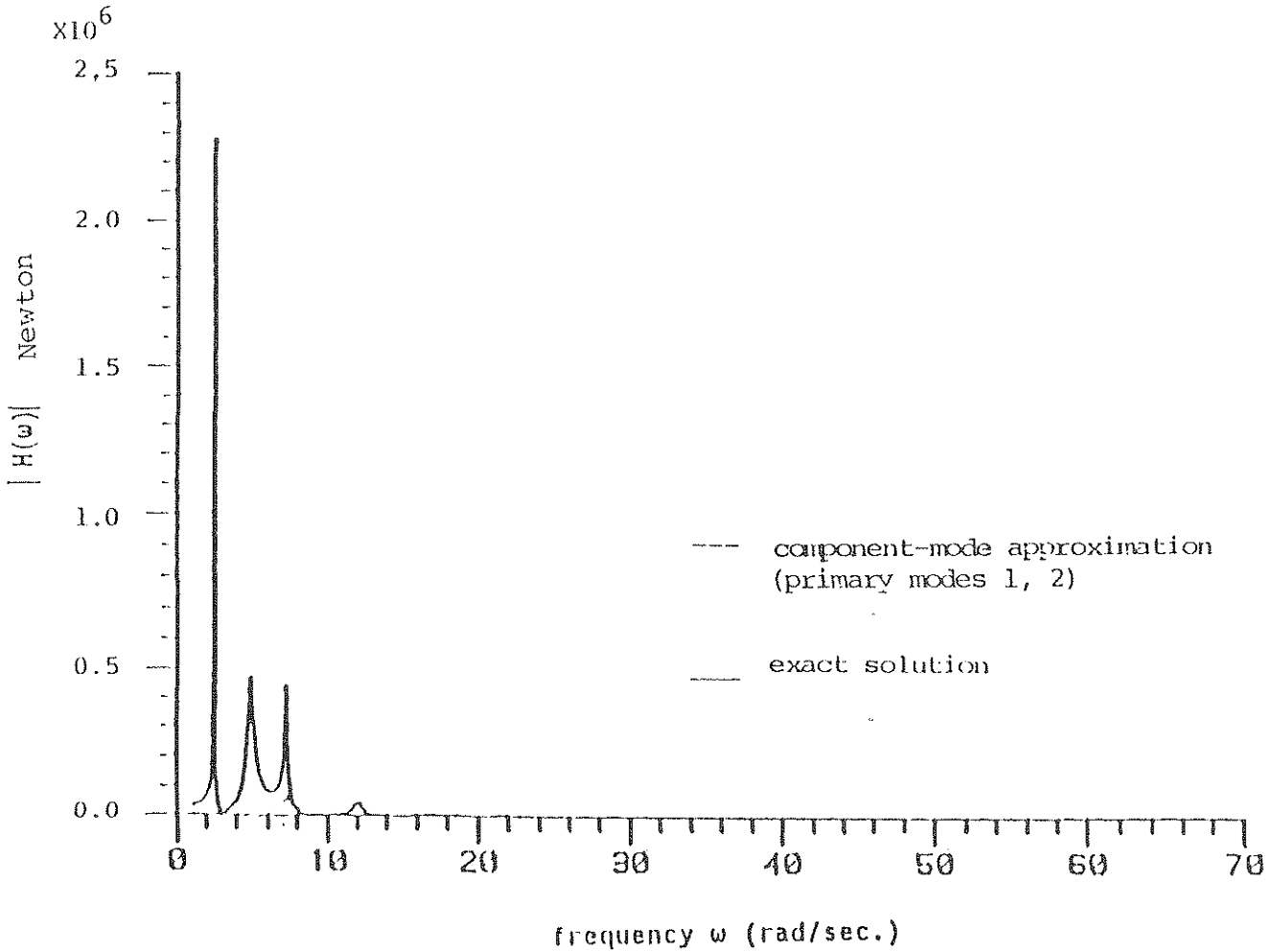


Figure 42. Modulus of frequency response function for interactive force acting at the equipment-building interface: component-mode approximation .vs. exact solution. Equipment on 4-th floor detuned to frequency mid-way between first two primary modes of building. ( Mass ratio = .01,  $c = 1.0 \times 10^7$  N/m/s).

#### 4.0 CONCLUDING REMARKS

A component-mode substructure approach provides an effective and efficient means of analyzing a p-s system. The approach is applicable to both cases of light and heavy secondary systems. Considerable reduction in computation can be realized if the secondary system has a low natural frequency for which only the lower modes of the primary system need to be included to accurately compute the secondary system response. As the natural frequency of the secondary system increases, the number of modes of the primary system to be included in the approximation also increases. In this case, a modified cascade approach is more efficient, in which the response near the natural frequencies of some selected primary modes is calculated on the basis of the component-mode approach including these primary modes, whereas the response for the remaining frequency region is calculated using the traditional cascade procedure. The selected primary modes normally include the one in tune with the secondary system and a few lowest primary modes. When damping in the primary system is sufficiently low, including only one primary mode, namely, the tuned primary mode, may be sufficient.



5.0 APPENDIX. EXACT TRANSFER MATRIX SOLUTIONS  
FOR AN EXAMPLE BUILDING-EQUIPMENT SYSTEM

Referring to figures 4(a-d), the motion of the j-th story unit of the building model, is governed by:

$$M_j (\ddot{X}_j + \ddot{G}) = U_j^+ - U_j^- + U_e \delta_{js} \quad (A-1)$$

$$U_j^- = U_{j-1}^+ = K_j (X_j - X_{j-1}) + C_j (\dot{X}_j - \dot{X}_{j-1}) \quad (A-2)$$

$$j = 1, 2, \dots, N$$

where the subscript j indicates a given story unit,  $U^+$  = shear force from above,  $U^-$  = shear force from below,  $X_j$  = translation of the j-th floor relative to the footing (which may be referred to as the 0-th floor),  $G$  = free-field horizontal ground translation during an earthquake, and  $U_e$  = the additional shear force on the s-th floor contributed by the attached secondary system. It is this additional shear force that accounts for the interaction between the primary and secondary systems. The effect of soil compliancy is neglected in the above formulation, but it can be included if so desired.

Taking the Fourier transform of the above equations and rearranging terms, we obtain the following frequency domain equations in matrix form:

$$\begin{bmatrix} \bar{X}_j \\ \bar{U}_j^+ \end{bmatrix} = \begin{bmatrix} 1 & \frac{1}{K_j + i\omega C_j} \\ -M_j \omega^2 & 1 - \frac{M_j \omega^2}{K_j + i\omega C_j} \end{bmatrix} \begin{bmatrix} \bar{X}_{j-1} \\ \bar{U}_{j-1}^+ \end{bmatrix} - M_j \omega^2 \begin{bmatrix} 0 \\ \bar{G} \end{bmatrix} - \delta_{js} \begin{bmatrix} 0 \\ \bar{U}_e \end{bmatrix} \quad (A-3)$$

$$j = 1, 2, \dots, N$$

where an over-bar denotes the Fourier transform, and  $\omega$  is the frequency of a steady state motion. More concisely, equation (A-3) may be written as

$$\begin{aligned} Z_j &= T_j Z_{j-1} - M_j \omega^2 G_o - \delta_{js} F & (A-4) \\ & j = 1, 2, \dots, N \end{aligned}$$

where  $T_j$  is known as a transfer matrix, it represents the mechanism that transfers the state at station  $j-1$  to station  $j$ , in the absence of  $G(t)$  and  $U_e$ . The boundary conditions are  $\bar{X}_o = 0$  at the footing, and  $\bar{U}_N = 0$  at the top floor,  $j=N$ . Similarly, for the equipment we have

$$Z_e = T_e Z_{e-1} - M_e \omega^2 G_o \quad (A-5)$$

where  $Z_e = [ \bar{Y}_e, 0 ]^T$ , and  $T_e$  can be constructed in the same way as  $T_j$  with  $M_j, K_j,$  and  $C_j$  replaced by  $M_e, K_e,$  and  $C_e,$  respectively. The shear force in the equipment, obtained from the second row of equation (A-5) can be simplified to the form

$$\bar{U}_e = - \left[ \frac{\tau_{21}}{\tau_{22}} \right]_e ( \bar{X}_e + \bar{G} ) \quad (A-6)$$

where  $\tau_{i,j}$  denotes the  $(i,j)$  element of a transfer matrix.

## 5.1 PRIMARY SYSTEM WITH IDENTICAL FLOORS

The analysis is simplified considerably when all the story units are identical. For this case, the transfer matrices for different stories of the primary system are identical, and it is possible to obtain closed form expressions for the frequency response functions of interest.

Discarding the subscript for the transfer matrices of the primary system since they are identical, the following simplified expressions can be obtained by inspection:

$$Z_j = T^j Z_0 - M \omega^2 \sum_{r=1}^j T^{j-r} G_0, \quad j < s \quad (\text{A-7})$$

$$Z_s = T^s Z_0 - M \omega^2 \sum_{r=1}^s T^{s-r} G_0 - F, \quad j = s \quad (\text{A-8})$$

$$Z_j = T^{j-s} Z_s - M \omega^2 \sum_{r=1}^{j-s} T^{j-s-r} G_0, \quad j > s \quad (\text{A-9})$$

$$Z_N = T^{N-s} Z_s - M \omega^2 \sum_{r=1}^{N-s} T^{N-s-r} G_0, \quad j = N \quad (\text{A-10})$$

We obtain from the first row of equation (A-8)

$$\bar{X}_s = \tau_{12}(s) \bar{U}_0^+ - M \omega^2 \sum_{r=1}^s \tau_{12}(s-r) \bar{G} \quad (\text{A-11})$$

By substituting equation (A-8) into equation (A-10), and making use of equations (A-6) and (A-11), we obtain from the second row:

$$\bar{U}_o^+ = M \omega^2 \bar{G} \left( \frac{P}{Q} \right) \quad (\text{A-12 a})$$

where

$$P = \sum_{r=1}^N \tau_{22}^{(N-r)} \left( 1 - \frac{M_e \omega^2}{K_e + i \omega C_e} \right) - \tau_{22}^{(N-s)} \sum_{r=1}^s \tau_{12}^{(s-r)} \frac{M \omega^2}{e} + \tau_{22}^{(N-s)} \left( \frac{M_e}{M} \right) \quad (\text{A-12 b})$$

and

$$Q = \tau_{22}^{(N)} \left( 1 - \frac{M_e \omega^2}{K_e + i \omega C_e} \right) - M_e \omega^2 \tau_{12}^{(s)} \tau_{22}^{(N-s)} \quad (\text{A-12 c})$$

Equation (A-12) can be simplified using two interesting properties common to all transfer matrices; namely, the determinant of a transfer matrix is equal to one, and its eigenvalues are reciprocal pairs. Denoting the two eigenvalues of the present 2x2 transfer matrix by  $\exp(\pm i\alpha)$ , it can be shown that

$$\cos \alpha = 1 - \frac{M \omega^2}{2(K + i\omega C)} \quad (\text{A-13})$$

Closed form expressions for several functions of this particular transfer matrix can be obtained from those derived in reference 13, by setting  $\beta=0$ , and replacing  $K$  by  $K+i\omega C$ . The expressions that are needed in the present study are:



$$\tau_{12}(j) = \frac{\sin j\alpha}{(K + i\omega C) \sin \alpha} \quad (\text{A-14})$$

$$\tau_{22}(j) = \frac{\cos (j + \frac{1}{2})\alpha}{\cos \frac{1}{2} \alpha} \quad (\text{A-15})$$

$$\sum_{r=1}^j \tau_{22}(j-r) = \frac{\sin j\alpha}{\sin \alpha} \quad (\text{A-16})$$

$$\sum_{r=1}^j \tau_{12}(j-r) = \frac{\sin \frac{1}{2}(j-1)\alpha \sin \frac{1}{2} j\alpha}{(K + i\omega C) \sin \frac{1}{2}\alpha \sin \alpha} \quad (\text{A-17})$$

With equations (A-13) through (A-17), it can be shown that equation (A-12) reduces to the following:

$$\bar{U}_o^+ = \frac{J_1}{J_2} \times \frac{2 (K+i\omega C) \sin \alpha/2 \sin N\alpha}{\cos (N+\frac{1}{2})\alpha} \bar{G} \quad (\text{A-18})$$

where

$$\begin{aligned} J_1 = & 1 - \frac{M_e \omega^2}{K_e + i\omega C_e} \\ & - \frac{2(M_e/M) \sin(s\alpha/2) \sin \frac{1}{2}(s-1)\alpha \sin \alpha \cos(N-s+\frac{1}{2})\alpha}{\cos^2 \alpha/2 \sin(N\alpha)} \\ & + \frac{(M_e/M) \cos(N-s+\frac{1}{2})\alpha \sin \alpha}{\cos(\alpha/2) \sin(N\alpha)} \end{aligned} \quad (\text{A-19})$$

$$\begin{aligned} J_2 = & 1 - \frac{M_e \omega^2}{K_e + i\omega C_e} \\ & - \frac{4(M_e/M) \sin^2(\alpha/2) \sin(s\alpha) \cos(N-s+\frac{1}{2})\alpha}{\cos(N+\frac{1}{2})\alpha \sin \alpha} \end{aligned} \quad (\text{A-20})$$

The ratio  $J_1/J_2$  in equation (A-18), depends on the parameters of the equipment, the parameters of the primary system, the location of the equipment, and the mass ratio  $M_e/M$ ; however, the remaining part of the equation depends only on the parameters of the primary system. Note that the ratio  $J_1/J_2$  approaches 1 as the mass of the equipment approaches zero, which provides a partial check because, in the limit, we

recover the known results for the primary system without the equipment [13].

With the knowledge of  $\bar{U}_s^+$ , the response of the primary system at various floors can be obtained. Specifically,

$$\bar{x}_j = \left\{ \beta(j) - 1 - \frac{\sin(j-s)\alpha}{(K + i\omega C)} \frac{\beta(s) U(j-s)}{\sin \alpha} M_e \omega^2 * \right. \\ \left. \left[ 1 - \frac{M_e \omega^2}{K_e + i\omega C_e} \right]^{-1} \right\} \bar{G}; \quad j = 1, \dots, N \quad (A-21)$$

$$\bar{U}_j^+ = \left\{ 2 (K + i\omega C) \mu(j) - \frac{\cos(j-s+\frac{1}{2})\alpha}{\cos(\frac{1}{2}\alpha)} \frac{\beta(s) U(j-s)}{\sin \alpha} M_e \omega^2 * \right. \\ \left. \left[ 1 - \frac{M_e \omega^2}{K_e + i\omega C_e} \right]^{-1} \right\} \bar{G}; \quad j = 1, \dots, N \quad (A-22)$$

where

$$\beta(j) = \frac{\sin(j\alpha) \sin(N\alpha) (J_1/J_2)}{\cos(N + \frac{1}{2})\alpha \cos \alpha/2} + \frac{\cos(j - \frac{1}{2})\alpha}{\cos \alpha/2} \quad (A-23)$$

$$\mu(j) = \frac{2 \cos(j + \frac{1}{2})\alpha \sin^2(\alpha/2) \sin(N\alpha) (J_1/J_2)}{\cos(N + \frac{1}{2})\alpha \sin \alpha} - \frac{\sin(\alpha/2) \sin(j\alpha)}{\cos(\alpha/2)} \quad (A-24)$$

and

$$U(j-s) = \begin{cases} 1 & \text{if } j \geq s \\ 0 & \text{if } j < s \end{cases} \quad (A-25)$$

Similar expressions for the secondary system can be obtained from equations (A-5) and (A-6). The results are:

$$\bar{Y}_e = \left[ \frac{\frac{\beta(s)}{M_e \omega^2}}{1 - \frac{M_e \omega^2}{K_e + i \omega C_e}} - 1 \right] \bar{G} \quad (\text{A-26})$$

$$\bar{U}_e = \left[ \frac{M_e \omega^2}{1 - \frac{M_e \omega^2}{K_e + i \omega C_e}} \beta(s) \right] \bar{G} \quad (\text{A-27})$$

## 5.2 CASCADE SOLUTION

By setting  $j = s$  and letting the mass of the equipment equal to zero in equation (A-21), we obtain the displacement of floor  $s$  relative to the ground, without the equipment. The response of the secondary system, modeled as a single degree-of-freedom oscillator, to this support excitation can be easily calculated (alternatively, one can use Eqs. A-26 and A-27 with  $J_1/J_2=1$  in the expression for  $\beta(s)$ ).

## 5.3 MODAL PROPERTIES OF PRIMARY SYSTEM

The modal properties of the multi-story building can be simply calculated when each story is identically constructed. The primary system in this case, is classically damped since the damping matrix is proportional to the stiffness matrix. Setting  $J_1/J_2$  equal to one, for example, (recall this is equivalent to ignoring the equipment) in equation (A-18), a total of  $N$  poles are found at

$$\alpha_i = \pi(2i-1)/(2N+1) \quad i=1,2,\dots,N \quad (\text{A-28})$$

which are the roots of

$$\cos (N+\frac{1}{2})\alpha = 0 \quad (\text{A-29})$$

Without damping, equations (A-13) and (A-28) determine the  $N$  natural frequencies. Setting  $c=0$ , and introducing the notation

$$\omega_o = \sqrt{\left(\frac{K}{M}\right)} \quad (\text{A-30})$$

the natural frequencies so obtained are:

$$\tilde{\omega}_i = 2 \omega_0 \sin \frac{1}{2} \alpha_i \quad i=1, \dots, N \quad (\text{A-31})$$

where  $\tilde{\omega}_i$  is the  $i$ -th undamped natural frequency. With damping present, the  $\omega_i$  obtained from equations (A-13) and (A-29) are complex. Then the modal damping ratio of the  $i$ -th mode may be determined as follows

$$\zeta_i = \frac{|\text{Im } \omega_i|}{\tilde{\omega}_i} \quad (\text{A-32})$$

where  $\zeta_i$  denote the damping ratio for mode  $i$ , and 'Im  $\omega_i$ ' is the imaginary part of  $\omega_i$ . Evaluation of equation (A-32) leads to the simple expression

$$\zeta_i = 2 \zeta_0 \sin \frac{1}{2} \alpha_i \quad i=1, \dots, N \quad (\text{A-33})$$

where

$$\zeta_0 = \frac{C}{2M\omega_0} \quad (\text{A-34})$$

In the above, it is assumed that all modes are lightly damped, which will be the case provided that

$$\zeta_i < 1 \quad (\text{A-35})$$

It is seen from equation (A-33), that when the damping mechanism is internal as assumed in this study, the modal damping is higher for a higher mode.

Following a similar procedure, it can also be shown that if the damping mechanism is external, (see figure 4e), the corresponding equation for the damping ratios are

$$\zeta_i = \frac{\zeta_0}{2 \sin \frac{1}{2} \alpha_i}, \quad i=1, \dots, N \quad (\text{A-36})$$

That is, the damping ratio decreases in each mode. For this case, the primary system is again classically damped since the damping matrix is proportional to the mass matrix.

With the natural frequencies for the primary system determined, the corresponding mode shapes can also be obtained. Setting  $M_e = 0$  in equation (A-21) for example, it can be shown that the frequency response function for the relative displacement at each floor reduces to the simple form

$$\bar{X}_j = \left( \frac{\cos (N + \frac{1}{2} - j)\alpha}{\cos (N + \frac{1}{2})\alpha} - 1 \right) \bar{G} \quad (A-37)$$

$$j = 1, \dots, N$$

The corresponding impulse response function due to a ground acceleration input is obtained from the expression

$$h_j(t) = \frac{1}{2\pi} \int_{-\infty}^{\infty} \omega^{-2} \left( 1 - \frac{\cos (N + \frac{1}{2} - j)\alpha}{\cos (N + \frac{1}{2})\alpha} \right) e^{i \omega t} d\omega \quad (A-38)$$

$$j = 1, \dots, N$$

It is known that the modal displacements which describe the shape of free vibration at each natural frequency are proportional to the residues [21]. Using this fact, we can compute the  $j$ -th element of mode  $i$  as follows:

$$\phi_i(j) = (-1)^{i+1} \cos (N + \frac{1}{2} - j)\alpha_i \sin \alpha_i \quad (A-39)$$

$$i, j = 1, 2, \dots, N$$



## 6.0 ACKNOWLEDGEMENT

Financial support from the IBM Inc. for J. A. HoLung while pursuing his Ph.D. degree in Mechanical Engineering at the Florida Atlantic University is gratefully acknowledged.





## 7.0 REFERENCES

1. Asfura, A., and Der Kiureghian, A., "Floor Response Spectrum Method For Seismic Analysis of Multiply Supported Secondary Systems", Earthquake Engineering and Structural Dynamics, Vol. 14, 1986, pp. 245-265.
2. Benfield, W. A., and Hrudu, R. F., "Vibration Analysis of Structures by Component Mode Substitution", AIAA Journal, Vol. 9, No. 7, July 1971, pp. 1255-1261.
3. Craig, R. R., "Coupling of Substructures for Dynamic Analyses", AIAA Journal, Vol. 6, No. 7, July 1968, pp. 1313-1319.
4. Der Kiureghian, A., Sackman, J. L., and Nour-Omid, B., "Dynamic Response of Light Equipment in Structures", Report No. UCB/EER-81/05, Earthquake Engineering Research Center, University of California, Berkley, Calif., April 1981.
5. Gladwell, G. M. L., "Branch Mode Analysis of Vibrating Systems", Journal of Sound and Vibration, 1, 1964, pp. 41-59.
6. Hale, A. L., and Meirovitch, L., "A General Substructure Synthesis Method for the Dynamic Simulation of Complex Structures", Journal of Sound and Vibration, 69 (2), 1980, pp. 309-326.
7. Hurty, W. C., "Dynamic Analysis of Structural Systems Using Component Modes", AIAA Journal, Vol. 3, No. 4, April 1965, pp. 678-685.
8. Igusa, T., and Der Kiureghian, A., "Dynamic Characterization of Two-Degree-of-Freedom Equipment-Structure Systems", Journal of Engineering Mechanics, ASCE, Vol. 111, No. 1, January, 1985, pp. 1-19.

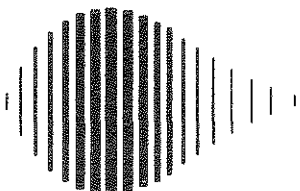
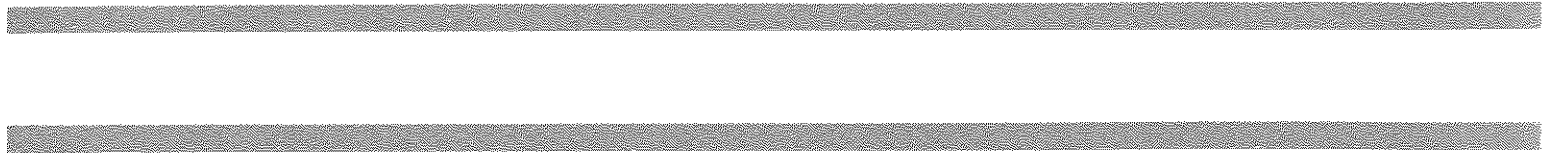
9. Igusa, T., and Der Kiureghian, A., "Dynamic Response of Multiply Supported Secondary Systems", Journal of Engineering Mechanics, ASCE, Vol. 111, No. 1, January, 1985, pp. 20-41.
10. Igusa, T., and Der Kiureghian, A., "Generation of Floor Response Spectra Including Oscillator-Structure Interaction", Earthquake Engineering and Structural Dynamics, Vol. 13, 1985, pp. 661-676.
11. Igusa, T., Der Kiureghian, A., and Sackman, J. L., "Modal Decomposition Method for Stationary Response of Non-Classically Damped Systems", Earthquake Engineering and Structural Dynamics, Vol. 12, 1984, pp. 121-136.
12. Lin, Y. K., Probabilistic Theory of Structural Dynamics, McGraw-Hill, New York, 1967, Reprinted by Kreiger Publishing Co., Malibar, Fl, 1976.
13. Lin, Y. K., and Wu, W. F., "A Closed Form Earthquake Response Analysis of Multistory Building on Compliant Soil", Journal of Structural Mechanics, 1984, pp. 87-110.
14. Lin, Y. K., and Wu, W. F., "Along-Wind Motion of Building on Compliant Soil", Journal of Engineering Mechanics, Vol. 110, January, 1984.
15. Sackman, J. L., and Kelly, J. M., "Seismic Analysis of Internal Equipment and Components in Structures", Engineering Structures, Vol. 1, No. 4, July 1979, pp. 179-190.
16. Singh, A. K., and Ang, A. H-S., "A Stochastic Model for Predicting Seismic Response of Light Secondary Systems", 5th World Conference on Earthquake Engineering, 1973.
17. Suarez, L. E., and Singh, M. P., "Exact Eigenproperties and Floor Response Spectra of Primary and Equipment Systems", Report No. VPI-E-86-10, Virginia Polytechnic

Institute and State University, Blacksburg, VA 24061,  
April, 1986.

18. Suarez, L. E., and Singh, M. P., "Seismic Response of SDF Equipment- Structure System", Journal of Engineering Mechanics, Vol. 113, No. 1, January, 1987.
19. Suarez, L. E., and Singh, M. P., "A Method for Dynamic Coupling with Nonclassical Damping Effects", Journal of Sound and Vibration, Vol. 121, No. 1, Feb. 1988 (to appear)
20. Suarez, L. E., and Singh, M. P., "A Modal Coupling Procedure for Structural Dynamics", Virginia Polytechnic Institute and State University, Blacksburg, Virginia, 1987.
21. Thornhill, J., and Smith, C. C., "Fourier and Spectral Analysis", notes prepared by Joe Thornhill, IBM, Austin, Texas, and Craig. C. Smith, Brigham Young University, Provo, Utah, 1980.







National Center for Earthquake Engineering Research  
State University of New York at Buffalo